



UNIVERSITÀ DEGLI STUDI DI ROMA
"TOR VERGATA"

DOTTORATO DI RICERCA IN INGEGNERIA CIVILE

indirizzo: INGEGNERIA AMBIENTALE

XXVII CICLO

**Valorization of BOF steel slag and
gasification ashes through suitable
treatments aimed at reuse**

Milena Morone

A.A. 2013/14

Tutor: Prof. Ing. Renato Baciocchi

Co-Tutor: Ing. Giulia Costa

Coordinatore: Prof. Ing. Renato Gavasci

Acknowledgements

I wish to express my gratitude to my tutor, Prof. Renato Baciocchi, for giving me the opportunity to study this scientific research topic and for allowing me to grow in the research field. Thanks for the valuable and useful discussions that we have had during this work. Thanks to my co-tutor, Giulia Costa, for the insightful advices and suggestions about this research.

Six month of this research has been carried out within the Department of Civil Engineering of the Katholieke University in Leuven. I would like to acknowledge Özlem Cizer for giving me the opportunity to pursue part of my research there. I am thankful for her introducing me to the field of alkali activation, that until then, was alien to me, and for the valuable support and interesting discussion that we had on this topic.

I would like to thank the PhD girls, for their genuine friendship and for making our office a peaceful place to work. Thanks to all of my friends that have always supported and incited me to strive towards my goal.

Finally, my gratitude goes to my family, to my parents and my brother Giuseppe, for helping, trusting and supporting me in any time, not only during this work, but throughout my life. I truly thank Giovanni, for his patience, love and happiness.

Abstract

The management of the great amount of solid residues and gaseous emissions resulting from thermal and industrial processes is one of the major critical issues to be dealt with by the different sectors involved. The physical, chemical and environmental properties of the solid streams are, in some cases, not suitable for their reuse and a relevant fraction is directly landfilled or limitedly reused for low-end applications. Hence, suitable treatments are needed to exploit and to valorize the potential of these by-products in order to reduce their landfilling and produce valuable products able to replace virgin raw materials.

The main objective of this doctoral thesis was to investigate new process routes for the valorization of two types of industrial residues, i.e. Basic Oxygen Furnace (BOF) steel slag and coal gasification ash.

The first and most relevant part of this work was addressed to slags generated from steel production, which generates high emissions of CO₂, making it one of the main industrial sources of greenhouse gases (GHG). In particular, the BOF steel slags were treated with a granulation and granulation/carbonation process, with the aim of producing secondary aggregates suitable for reuse in civil engineering applications and of storing CO₂ in a solid and thermodynamically stable form, thus at least partially contributing to the reduction of GHG emissions from steelmaking plants. The results of the tests, carried out in a rotary drum granulator and by mixing the slag with water, indicated that the particle size of the slag increased progressively with reaction time and significant CO₂ uptake values (between 120 and 150 g CO₂/kg) were measured even after short reaction times (30 or 60 minutes). The leaching behavior of the obtained granules showed to comply with the limits for reuse set by the Italian legislation. However, the mechanical performance of the granules, evaluated by applying the Aggregate Crushing Value (ACV) test, resulted far from that achieved by natural gravel. The mechanical properties of the artificial aggregates were improved by applying both treatments to slag-cement mixtures, by replacing 10% and 20% by wt. of slag with cement. In this case, the mechanical performance was improved regardless the amount of cement employed, reaching ACV similar to those reported in the British Standard for igneous rock, i.e.

16%. Nevertheless, as the production of cement is related to high environmental impacts, an alternative and more sustainable option was evaluated with the aim to increase the mechanical performance of the granules. Indeed, in order to accelerate the original latent hydraulic properties of the slag, the alkali activation process was exploited by using two different alkali solutions, i.e. a mixture of sodium hydroxide/sodium silicate and sodium hydroxide/sodium carbonate. It was found that the BOF slag mortars activated with the sodium hydroxide/sodium silicate solution and cured under a continuous flux of CO₂ at 50 °C, showed the highest mechanical strength. So, this alkaline solution was used as binder in the granulation-carbonation treatment, with the aim of enhancing the mechanical properties of the obtained aggregates. The results of the tests showed that the maximum mean diameter achieved for the activated granules was 13 mm, with maximum CO₂ uptake of the activated granules resulted equal to 40 gCO₂/kg steel slag. As for the environmental behavior of the treated material, only the release of Cr and V of the activated granules exceeded the Italian limit for reuse. More important, the use of alkalis showed to exert a relevant influence on the strength of the granules, that after both the granulation and granulation-carbonation treatments showed an ACV comparable or even lower than that of natural gravel (20 %).

The second part of this work was addressed at the characterization and valorization of the ashes produced by the Zecomix (Zero Emission COal MIXed technology) platform, collected both directly from the solid bed (bed ash) and from the cyclone installed downstream the coal gasifier (fly ash). Both ashes were composed mainly by Mg, Si and Fe, typical of the olivine that made up the bed of the gasifier, whereas the total organic carbon was 5% in the bed ash and 27% in the the fly ash. Both gasification residues underwent a particle size and density separation procedure, allowing to obtain an organic and an inorganic fraction, which could then be separately reused.

Sommario

La gestione dei rifiuti solidi e gassosi derivanti da processi termici è una delle principali criticità da affrontare per i diversi settori industriali coinvolti. Le proprietà fisiche, chimiche e ambientali di tali residui non li rendono spesso adatti per il riutilizzo, generalmente provocandone lo smaltimento in discarica o eventualmente l'impiego in applicazioni di scarso valore. Ne risulta la necessità di sviluppare trattamenti idonei a valorizzare il potenziale di questi sottoprodotti, al fine di ridurre lo smaltimento in discarica e produrre prodotti finali in grado di sostituire materie prime vergini.

L'obiettivo principale di questa tesi di dottorato è stato pertanto quello di indagare nuovi trattamenti per la valorizzazione di residui industriali prodotti da diversi processi termici. La prima e più rilevante parte di questo lavoro ha riguardato lo studio di scorie provenienti da impianti per la produzione dell'acciaio. In particolare, le scorie BOF sono state trattate con un processo di granulazione e di granulazione/carbonatazione, con l'obiettivo di produrre aggregati secondari idonei al riutilizzo in applicazioni di ingegneria civile e di stoccare CO₂ in forma solida e termodinamicamente stabile, contribuendo in questo modo, seppur parzialmente, alla riduzione delle emissioni di CO₂ dell'acciaieria. I risultati dei test, condotti su scala di laboratorio in un reattore a tamburo rotante dotato di un coperchio e di un sistema per l'alimentazione della CO₂ e miscelando le scorie con acqua, hanno mostrato che la dimensione delle particelle aumenta progressivamente con il tempo di reazione e valori significativi di CO₂ uptake (tra 120 e 150 g CO₂/kg) sono stati misurati anche dopo tempi di reazione brevi (30 minuti). Il comportamento alla lisciviazione dei granuli ottenuti rispetta i limiti previsti per il riutilizzo fissato dalla normativa italiana. Tuttavia, le prestazioni meccaniche dei granuli non sono risultate adatte per permetterne il riutilizzo in applicazioni dell'ingegneria civile. Quindi, con l'obiettivo di migliorare le proprietà meccaniche degli aggregati, i trattamenti di granulazione e granulazione-carbonatazione sono stati applicati ad una miscela scorie-cemento, sostituendo il 10% e 20% in peso di scorie con cemento. In questo caso, si è osservato che le prestazioni meccaniche migliorano, indipendentemente alla quantità di cemento nella miscela, raggiungendo valori di ACV

simili a quelli riportati nel British Standard per rocce ignee, ossia 16%. Inoltre, è risultato che la carbonatazione non influenza le proprietà meccaniche dei granuli ottenuti, per tutte le miscele testate. Ciononostante, al di là del cemento cui sono associati alti impatti ambientali, sono state valutate altre opzioni alternative e più sostenibili in grado di migliorare le performances dei granuli prodotti. Al fine di accelerare le originali latenti proprietà idrauliche delle scorie BOF, è stato sfruttato il processo di attivazione alcalina utilizzando due diverse soluzioni alcaline (una miscela di idrossido di sodio/silicato di sodio e idrossido di sodio/carbonato di sodio). Si è osservato che la resistenza meccanica è risultata maggiore per i campioni di scorie miscelati con la soluzione di idrossido e silicato di sodio. Quindi, sulla base di questi risultati, tale soluzione alcalina è stata utilizzata per studiare l'effetto del processo in combinazione con il trattamento di granulazione-carbonatazione, con l'obiettivo di migliorare le proprietà meccaniche degli aggregati. I risultati dei test hanno mostrato che il diametro medio massimo raggiunto dai granuli era pari a 13 mm e che il valore massimo di stoccaggio della CO₂ dei granuli contenuti l'attivatore alcalino è risultato pari a 40 gCO₂/kg di scoria. Quanto al comportamento ambientale del materiale trattato, sono state osservate differenze tra le prove di lisciviazione effettuate con granuli attivati frantumati e non frantumati, ma in entrambi i casi le concentrazioni di Cr e V sono risultate superiori al limite imposto per il riutilizzo dalla normativa italiana. Inoltre, l'utilizzo dell'attivatore influenza la resistenza dei granuli che dopo entrambi i trattamenti, hanno fornito valori di ACV confrontabili o inferiori di quelli ottenuti per la ghiaia naturale (20%). La seconda parte del lavoro ha riguardato la caratterizzazione e l'applicazione di processi per la valorizzazione di ceneri prodotte dalla piattaforma Zecomix, i cui residui solidi sono stati raccolti dal letto solido del gassificatore e dal ciclone posto a valle dello stesso. Si è osservato che le ceneri sono costituite principalmente da Mg, Si e Fe, tipici elementi dell'olivina utilizzata nel letto fluido. Il contenuto di carbonio organico totale è risultato maggiore nel campione di ceneri dal ciclone (27% in peso) rispetto a quello ottenuto nel campione di ceneri pesanti (5% in peso). Dopo la caratterizzazione, i campioni sono stati sottoposti ad una procedura di separazione per vagliatura e per densità, con l'obiettivo di valutare le più idonee applicazioni per ciascun residuo ottenuto.

Table of contents

Acknowledgements	i
Abstract	iii
Sommario	v
Table of contents	vii
Introduction and aims of the thesis.....	1

SECTION I

TREATMENTS AIMED AT THE VALORIZATION OF BOF STEEL SLAG 5

Chapter 1

Background	7
1.1. Properties of steel slag and main reuse options	7
1.2. Treatments aimed at reuse	11
1.2.1. Accelerated carbonation	12
1.2.2. Granulation	17
1.2.3. Combination of the granulation-carbonation treatment for the valorization of residues	22
1.2.4. Alkali activation	24

Chapter 2

Application of the carbonation-granulation treatment on BOF steel slag.....	33
2.1. Introduction.....	33
2.2. Tests performed with BOF steel slag.....	34

Table of contents

2.2.1.	Materials and methods.....	34
2.2.2.	Results and discussion.....	37
2.3.	Further investigation: evaluation of the effects of cement used as binder for the production of granules	52
2.3.1.	Materials and methods.....	53
2.3.2.	Results and discussion.....	54
2.4.	Main findings.....	64

Chapter 3

Effect of coupling alkali activation and CO₂ curing on BOF steel slag..... 67

3.1.	Introduction.....	67
3.2.	Materials and methods	70
3.2.1.	Materials and alkaline solution composition.....	70
3.2.2.	Methods	72
3.3.	Results and discussion	77
3.3.1.	Characterization of the untreated materials	77
3.3.2.	Screening test: evaluation of the short-term reactions by heat of hydration	79
3.3.3.	Long-term reactions: effect of the process on the mineralogy of the BOF slag	91
3.3.4.	Extent of CO ₂ uptake.....	106
3.3.5.	Mechanical strength of the slag mortars.....	110
3.4.	Main findings.....	112

Chapter 4

Investigation of the effects of alkalis on the granules produced by carbonation-granulation treatment

115

4.1.	Introduction.....	115
------	-------------------	-----

4.2.	Material and methods.....	116
4.2.1.	Materials	116
4.2.2.	Applied treatments.....	118
4.3.	Results and discussion	120
4.3.1.	Effect of the treatment on the particle size distribution of the obtained granules	120
4.3.2.	CO ₂ uptake kinetics	123
4.3.3.	Effect of the treatment on the leaching behavior of the material	126
4.3.4.	Effect of the treatment on the mechanical properties of the material.....	133
4.4.	Main findings	135

SECTION II

TREATMENTS AIMED AT THE VALORIZATION OF COAL GASIFICATION ASH	137
--	------------

Chapter 5

Background	139
5.1. Description of the Zecomix platform.....	139
5.2. Overview of the main characteristics and reuse options of coal gasification ash	142

Chapter 6

Characterization and density separation procedure of coal gasification residues generated from the Zecomix platform.....	145
6.1. Introduction.....	145
6.2. Materials and methods	148
6.2.1. Materials and methods of characterization	148

Table of contents

6.2.2.	Particle size and density separation procedures of the gasification residues	149
6.3.	Results and discussion	150
6.3.1.	Results of the characterization.....	150
6.3.2.	Results of the tested treatments on the gasification residues	157
6.4.	Main findings	168
	Conclusions and final remarks	171
	References.....	175
	Publications	193

Introduction and aims of the thesis

The proper management of industrial waste and the reduction of greenhouse gas (GHG) emissions represent two of the main environmental concerns for the industrialized world. This is particularly relevant for intensive industrial processes, based on the thermal treatment of raw materials, such as those required for cement or steel production. These are typically characterized by the generation of large amounts of solid waste residues (e.g. slag, dust, combustion or gasification ash) whose reuse is not always feasible, due to the variability of the material characteristics, the lack of a suitable national legislation on the proper management of these industrial by-products, the scarce presence of low-cost technologies to produce valuable secondary products and the poor attention paid by the market to the application of products derived from industrial waste. As a result, although there is a growing awareness about the environmental problems related to the final disposal of such residues, still a relevant fraction of them is without a well-established management pathway and has to be landfilled. Volume stability, particle size distribution or the leaching of regulated elements are only a few of the technical and environmental issues to be addressed. In this sense, several efforts are being made in view of employing alternative binders in civil engineering applications, such as partial or total replacement of cement or of the natural raw materials employed in concrete manufacturing (Taylor et al., 2010), but still a lot needs to be done in this direction. Concerns about global climate change are also growing and, according to the third IPCC report, there is a strong evidence that most of the warming observed over the past 50 years is attributable to human activities, with carbon dioxide providing the largest contribution. At present, thermal processes have a vast impact on the contribution of anthropogenic CO₂ emissions and the energy use in the industrial sector accounts for one third of the total CO₂ emissions. Specifically, the iron and steel industry emitted 2.3 GtCO₂ worldwide in 2007, while the cement industry almost 2 GtCO₂, accounting for nearly 10% and 5% of the global CO₂ emissions, respectively. These values are also expected to grow, given that the worldwide crude steel and cement production show to continue to increase (Kuramochi et al., 2012).

Hence, beyond the ongoing efforts of the industries to reduce the CO₂ emissions on-site in the plant, the development of long-term carbon storage is a necessary step.

Coming to the specific issues discussed here, the first and most relevant part of this Ph.D. work was addressed to the investigation of new process routes for the valorization of a specific type of alkaline slag produced during steel manufacturing, Basic Oxygen Furnace (BOF) Slag. Furthermore, the possibility of tackling, at least partially, the CO₂ emission reduction issue, as these by-products are typically associated to CO₂ source points was also addressed. Such a process should therefore allow to obtain a material of suitable particle size, environmental (i.e. leaching) behavior and mechanical properties in order to reuse it in civil engineering applications, while in the meantime possibly aiming at contributing, at least partially, to the reduction of CO₂ emissions from the steel manufacturing plant. Looking at the relevant literature, accelerated carbonation has been so far investigated as one of the options for achieving the permanent storage of CO₂ by binding it into solid carbonate minerals. For this process, beyond the use of minerals, alkaline waste residues derived from thermal treatments have been employed as a suitable source of alkalinity, while also promoting the chemical and leaching stability of the treated waste. Nevertheless, although this treatment affects some of the properties of the slag (e.g. mineralogy and leaching of major and trace compounds), it does not exert a relevant influence on its particle size distribution, which, as already said before, is an important issue in view of the reuse of the residues as aggregates in civil works. The particles' agglomeration process can be achieved through a granulation treatment, typically performed in a rotating drum with a liquid binder. Nevertheless, the production of well-sized granules does not necessarily assure the achievement of an adequate strength of the materials, able to meet the mechanical requirements for reuse in civil engineering applications as bound (i.e. with binding agents such as cement for concrete production) or unbound aggregates (i.e. used as received, for example as filling material in road sub-base layers). Hence, other treatments may be required for enhancing the mechanical performances of the yielded granules. Namely, alkali activation has shown to be a treatment able to improve the hardening reactions of amorphous residues rich in calcium and silicon, e.g. blast furnace slag derived from the iron production. Alkali activation is a chemical process in which the raw material,

usually amorphous, is mixed with specific alkaline solutions (e.g. sodium or potassium alkalis, carbonates or silicates) in order to favor the dissolution of the reacting species and to enhance the hydration reactions leading to the formation of binding phases, such as a calcium silicate gel, that yields a compact and strong product. The sustainability of this process has been widely investigated, and most of the workers agree that the carbon dioxide emissions associated to the production of the alkali solution, mainly those related to sodium silicate, are quite high. However, the production of alkali activated binders, based on a solid waste, used instead of cement, can be associated to a level of carbon dioxide emissions lower than those emitted for the production of cement itself (Duxson et al., 2007; Mc Lellan et al, 2011; Habert et al., 2011). The current research study was hence firstly addressed to investigate the applicability of a combined granulation and carbonation treatment as a valorisation technique for the BOF slag, with the aim of producing artificial aggregates suitable for civil engineering applications. Through properly designed lab-scale tests, it was possible to assess the effect of CO₂ concentration (ambient and 100%), of the type of binder (water or a solution of cement or of a proper alkali activator) and of other operating conditions on the particle size distribution, environmental behaviour and mechanical properties of the obtained granules.

The second part of this Ph.D. work was addressed to the valorisation of the ashes produced by the Zecomix (Zero Emission COal MIXed technology) platform, an integrated pilot scale plant where coal is gasified and the yielded synthetic gas is decarbonised in order to be used as a H₂ rich fuel in a gas turbine. During the gasification experiments performed in the Zecomix unit, the bed ash is typically left in the reactor for more than one cycle to increase carbon conversion, decrease the use of fresh olivine and also because the thermally treated olivine showed an enhanced performance in terms of tar catalytic cracking. However, after the ash content of the bed increases above 5-10%, the reactor is emptied and the bed is re-composed with fresh olivine. Hence, specific management options for the discharged bed ashes are required, as well as for the fly ashes produced from the cyclone downstream the gasification unit. This part of the research was aimed to identify valorization strategies for the solid residues generated by the Zecomix gasification unit that may allow to both minimize or

avoid landfill disposal while recovering energy and material that may be possibly reused within one of the processes making up the Zecomix platform. Therefore, the characterisation of these residues was carried out and then, the assessment of an experimental protocol was developed, consisting of a particle size and density separation treatment, with the aim of separating the organic and inorganic fractions of the residues in order to identify the most suitable valorisation-routes for both of them.

The two main themes addressed by the present study are presented in the thesis in the following two sections:

- Section I, that discusses the treatments aimed at the valorisation of the BOF steel slag.
- Section II, that deals with the characterization of the coal gasification ash from the Zecomix plant and the treatments aimed at its valorization.

In particular, Section I is structured in four main chapters: Chapter 1 reports a general overview of the main characteristics of the BOF steel slag, focusing on the issues related to the reuse of this type of residue. Afterwards, a short review of the processes investigated in this thesis and aimed at the reuse and valorization of these materials is provided, which includes accelerated carbonation, granulation and alkali activation. In Chapter 2, the study of the granulation-carbonation treatment applied to the BOF steel slag is presented and the main results are reported. Chapter 3 shows the main results obtained from the application of the alkali activation process on the BOF steel slag, while Chapter 4 presents the findings achieved by combining the alkali activation process with the granulation-carbonation one. Following the order of the chapters adopted in the first section, Section II is divided in two main chapters: Chapter 5, in which a general overview of the Zecomix pilot-scale plant is given and the main characteristics and reuse options for coal gasification ash are discussed; Chapter 6, where the main results of the characterization of the ashes derived from the gasifier and the cyclone of Zecomix platform are reported, along with the results achieved from the particle size and density separation treatments applied on these residues. Finally, in the Conclusions and final remarks section, the most relevant results of this work are summarized and a perspective for further investigation of the proposed treatments is provided.

SECTION I

TREATMENTS AIMED AT THE VALORIZATION OF BOF STEEL SLAG

Chapter 1

Background

1.1. Properties of steel slag and main reuse options

The iron and steel industry is the largest energy-consuming manufacturing sector in the world, accounting for 10-15% of total industrial energy requirements (IEA GHG, 2002). Today, the production of steel is carried out in two main types of converter, i.e. the Basic Oxygen Furnace (BOF) and the Electric Arc Furnace (EAF), that are fed by pig iron and iron scraps, respectively. Namely, the BOF unit is commonly located in an integrated steel production plant downstream of the blast furnace (BF) that produces the molten (or pig) iron, and upstream of the ladle furnace unit in which further refinement of the molten steel is carried out through desulfurization, desiliconisation and dephosphorization processes (Yildirim and Prezzi, 2009). Fluxing agents, such as lime or dolomite, are usually added into the the different units in order to remove undesired elements, such as sulphur and phosphorus, from the hot metal. These compounds are retained by a fluid layer of slag, consisting of a chemical combination of SiO_2 , obtained from the oxidation of the Si present in the hot metal, and the charged fluxes. At the end of the process, the slag is removed from the furnace trough densimetric separation (Mahieux et al., 2009).

Among the different technologies adopted for the production of steel, it is estimated that the integrated steel making process (BF/BOF) accounted for above 70% of the world's total output of crude steel in 2013 (1600 million tons). This figure is only slightly lower

for Europe, as it proved to be 60% of the global steel production (166 million tons), confirming the widespread consolidation of the oxygen blow technique (World steel Association, 2014). However, besides this, steelmaking industries produce significant amounts of alkaline solid residues, ranging between 10 and 15% by weight of the total yielded steel, depending on the characteristics of the manufacturing process (Proctor et al., 2000). Making reference to EU data, the BF slag produced in 2012 were almost 23 million tons, while around 21 million tons of steel slags were generated in 2012, 46% of which made up by Basic Oxygen Furnace (BOF) slag, followed by Electric Arc Furnace (EAF) slag (38%) and secondary steel slag (17%) (Euroslag, 2012). Apart from blast furnace slag, that finds valuable applications as a cement substitute (Babu and Kumar, 2000; Oner and Akyuz, 2007; Shariq et al, 2008) or as coarse aggregate in substitution of natural raw materials in concrete manufacturing (Etxeberria et al., 2010), most steel slags are still landfilled, or reused for low-end applications. However, as reported in Figure 1.1, although the main reuse options for steel slag are in road construction (43%), as base or sub-base layer, or as aggregates in cement production (5%), more than 10% of these residues are still disposed of in landfills.

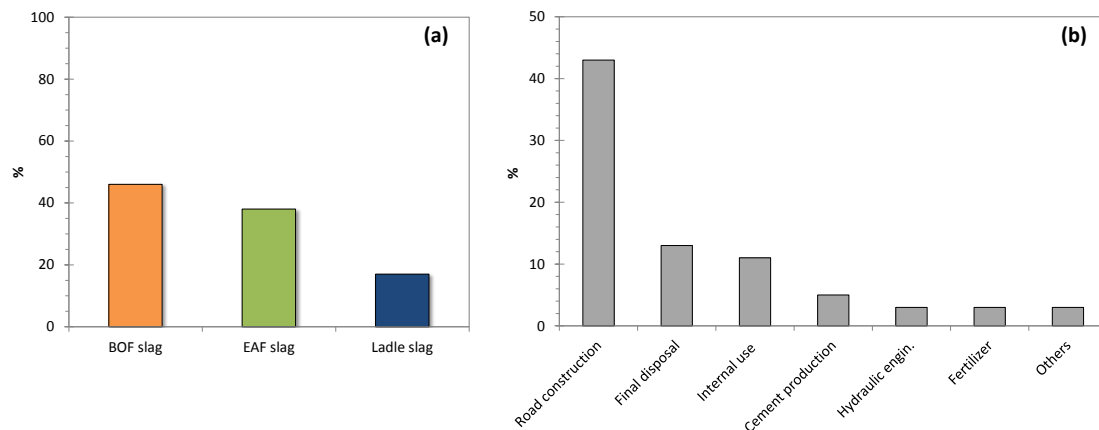


Figure 1.1 (a) Production and (b) reuse options of steel slag in Europe in 2012 (adapted from Euroslag, Statistics 2012)

This figure is even higher for BOF slag, as roughly 25% of these residues are typically landfilled after undergoing a metal recovery step (Bohmer et al., 2008), or at best reused

for low end applications. In order to improve the current management practices for BOF slag, different experimental studies have focused on the possibility of using these materials in place of natural aggregates in civil engineering applications. In particular, the main options tested for steel slag reuse include: production of hydraulic binders (e.g. Reddy et al., 2006; Mahieux et al. 2009) use as aggregates in asphalt mixtures (Xue et al., 2006; Shen et al., 2009) or as landfill liner materials (Herrmann et al., 2010).

Table 1. 1 shows the chemical composition (in terms of oxide content) of BOF slag reported by different studies. It can be notes that CaO is the main constituent, with contents ranging from 37 to 52%, followed by Fe₂O₃, with quite variable concentrations depending on the study considered, SiO₂ (8-18%) and MgO (0.8-14.1%). Ca and Mg components are mostly in the form of silicates, however for this type of slag, significant contents of free calcium and magnesium oxides have been reported. This is an important aspect to take into account for the reuse of BOF slag in bound (e.g. aggregates used in concrete production with binding agents, such as cement) or unbound applications (e.g. aggregates used as received, as filling material in road base layers) (Motz and Geisler, 2001). In fact short-term hydration and long-term carbonation reactions of free lime or periclase can lead to the swelling of the slag over time, leading to a poor volumetric stability and hence to a low technical performance of the material. As a rule of thumb, the maximum free lime content should preferably not exceed 4% (Wang et al., 2010), although some authors suggested a higher limit, equal to 7%, for unbound applications (Geiseler, 1996). Deneele et al. (2005) found that the expansions of BOF slag, evaluated from the packing density measured after mechanical compaction of a given mass of material, is highly dependent on its particle size. Indeed, the swelling resulted higher for slag having a particle size below 2 mm. Manso et al. (2006), with the aim of evaluating the durability of concrete with EAF steel slag as aggregate, exposed the material for 90 days to moist atmospheric conditions, so to provoke the hydration of free lime and periclase in the slag, in order to stabilize it and prevent further expansion phenomena. Elsewhere (Yildirim and Prezzi, 2009) it is reported that if the steel slag does not meet the required limit regarding expansion, set at 0.5% by the Pennsylvania Test Method Specification, the material should be aged for six months or longer until swelling complies with the standard limit.

Table 1. 1 Chemical composition of BOF slag reported in different literature studies, expressed as oxides content %.

References	Oxide amount (% by wt.)				
	CaO	SiO ₂	Al ₂ O ₃	MgO	Fe ₂ O ₃
Altun et al. (2002)	37.02	18.01	2.61	14.1	14.1
Chaurand et al. (2007)	41.3	12.5	2.4	4.3	31.2
Das et al. (2007)	47.88	12.16	1.22	0.82	n.r.
Mahieux et al. (2009)	47.5	11.8	2	6.3	22.6
Nicolae et al. (2007)	40.1	17.8	2.04	6.32	6.58
Poh et al. (2006)	41.44	15.26	4.35	8.06	9.24
Reddy et al. (2006)	52.3	15.3	1.3	1.1	n.r.
Shen et al. (2009)	39.3	7.75	0.98	8.56	38.06
Tossavainen et al. (2004)	45	11.1	1.9	9.6	10.9

n.r.: not reported

However, weathering of the slag under atmospheric conditions outside the steel plant to allow the transformation of free lime to calcium hydroxide takes time and requires a suitable storage site. Moreover, this process produces a material with a fine particle size distribution, caused by disintegration of slag upon volume increase ($\text{CaO} \rightarrow \text{Ca(OH)}_2$) (Motz and Geisler, 2001). This may represent another important limiting factor for the reuse of BOF slag, as slag fractions presenting a diameter below 4.75 mm have been indicated as unsuitable for replacing natural fine aggregates due to poor mechanical characteristics (Xue et al., 2006). The grain size distribution of BOF slag reported in the literature is quite variable. This is mainly related to the different treatments that may be applied in the steel plant on the slag, i.e. metal recovery process, to separate the metallic part ($d > 250$ mm), and crushing, for either metal recovery or to achieve an appropriate size distribution (Yildirim and Prezzi, 2009). Nevertheless, applying these treatments on the slag outside the steel production plant implies the production of residues with a quite fine average particle size, which may hence result inadequate for technical applications (Shen et al., 2003).

The reuse of BOF slag in civil engineering applications may be also constrained by the need of complying with environmental acceptance criteria set by national legislations, generally based on the results of leaching tests. Due to the alkaline nature of BOF slags, leachate pH may exhibit values even above 12 (Geiseler, 1996), thus exceeding, for instance, the national Italian criteria for the reuse of waste (Ministerial Decree 2006/186), that requires the pH to fall within the 5.5-12 range. As far as the leaching of trace contaminants is concerned, Cr and V may represent an issue, as their content in steel slags is typically higher than in natural road construction materials (Proctor et al., 2000). Nevertheless, it has been generally reported that leaching of these metals from BOF slags is quite limited. This seems to be particularly the case for Cr that is present in BOF slag as Cr(III), which is less mobile than the oxidized form [Cr(VI)] (Chaurand et al., 2006; de Windt et al., 2011).

1.2. Treatments aimed at reuse

As previously reported, the reuse of BOF slag may be hindered owing to both technical and environmental aspects, such as the volumetric expansion associated to free calcium and magnesium oxide content and particle size distribution, which in case of grinding for metal recovery may not be suitable for the reuse of this type of residue as aggregates in the civil work. On the other hand, the leaching of trace elements (e.g. Cr and V) and the pH may exceed the compliance criteria for reuse or environmental reclamation. Currently, the main management options applied in Italy for BOF steel slag are landfill disposal or quarry backfilling. Therefore, to reuse these materials in high-grade applications, specific treatments are needed. In the present thesis, the application of a combined carbonation and granulation treatment, along with alkali activation was investigated, in order to produce aggregates suitable for the reuse in civil engineering applications, while also storing part of the associated emissions of CO₂. In this regard, it was reported that accelerated carbonation may exert a positive effect on the leaching behaviour and the mechanical properties of alkaline materials, allowing also to store

CO₂; granulation may exert a relevant influence on the particle size distribution of the slag, and alkali activation may allow to enhance the hydraulic properties of the BOF slag and improve its mechanical strength.

This section discusses the individual processes that were selected for treating the BOF steel slag; in particular for each type of treatment, the main mechanisms and factors, along with their applications to different types of residues, are presented.

1.2.1. Accelerated carbonation

Carbonation is the process that refers to the chemical reaction occurring between CO₂ and an alkaline solid, containing calcium and magnesium oxides and silicates, that leads to the formation of the corresponding inorganic carbonates phases. Natural carbonation of calcium and magnesium bearing minerals is a slow process, occurring in geological timeframes (Lackner et al, 1995). However, it is possible to accelerate these reactions by exposing the material to a concentrated flux of CO₂ and modifying specific operating conditions, such as temperature and CO₂ partial pressure or the liquid to solid ratio. The main routes for accelerated carbonation are classified as *indirect*, where the alkaline metals are first extracted from the mineral matrix and then precipitated as carbonate, and *direct*, where carbonation occurs in a single process step. In the indirect route, the dissolution of the metal is usually achieved by adding an acid, e.g. HCl or acid acetic (Park et al., 2003), other solvents, such as molten salts (Huijgens and Comans, 2005) or by using CO₂ at high pressure (Hänchen et al., 2006). However, besides the fast reaction rate of carbonation and the formation of pure carbonates, this type of process usually presents a high energy requirement or the use of chemicals, whose recycling may represent a critical issue to deal with. The direct route is usually classified in two main types: gas-solid (dry) and aqueous (wet) carbonation. In the former process, the formation of carbonates occurs directly contacting gaseous CO₂ with mineral or residue containing Ca or Mg oxide phases at various temperature and pressure ranges (Lackner et al., 1995). However, the slow kinetics of the process especially for silicate phases, the significant energy input required and also thermodynamic limitations have led to

conclude that this route has little potential of becoming an industrially viable process and, apart from a few exceptions (Zevenhoven et al., 2008), its investigation has been basically abandoned. Wet carbonation processes may be performed either in a slurry phase (gaseous phase supplied to an aqueous suspension of the material) at liquid to solid (l/s) ratios of 5-50 l/kg (Huijgen et al., 2005; Baciocchi et al., 2015), or via the wet or thin-film phase (humidified material directly contacted with the gaseous phase) at l/s ratios <1.5 l/kg (Johnson et al., 2003). Carbonation in slurry conditions, usually performed on materials containing silicates in order to enhance their dissolution, requires a significant amount of water (l/s ratios of 2-10 l/kg) to allow the reaction to occur, whose final treatment/disposal is also an issue. The wet-route has been applied to different types of residues including those containing a high amount of soluble contaminants so to avoid the production of a liquid effluent that would require treatment; in addition this process was found to be effective also under mild operating conditions in enhancing the dissolution kinetics of the reactive phases (Baciocchi et al., 2010a). In this Ph.D. work, the wet-carbonation route was used to treat the BOF steel slag in combination with the granulation process, that also requires a l/s ratio lower than 1 l/kg to be effective. Therefore, the following sections report the wet carbonation route mechanism, along with the factors and the main applications carried out to treat the residues.

1.2.1.1. Mechanism of the process (wet-route)

The wet-route carbonation reaction occurs through the diffusion of carbon dioxide into the thin aqueous layer where the oxide phases of the solid dissolve leading to the formation of a carbonate layer surrounding the non-carbonated one, constituting the inner core of the grains (Fernández-Bertos et al., 2004). The carbonation process involves different steps, which include: the diffusion and dissolution of CO₂ and the dissolution of the Ca-containing species present in the solid, schematically reported below (Fernández-Bertos et al., 2004 quoting Maries, 1985):

- Diffusion of CO₂ in air and permeation through the solid
- Solvation of CO_{2(g)} to CO_{2(aq)}, hydration of CO_{2(aq)} to carbonic acid (eq. 1.1) and instantaneous ionisation of H₂CO₃ to H⁺, bicarbonate ions (eq. 1.2) and carbonate ions (eq. 1.3). The hydration of CO₂ is considered the rate-determining step in all the process and these reactions are accompanied by changes in the ionic equilibrium of the pore solution, hence by a decrease of the pH.



- The dissolution and release of the Ca²⁺ ions from the calcium-containing species present in the solid (Eq. 1.4) and precipitation of CaCO₃ with production of H₂O and heat (Eq. 1.5), reported below:



The carbonation process may also involve calcium silicate phases, like C₂S or C₃S, through a preliminary hydration step followed by carbonation of the hydrated products, i.e. calcium silicate hydrate (C-S-H) and Ca(OH)₂ (Papadakis et al., 1989). The latter one reacts following Eq. 1.4 and 1.5, whereas C-S-H may undergo decalcification reactions leading to CaCO₃ and silica gel (S-H). Young et al. (1974) stated also that, in the first minutes, the reaction of C₃S with carbonic acid, obtained from carbon dioxide dissolution, allowed to accelerate the hydration of the silicates to form the carbonation products.

1.2.1.2. Factors affecting the process

The effectiveness of the carbonation process is correlated to the reactivity of the material and to the diffusivity of CO₂ into the solid matrix. The former depends on the chemical composition of the solid and on the degree of hydration. On the other hand, the diffusivity of CO₂ is controlled by the grain size of the material, which in turn affects the pore system, and by exposure conditions (Fernández Bertos et al., 2004).

Carbonation is effective if the treated material is rich in Ca; besides, the higher the concentration of this element in the system, the higher is the extent of carbonation. At the same time, high Ca/Si ratios also typically lead to a higher degree of carbonation and phases such as ferrite may also allow to produce calcium carbonate by their decomposition in the presence of CO₂ (Lange et al., 1996). The presence of water is crucial to ensure that carbonation takes place, since it takes part in the solvation and hydration of CO₂. Actually, too much water limits the rate of reaction, since the pores are filled and hence the diffusion of CO₂ is hindered. Conversely, a low content of water, which may be also ascribed to the exothermic carbonation reactions that cause the evaporation of water and so premature drying of the material, does not ensure the completion of the reaction (Lange et al., 1996; Young et al., 1974). Hence, depending on the properties of the material an optimum water to solid ratio needs to be found for achieving the maximum CO₂ uptake.

Different physical properties of the material, such as micro-porosity and permeability, affect the diffusion of CO₂. Low porosity reduces the diffusion of CO₂ in the material and hence results in a lower amount of precipitated calcium carbonate. Fine particles with a high water content show a higher degree of carbonation because of the higher surface exposed to react with CO₂. Moreover, Johnson et al., (2003) found that the finer particles (<0.125 mm) of a calcium-magnesium silicate rich material showed the higher amount of CaO and hence, were more reactive towards CO₂.

The kinetics and extent of carbonation depend also on the operating conditions, such as the total and partial CO₂ pressure, temperature and relative humidity. A higher amount of CO₂ in the gas phase, as well as a higher total pressure, should lead to an increase of the rate of carbonation (Fernández-Bertos et al., 2004). Results of batch carbonation

tests, carried out by Baciocchi et al. (2013) on a milled sample of BOF steel slag, at set total pressure and temperature (10 bar and 100 °C) and CO₂ concentrations of 10, 40 and 100%, showed that the maximum CO₂ uptakes (20% at a p_{CO2}=100%) varied as function of the partial pressure, suggesting that the CO₂ solubility exerted a key factor on the process yield. On the other side, at a set CO₂ concentration of 100%, it was found that increasing the total pressure from 1 to 10 bar appeared to slightly affect the kinetics of the carbonation reaction of AOD stainless steel slag (Baciocchi et al., 2009). Other works (Cizer et al., 2012) followed the uptake of CO₂ in a well-compacted lime mortar sample and found that it is independent from the gas phase concentration of CO₂, ranging from 15 to 72%. Another important parameter to be monitored is the relative humidity (RH) of environment; some authors have indicated that the optimum RH value at which carbonation takes place is 50%-70% (Papadakis et al., 1989). It has been observed that RH values above this range may hinder the diffusion of the gas inside the pores filled with water, while the kinetics of carbonation may become lower below it. Regarding the temperature effect, it was found that the carbonation reaction proceeds slowly at ambient temperature and can be accelerated increasing the operating temperature, as a result of the increased dissolution of calcium ions from the particles of the solid. However, this is true up to a certain threshold, set equal to 60 °C by Liu et al. (2001), above which the solubility of CO₂ in water decreases, leading to a decrease of the rate of carbonation.

1.2.1.3. Application of the process for the valorization of alkaline residues

Natural carbonation proceeds too slowly to be considered an effective option for CO₂ storage. Mineral carbonation, that involves the accelerated reaction of CO₂ with natural ores, such as wollastonite (CaSiO₃), olivine (Mg₂SiO₄) and serpentine (Mg₃Si₂O₅(OH)₄), has been widely investigated as a CO₂ storage option (Lackner et al., 1995; Park et al., 2003; Prigiobbe et al., 2009). Recently, accelerated carbonation has also been applied to alkaline solid residues. The waste materials that show to be reactive towards CO₂ derive mainly from industrial thermal processes and include cement

wastes (Huntzinger et al., 2009), steel slag (Huijgen et al., 2005; Bonenfant et al., 2008; Baciocchi et al., 2010a) and incineration ashes (Arickx et al., 2006; Li et al., 2007; Baciocchi et al., 2010b). These residues show a high alkaline pH and a variable but sufficient content of available phases for the reaction with CO₂, because Ca oxides, rather than Mg ones, are the predominant components of these systems (Huijen and Comans, 2005). They are suitable at low costs and are usually associated with the CO₂ source; besides, they are more reactive towards carbonation than natural ores. Moreover, due to their chemical instability, they require a lower degree of pre-treatment and less energy intensive operating conditions, with respect to natural minerals. For instance, different types of steel slag, including BOF residues, treated by accelerated carbonation in a static reactor under wet conditions, i.e. applying a liquid to solid (L/S) ratio lower than 1 l/kg, have shown a significant reactivity with CO₂, even under mild operating conditions (T=20-50 °C; p=1-10 bar), reaching a CO₂ uptake of 20-21% after 24 h carbonation (Baciocchi et al., 2012).

Several studies have indicated that the leaching behavior and mechanical properties of alkaline materials, such as steelmaking slags, may be affected by accelerated carbonation treatment (Johnson et al., 2003; Fernández Bertos et al., 2004; Chen et al., 2007; Baciocchi et al., 2010a). Indeed, carbonation may lead to a relevant pH reduction of these types of residues due to the conversion of alkaline hydroxides to neutral carbonates. This effect causes a change of the mobility of major and trace metals and it results of great importance particularly in the case of the solubility of regulated hazardous elements (van Gerven et al., 2004; Baciocchi et al., 2010a; Santos et al., 2012). Moreover, a higher strength of the residues upon carbonation has been reported and related to the increase of the density of the treated material (Johnson et al., 2003).

1.2.2. Granulation

The granulation treatment represents a particle size enlargement process, which is achieved by contacting a dry powder with a liquid binder (water or a solution of organic additives at different liquid-to-solid ratios depending on both the binder and feed

material properties) in a dynamic device, such as a fluidized bed, a high shear mixer, a disc granulator or a rotating drum (Medici et al., 2000; Marruzzo et al., 2001; Wauters et al., 2002). In a granulation process, the liquid binds the solid particles together and, through the combination of capillary and viscous forces, leads to the formation of more permanent bonds (Iveson et al., 2001a). Moreover, based on the improved characteristics of the final granules, i.e. increased bulk density, reduced dustiness and facilitated granules handling, the granulation treatment have been widely applied in different industries, including agricultural, chemical and food production (Iveson et al., 2001a).

1.2.2.1. Mechanism of the process

The agglomeration process can be divided into three main different mechanisms (see Figure 1.2), that can occur sequentially or simultaneously (Tardos et al., 1997; Iveson et al., 2001a):

- wetting and nucleation, which corresponds to the initial phase of the process, when the powder comes into contact with the liquid binder and the nuclei are formed. The initial distribution of the liquid inside the granulator occurring in this phase highly affects the final granule size distribution of the material (Butensky and Hyman, 1971; Hapgood et al., 2009).
- consolidation and growth, in which agglomeration is caused by the collisions among the nuclei, between the wet nuclei and dry material or among the nuclei and the walls of the reactor. In this phase, the consolidation of the nuclei occurs with the expulsion of the air from the material, while the growth takes place by coalescence, i.e. when two or more well-formed granules collide and form a single agglomerate, or by layering, when the fine material adheres on the surface of the already existing granules (Iveson et al., 2001a). The granule growth behaviour was considered by Iveson and Litster (1998a) as a function of two main parameters, the

liquid content and the impact deformation of the granules, related to the speed of the reactor.

- breakage and attrition, that occurs when wet (breakage phenomenon) or dry (attrition phenomenon) granules break due to the impact among themselves or to the impact of the granules with the walls of the reactor. The extent of breakage increases with time, resulting in the generation of fine particles, and it is controlled by the velocity of impact or by the dimensions of the equipment, i.e. the breakage shows to increase for increasing the diameter of the drum (Litster and Sarwono, 1996; Mishra et al., 2002).

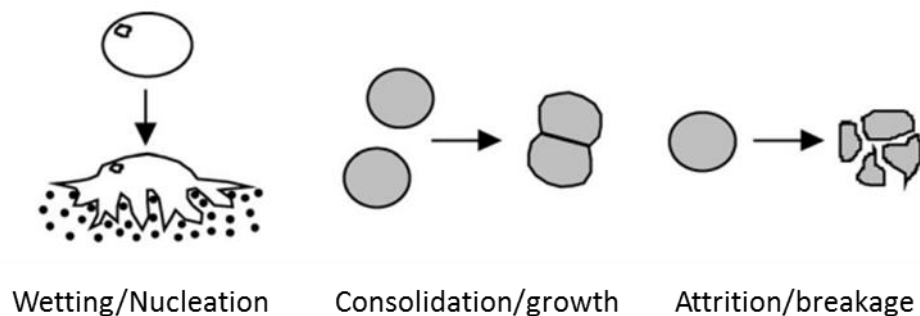


Figure 1.2 Scheme of the agglomeration phases (Litster, 2003)

Actually, the behavior of the material in the granulator may not follow exactly the above-mentioned steps and, when it occurs, this leads to a non-granulating system, referred as e.g. the “nucleation only behavior”, in which the lack of suitable amount of binder does not promote further growth; “crumb behavior”, in which while there is enough binder, the particles are too weak to form permanent granules, and “slurry”, where the amount of binder is too high that the final product is over-wetted (Iveson and Litster, 1998a).

1.2.2.2. Factors affecting the process

The key parameters that affect the granulation process generally depend on the properties of the solid material (initial particle size distribution), on the liquid binder

(amount, viscosity, delivery and distribution) and on the equipment used (speed and geometry) (Adetayo et al., 1993; Tardos et al., 1997). The primary particle size distribution (PSD) directly influences the granule growth behavior, since it affects the granules strength and the consolidation behavior. If the initial PSD is fine, the formed granules are stronger and they do not deform sufficiently to stick together, so tend to grow slowly and reach a smaller maximum size. Conversely, above a critical size that depends on the characteristic of the feed material used in the experiments, the granules are weak and form a crumb system (Iveson et al., 2001a). The growth behavior and strength of the granules are strongly influenced by granules porosity that controls granule deformability and liquid saturation. Indeed, in some systems, the granules may not rapidly grow, settling the so called “nuclei formation only”; in this case, if during the consolidation process the entrapped air and liquid binder are squeezed out from the granules to the layer surface, hence reducing their porosity, it is possible to achieve the desired growth (Iveson and Litster, 1998a). The binder content directly influences the finale size of the product, since increasing the binder amount in the mixture leads to steadily reach the maximum pore saturation, which if exceed a critical point, could shift the granule growth towards a slurry condition. Furthermore, increasing the binder content reduces the time required for granules to become saturated and hence, accelerates the rate of consolidation, by also increasing the final granule size (Iveson et al., 1996). On the other hand, binder dispersion, consolidation and growth of the granules are affected by a different extent from the viscosity of the binder. Indeed, in the former case, increasing the binder viscosity inhibits binder atomisation and dispersion, leading to the formation of an initial large nuclei and to a slow and less uniform binder dispersion in the material (Iveson et al., 2001a). An optimum binder viscosity is required for the growth of granules (Kenningley et al., 1997), above which the effect of binder viscosity on granule deformability becomes dominant and granule growth is inhibited. Binders with low viscosity promote an initial faster growth, and once the liquid is squeezed out to the surface, the granules show a faster final growth. Conversely, if the viscosity is too high, it may prevent the squeezing out of the liquid and thus may hinder the further growth of the material.

Other relevant process variables, such as the equipment characteristics and the operating conditions, exert a strong influence on the agglomeration process. Granulation can be achieved in different types of mixers, ranging from rotating drums and pans to high shear mixers and fluidized bed, each of one exerting a different rate of granules consolidation. Usually, increasing the equipment speed increases the rate of consolidation, and hence the growth. Agglomeration at higher speed, usually experienced in the high shear mixers, increases the granule deformability, reduces the porosity and allows to produce granules with enough strength (Iveson et al., 2001a). In a drum granulator, the speed, rotation and drum fill also play an important role, since speed and fill should be sufficient to induce optimal particle mixing rotation, while the tilt affects the size and strength (Sherritt et al., 2003).

The high number of variables occurring in a granulation process led Iveson and Litster (1998b) to find a qualitatively representation of the particle growth through a growth regime map, using different drum granulation experimental data. The qualitative map correlates the agglomerate growth to the effect of pore saturation and granules deformation, highlighting the thin boundaries that occur for the transition between the different growth regimes. However, the limiting view of a two-dimensions regime map has been pointed out by the same authors, since considering only these two parameters, without taking into account the binder viscosity, is not sufficient for describing the material growth (Iveson et al., 2001b). Hence, the authors stated that the map may be used as a qualitative tool for comparing the behavior of different materials with binders of similar viscosities in the same equipment or as a guide for planning the experiments, since it gives an overview on what needs to be changed for reaching the desired characteristics of the final product.

1.2.2.3. Application of the process for the valorization of the residues

Granulation has been widely studied in the literature with the aim of understanding the basic concepts of the process so to optimize the operating conditions for producing granules with the desired properties (controlled size distribution, specific porosity and

bulk density, suitable structure stability and strength). Moreover, in order to fulfill this aim, the researchers focused on the effect of granulation on primary raw materials, such as glass ballotini (Iveson and Litster, 1998a), chalcopyrite (Wauters et al., 2002), calcium carbonate powder (Keningley et al., 1997), because of their uniform composition and size distribution. Beyond this aspect, different studies (Medici et al., 2000; Baykal and Döven, 2000; Scanferla et al., 2009; Cioffi et al., 2011) have started to focus on the application of disc granulation to waste materials deriving from thermal treatment, such as fly ash and bottom ash from waste incineration, and contaminated soils, with the aim of producing aggregates to be used as filling material or for concrete manufacturing. In this case, binders such as lime or cement (Cioffi et al., 2011), as well as chemical additives, such as super-plasticizers (Scanferla et al., 2009), are typically added in order to improve the mechanical characteristics of the final product. The main aim of these works is the valorisation of these residues by producing a valuable final product, e.g. light weight¹ aggregates (LWA), mainly for avoiding landfill disposal.

1.2.3. Combination of the granulation-carbonation treatment for the valorization of residues

Recently, the combination of accelerated carbonation and granulation was investigated on quarry waste (Gunning et al., 2009), municipal solid waste incineration (MSWI) air pollution control residues (APCr) (Gunning et al., 2013) or contaminated soil and sediments (Melton et al., 2008) for producing artificial aggregates. The aim of these works was to analyze the combined effects of both treatments carried out in the same reactor on granule properties, e.g. particle size and mechanical performance, and on the extent of carbonation.

Gunning et al. (2009) treated the quarry fines, a low quality by-product of the quarrying industry, by mixing them with several types of thermal residues (e.g. biomass ash,

¹ Based on the particle density, the aggregates are classified as “natural weight aggregate”, with a density typically equal to 2600 g/l, while the “light weight aggregate” have a particle density ranging from 800 to 2000 g/l (Cheeseman et al., 2005)

cement kiln dusts, municipal waste incineration bottom ashes and fly ashes, paper and wood ash) at different weight ratios, ranging from 10 to 50%, and using water as liquid binder. A flow of carbon dioxide was fed to the rotary granulator reactor at ambient temperature and pressure, in order to allow the carbonation reactions to take place while the granules are forming. Moreover, a pilot scale facility was developed for producing 100 kg of aggregates/h. The aggregates produced by blending quarry fines with cement kiln dust, paper and wood ash showed a strength comparable to that of commercial lightweight expanded clay aggregate (LECA) and Aardelite. The aggregates produced from the pilot-scale set-up, made by paper ash and quarry fines, showed a CO₂ uptake variable from 5% to 8% and a strength comparable or even higher than that of natural aggregates. The production of lightweight aggregates was then developed on industrial scale by treating APCr with reagents, where needed, and carbon dioxide (Gunning et al., 2013). The yielded aggregates showed to comply with the specifications reported in the End-of-Waste criteria, that set an average individual aggregate compressive strength of 0.1 MPA and a maximum bulk density equal to 1200 g/l. The authors also reported that the annual aggregate production of the facility is equal to 36000 tons/year and that, during manufacturing, the fluctuations of the main aggregate properties (bulk density and mechanical strength) were correlated to the changes in the properties of the feed material, mix formulation and process parameters tested.

Melton et al. (2011) applied the granulation/carbonation treatment as a valorisation technique for treating a contaminated soil and sediments with water and Portland cement in a rotary drum at laboratory-scale. A set of experiments was carried out for the determination of the optimal working range of different key parameters (e.g. water and binder content, time and carbonation method) for the optimization of the process. Aggregate production was carried out according to the optimum mixtures obtained at small scale. They found that most of the aggregates were characterized by a size greater than 4 mm and the extent of carbonation was found to be dependent on the particle size of the granules. This finding, supported by a microstructural analysis of the granules, was then correlated to a non-uniform diffusion of CO₂ into the aggregates, since increasing the diameter of the granules, the amount of carbonates in the core of the aggregates showed to decrease.

As to our knowledge, the granulation/carbonation treatment has not been so far applied as a valorisation route for other industrial residues, such as the steel slag.

1.2.4. Alkali activation

Alkali activation refers to the chemical process in which a material is mixed with specific alkaline solutions in order to favor the dissolution of the reacting species and to enhance the hydration reactions leading to the formation of a compact and strong product (Song et al., 2000; Rashad et al., 2013). This treatment has been widely investigated in order to identify alternative binders to cement for concrete production, for two main reasons: to reduce the amount of cement needed for civil engineering applications, thus partially cutting the carbon dioxide emissions related to it, and replace cement because of several problems of durability related to the disintegration of old cement-based structures (Mehta, 1991). Materials such as ground granulated blast furnace slag (GGBFS) have been already used as binder in place of cement and different works pointed out the improved performance of the resulting concrete, in terms of mechanical strength and durability (Babu et al., 2000; Pal et al., 2003). Nevertheless, this residue shows latent hydraulic properties, which implies that it has hydraulic properties when activated in suitable conditions. Purdon (1940) firstly investigated the activation of blast furnace slag with sodium hydroxide, finding that the process consists of a first step, in which silica, aluminum and calcium are firstly dissolved, followed by the formation of the corresponding hydrates. More recently, Shi and Day (1995) reported that it is possible to achieve a compressive strength of 160 MPa from GGBFS activated with sodium silicate after 90 days curing at room temperature, with respect to the compressive strength obtained from pastes without activator, that reach only 0.8 MPa. Other materials, such as fly ash, derived from thermal treatments, or metakaolin ($\text{Al}_2\text{O}_3 \cdot \text{SiO}_2$), an anhydrous aluminosilicate produced by the thermal decomposition of kaolinite, were also alkali activated. The first investigation in this field was carried out from Davidovits and Cordi (1979), who patented a new product obtained from the activation of metakaolin, named geopolymer. According to the authors, this name refers

to the fact that once the material is activated, it polymerizes, i.e. it transforms and hardens at low temperature. Actually, over the last years, a broad discussion was initiated on the definition of the alkali activation process in the literature. It was concluded that alkali activated materials should be used as a general term, while the term geopolymer should only be used when a zeolite-like phase is obtained as a result of the activation reaction (Palomo et al., 1999; Pacheco-Torgal et al., 2008a).

1.2.4.1. Mechanism of the process

The reaction mechanism that explains the hardening of the alkali activated binders is highly dependent on the composition of the prime material as well as on the nature of the alkaline activator. In particular, as reported in the previous section, two different models are used to explain the mechanism of alkali activation: the first one is in the case of an activation of system based on a high content of Ca and Si (blast furnace slag), having C-S-H as the main reaction product. The second model refers to the activation of residues with a high content of Si and Al (fly ash and metakaolin), for which the final product is characterized by the formation of an amorphous zeolite-like polymer (Li et al., 2010a).

Glukhovskiy et al. (1980) proposed a general mechanism for the alkali activation of metakaolin, based on different reactions of destruction-coagulation-condensation-crystallization characterized by three main steps. The first step, defined “destruction-coagulation”, is represented by a breakdown of the Si-O-Si and Al-O-Si bonds that occurs when the pH increases. The disaggregation of the solid phase allows to transform these groups into a colloid phase and, in the early age, the amorphous component of the solid particles dissolves in the presence of a high alkaline solution. The second step, called “coagulation-condensation”, is characterized by the accumulation of the destroyed products to form a coagulated structure where poly-condensation takes place. The rate of this step is determined by the state of the dissolved ions and the existence of the required conditions for gel precipitation. Indeed, the silicic condensation is favored at basic pH values, for which the disaggregation of the Si-O-Si bond gives rise to

$\text{Si}(\text{OH})^4$ like hydroxylated complexes. The generation of a condensed and crystallized structure represents the third and last step. The main differences between traditional zeolitic systems and alkaline activated binding derive from the different experimental conditions employed in the synthesis process. Other authors (van Jaarsveld et al., 1998; Xu and van Deventer, 2000) also explained that the alkaline activation of metakaolin results in the release of silicate and aluminate species into solution, and the initial release of Al may be even more rapid than that of Si. Hence, the dissolved Al may react with the silicate supplied by the activating solution leading to the formation of aluminosilicate oligomers. This is why the use of a sodium silicate solution ($\text{Na}_2\text{OSiO}_2 \cdot \text{H}_2\text{O}$) lead to a better activation and thus better mechanical properties than a solution of sodium hydroxide (NaOH). After that, the formed gel grows and eventually crystallizes to form zeolites. For the fly ash, the activation occurs at low solution to solid ratios and at very high OH^- concentration. In these conditions, the growth of the zeolitic phase in a crystal form is extremely slow and therefore, an amorphous cementitious matrix, the so-called aluminosilicate gel, is stabilized. However, upon the alkali activation of fly ash, Fernández-Jiménez and Palomo (2005) observed the presence of crystalline zeolite phases like hydroxysodalite ($\text{Na}_4\text{Al}_3\text{Si}_3\text{O}_{12}\text{OH}$) and herschelite ($\text{NaAlSi}_2\text{O}_6 \cdot 3\text{H}_2\text{O}$), that probably represents the phases thermodynamically stable towards which the system should evolve with time. They also found that when the activating solution is a mixture of NaOH and Na_2CO_3 , the incorporation of carbonates into the system allowed the formation of sodium bicarbonates among the reaction products.

The reaction mechanism of the alkali activation of blast furnace slag is more complicated than that reported for fly ash, mainly because it is still unclear how the calcium is structurally bound in the aluminosilicate phase glass phase constituting the slag (Li et al., 2010a). However, the presence of Ca in the glassy phase promotes a higher disorder in the slag and increases also the degree of depolymerization of the system, leading to the higher reactivity towards alkalis. According to Krizan and Zivanovic (2002), who studied alkali activation with a high concentration of OH^- , the process begins with the dissolution of the slag bonds Ca-O, Mg-O, Si-O-Si, Al-O-Al and Al-O-Si, followed by the formation of a Si-Al layer on the surface of slag grains, after which the formation of the reaction products occurs. Song et al. (2000) activated a

blast furnace slag with NaOH and they observed that the formation of Ca compounds as reaction product is highly dependent on the pH of the solution. Indeed, they found that the solubility of Si increased with pH and that, in the beginning of the reaction, the active silicate ions react with Ca^{2+} to form a calcium silicate hydrate gel (C-S-H), whose formation is highly affected by the pH of the solution. It has been reported elsewhere that C-S-H is not present as reaction product when a solution with a pH below 9.5 is used (Greenberg and Chang, 1965). This gel represents the main reaction product of the activation of either blast furnace slag or fly ash and this finding is of great importance for the purpose of the research in this field since this compound is the main binding phase resulting from the hydration of cement (Richardson, 1999). However, it was reported that in the presence of a high sodium content derived from the alkali solution, the C-S-H gel may incorporate part of it, with a decrease in the Ca/Si ratio, through the replacement of the Na^+ ion by Ca^{2+} (Stade, 1989; Macphee et al., 1989). Nevertheless, some authors did not find the formation of C-S-H under specific conditions, i.e. with a Na-silicate solution modulus² of 1.2 (Yip et al., 2005).

1.2.4.2. Factors affecting the process

The main parameters that affect the alkali activation process are the composition of the raw material, the type and concentration of alkaline activator and curing conditions.

Any material composed of silica and aluminum can be treated with alkalies (Pacheco-Torgal et al., 2008b) and depending on their chemical composition, Palomo et al. (1999) have classified the **prime materials** in the following two major categories:

- Materials rich in Si and Ca, e.g. blast furnace slag, which usually react with a mild alkaline solution, having C-S-H as the main reaction product.

² The silica modulus of a solution composed of alkali hydroxide and the corresponding silicates represents the ratio of SiO_2 and the M_2O (where M is an alkali ion, e.g. Na or K)

- Materials rich in Si and Al, e.g. metakaolin and fly ash, which usually react with an alkaline solution at high concentrations and are characterized by a polymeric final product.

The blast furnace slag is a glassy ground material formed when molten slag is rapidly cooled and then ground for improving its reactivity. It is mainly constituted by SiO_2 , CaO , MgO and Al_2O_3 , which are the common components of commercial silicate glasses. Haha and co-authors (Haha et al., 2011; Haha et al., 2012) investigated the effect of the MgO and Al_2O_3 content of the slag on the kinetics of slag reaction and on the compressive strength achieved employing different activators. Regarding fly ash, Fernández-Jiménez and Palomo (2003) found that different parameters influence the reactivity of this residue towards alkalis, such as the reactive silica content, the amorphous phase content and the particle size distribution. The high reactive silica, involving the formation of the main reaction product, an aluminosilicate gel, was indicated as the responsible for the high mechanical strength of the final activated product.

As for the nature of **alkaline activators**, they were classified by Glukhovsky (1981) into the following six groups (M denoted the alkali ion, e.g. Na, K):

- Alkalis: MOH
- Non-silicate weak acid salts: M_2CO_3 , M_2SO_3 , M_3PO_4 , MF
- Silicates: $\text{M}_2\text{O}\cdot n\text{SiO}_2$
- Aluminates: $\text{M}_2\text{O}\cdot n\text{Al}_2\text{O}_3$
- Aluminosilicates: $\text{M}_2\text{O}\cdot \text{Al}_2\text{O}_3\cdot (2-6)\text{SiO}_2$
- Non-silicates strong acid salts: M_2SO_4

However, the mixtures of sodium or potassium hydroxide (NaOH , KOH) with sodium silicate or potassium silicate ($n\text{Na}_2\text{SiO}_3$, $n\text{K}_2\text{SiO}_3$) are the most common alkaline activators (Pacheco-Torgal et al., 2008b). Depending on the chemical composition of the prime material, the concentration and type of alkaline activators have been varied in different studies, mainly for achieving a final activated product with a suitable mechanical performance to be reused as binder. Indeed, the amorphous content of silica

and alumina in the prime material, having a higher internal energy than the crystalline phases, affects the reactivity towards alkali activation (Pacheco-Torgal et al., 2008b). Generally, since the chemical composition of the materials in question differs substantially, also the composition of the activators changes accordingly and, very often, even for the same category of material, the optimum activator dosage may change. Usually, the composition of the activators is expressed as the M_2O content or silica modulus, i.e. SiO_2/M_2O for the silicates, otherwise it can be also expressed in terms of oxide content or molarity of the alkali solution, when only an alkali hydroxide or salt is used as activator.

According to Fernández-Jiménez et al. (1999), the most important parameters that affect the mechanical strength of alkali activated blast furnace slag (BFS) mortars are, in ascending order, the nature of the alkaline activator, the activator concentration the curing temperature and the specific surface of the slag. In particular, they observed that to achieve the highest and earliest mechanical strength, the slag has to be activated with a mixture of $Na_2SiO_3 \cdot H_2O$ and $NaOH$, followed by $NaOH$ and then by Na_2CO_3 . The fact that sodium carbonate did not provide an earlier mechanical strength was related to the initial low reaction rate due to the lower pH of the solution and hence to lower initial strength development. However, at later ages, higher strength was found using the sodium carbonate solution instead of the sodium hydroxide one, because of the formation of carbonate compounds that increase the mechanical strength. The authors also noticed that the optimum concentration of Na_2O of the alkaline activator should vary between 3 and 5%. It is commonly agreed that the activation of blast furnace slag with a water-glass based activator (Na_2SiO_3) increases the dissolution of the prime materials and hence leads to a higher mechanical strength (Zivica, 2007). Usually, the silica modulus of the silicates showed to vary between 0.75 (Atis et al., 2009) and 2.52 (Douglas and Brandstetr, 1990), with highly variable optimum values. Bakharev et al. (1999a) achieved an optimum strength by using a Na_2O concentration of 8% for a silica modulus of 1.25. Wang et al. (1994) stated that water-glass was the best activator in terms of mechanical performances of the slag mortars and the best alkali dosage was in the range of 3-5.5% of Na_2O by slag weight, with a silica modulus ranging from 1 to 1.5. The molarity of the sodium hydroxide solution is often too low for activating the

blast furnace slag, as reported in Song et al. (2000) where two solutions of NaOH of 1M or 0.1M were used. On the other hand, alkali activation of fly ash usually required higher concentration of the alkali, as reported in Palomo et al. (1999) where good results in terms of mechanical strength were obtained with a NaOH concentration of 12M. However these authors have also underlined the importance of using soluble silica, instead of hydroxide, in order to promote the polymerization reactions.

Beyond the above mentioned parameters, mainly related to the composition of the raw materials, other key factors that affect the alkali activation process are the **relative humidity and curing temperature** applied. It should be noted that in the literature different curing conditions were tested and reported for different prime materials activated with different activators. First, placing the specimen in a curing chamber, the relative humidity should be kept sufficient to prevent water evaporation, that causing micro-cracking into the system, leads to a reduction of the final mechanical strength. Indeed, most of the experimental studies on alkali slag were performed by placing the samples in a curing chamber at ambient temperature (usually $T=20\text{ }^{\circ}\text{C}$) and high relative humidity, i.e. 90% (Brough and Atkinson, 2002; Krizan and Zivanovic, 2002). However, other works report different curing conditions, e.g. RH=50% (de Vargas et al., 2011) or 65% (Atis et al., 2009). Regarding the effects of the curing temperature, Fernández-Jiménez et al. (1999) report that, at the early ages of curing, increasing the temperature (from $25\text{ }^{\circ}\text{C}$ to $45\text{ }^{\circ}\text{C}$) has a positive effect on the early strength of the material based on blast furnace slag, regardless the type of activator employed, although at later curing times, the effect seemed to reverse. This may be correlated to the increase in slag solubility and to the production of large amounts of reaction products in the first stage of the reaction, while, as the reaction time increased, the higher paste densification slowed the following reactions as the diffusion process became difficult, hence reducing the amount of reaction products. Burciaga-Diaz et al. (2013) found that a temperature increase from $20\text{ }^{\circ}\text{C}$ to $60\text{ }^{\circ}\text{C}$ promotes higher strength for slag activated with sodium silicate at a Na_2O concentration equal to 2.5% and 3.5%. Wang et al. (1994) stated that the effect of temperature is almost irrelevant when different types of slag are activated with solutions at high concentrations. As far as the effect of temperature on fly ash is concerned, the obtained literature findings were similar for the BFS, where an overall

strength increase for increasing temperature at early curing times was observed with an inverse effect at longer curing times (Puertas et al., 2000).

Chapter 2

Application of the carbonation-granulation treatment on BOF steel slag

2.1. Introduction

Steel making plants produces large amount of solid residues and among these BOF steel slag are one of the most abundant; BOF slags are typically landfilled or reused limitedly for low-end applications, because some of its properties (i.e.: high free lime content, fine particle size and excessive mobility of specific elements) have shown to affect its technical performance and/or environmental behavior, thus hindering its recycling potential. Efforts should be made in order to develop valorization routes aimed at enhancing the reuse of such residues. Nevertheless, it should be taken into account that the steel industry also generates large amount of carbon dioxide that nowadays represents a well a problem to deal with. Hence, with this aim, this chapter reports the results obtained from the application of a combined granulation and carbonation treatment, as a technique for BOF slag valorization, also allowing to store a fraction of

the CO₂ emissions. The effects of this process are compared with those exerted by granulation under atmospheric air, so to analyze the influence of carbonation on particle aggregation and on the properties of the products. Specifically, the chapter reports and discusses the results of the granulation and granulation-carbonation experiments carried out on samples of BOF slags in a laboratory scale granulation device at different reaction times, in terms of the effects exerted on the physical properties, CO₂ uptake, mineralogy, leaching and mechanical behavior of the obtained granules. Finally, further investigations were carried out with the aim of enhancing the mechanical strength of the slag based aggregates, by performing tests on a slag-cement mixture with different percentages of cement. The above-mentioned characterization methods were applied also for the granules yielded from this treatment.

2.2. Tests performed with BOF steel slag*

2.2.1. Materials and methods

The slag used in this study is a by-product of a steel making plant employing the basic oxygen furnace (BOF) process. The sample was collected from the slag storage site directly after crushing and magnetic separation for iron and steel recovery. The particle size of the untreated material was lower than 2 mm with a d₅₀ value of 0.45 mm. The main chemical constituents of the BOF slag (see Table 2. 1), as determined by alkaline fusion with Li₂B₄O₇ at 1050 °C and ICP-OES analysis of the obtained solutions were: Si (356.91 g/kg), Ca (239.26 g/kg), Fe (196.03 g/kg), Mg (46.57 g/kg) and Mn (22.42

*This section is based on a published paper:

Morone M., Costa G., Poletti A., Pomi R., Baciocchi R. (2014). “*Valorization of steel slag by a combined carbonation and granulation treatment*”. *Minerals Engineering* 59, 82-90

Table 2. 1 Elemental composition of untreated BOF slag expressed as % on a dry weight basis for major elements and mg/kg for trace compounds.

Major Element	Concentration (%)	Major Element	Concentration (%)	Trace Element	Concentration (mg/kg)
Al	1.51	Mg	4.66	Ba	64.61
Ca	23.93	Mn	2.24	Cu	270.21
Cr	0.17	Na	0.31	Ni	18.88
Fe	19.6	V	0.032	Pb	29.86
K	0.13	Si	35.69	Zn	100.22

g/kg); these values are quite similar to the concentrations reported in other studies for this type of steelmaking slag (Proctor et al., 2000, Belhadj et al., 2012). Both the granulation and granulation-carbonation experiments were performed using a laboratory scale granulator (power consumption of 180 W) with a diameter of 0.3 m and a height of 0.23 m, equipped with a blade and operated at 24 rpm applying a tilt of 50° during all experiments. Granulation experiments were performed at ambient temperature and pressure, maintaining the reactor under atmospheric air (Figure 2. 1a); the granulation-carbonation experiments were performed at ambient temperature too, placing a custom-made Perspex lid with a CO₂ feeding system over the reactor (Figure 2. 1b). In this second type of tests, 100% CO₂ was used and the pressure was maintained at 1 bar.

For both types of experiments, air-dried slag (approximately 500 g) and deionized water were premixed in a plastic bag, at the liquid to solid ratio that resulted optimal for the granulation of this material at the tested conditions, i.e. 0.12 l/kg. In order to obtain a homogeneous initial particle size distribution for all the experiments, the mixture was then pushed through a 2 mm sieve, following the procedure widely adopted in other studies on granulation (Iveson et al., 1996; Wauters et al., 2002). Experiments were performed at different reaction times (30, 60, 90 and 120 minutes) and the product of each test, after curing under atmospheric conditions for 7 days, was analysed to determine its particle size distribution applying the ASTM D422 standard procedure.

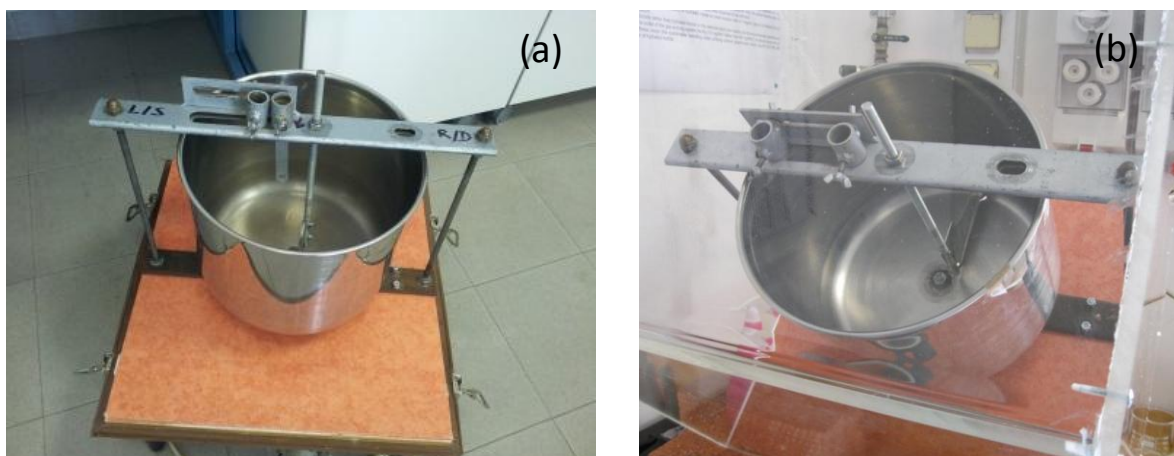


Figure 2. 1 Laboratory scale device used for the granulation experiments (a) under atmospheric air and (b) with a Perspex lid to supply a continuous flow of CO₂.

Each material was then divided by sieving into the following size fractions: Class A ($d > 9.53$ mm); Class B ($4 < d < 9.53$ mm); Class C ($2.36 < d < 4$ mm); Class D ($d < 2.36$ mm). Subsequently, each fraction as well as the untreated BOF slag was characterized in terms of its density, carbonate content, mineralogy and leaching behaviour. In addition, in order to obtain enough sample to perform the batch compliance leaching test (UNI EN 12457-2) and the carbonate content analysis, the finest classes (i.e. C and D) were mixed. The density of the samples was assessed applying the UNI EN 1097-6 procedure. The carbonate content was evaluated by inorganic carbon analysis using a Shimadzu TOC VCPH analyser equipped with a SSM-5000A solid sampler. The mineralogical composition was determined by powder XRD analysis with Cu K α radiation using a Philips Expert Pro diffractometer equipped with a copper tube operated at 40 kV and 40 mA, applying an angular step of 0.02° for 2 seconds with 2θ spanning from 5 to 85° . The leaching behaviour was assessed by following the EN 12457-2 standard compliance test that involves grinding of the material presenting a grain size above 4 mm. In addition, the leaching behaviour of the unground granules obtained from each treatment was also assessed by applying a L/S ratio of 10 l/kg and a contact time of 24 hours, followed by ICP-OES analysis of eluates, employing an Agilent 710-ES spectrometer. Leaching tests were carried out in duplicate. Moreover, the mechanical strength of the granules was evaluated by performing the Aggregate

Crushing Value (ACV) test, applying the British Standard BS 812-110/112, which gives a relative measure of the resistance of an aggregate to crushing under a gradually applied compressive load. This value is expressed as the ratio between the amount of fines formed and the total mass of the test specimen, as reported in the following equation:

$$ACV = \frac{M_2}{M_1} \times 100 \quad (2.1)$$

Where M_2 (g) is the mass of the fine material passing a standard sieve and M_1 (g) is the initial total mass of the test specimen.

2.2.2. Results and discussion

2.2.2.1. Effect of the treatment on the physical properties of the obtained granules

Both granulation and granulation-carbonation processes exerted a relevant effect on the particle size distribution of the material (see Figure 2.2). The average diameter of the obtained granules resulted in both cases between 4 mm and 10 mm and showed to increase with reaction time. The d_{50} (diameter of particles with 50% passing) value of the treatment product was an order of magnitude greater than that of the initial BOF slag (0.4 mm). Since the granule size distribution is generally considered the most variable parameter in a granulation test, multiple experiments were performed for selected reaction times. Results showed that, despite some variations, overall the modifications of the particle size of the slag obtained after each treatment at a specific reaction time, were quite comparable. For instance, for the granulation carbonation test carried out for 30 minutes, the particle size distribution curves resulting from two repeated tests were compared by calculating the d_{90} (diameter of particles with 90% passing); d_{50} and d_{10} (diameter of particles with 10% passing) values for each curve.

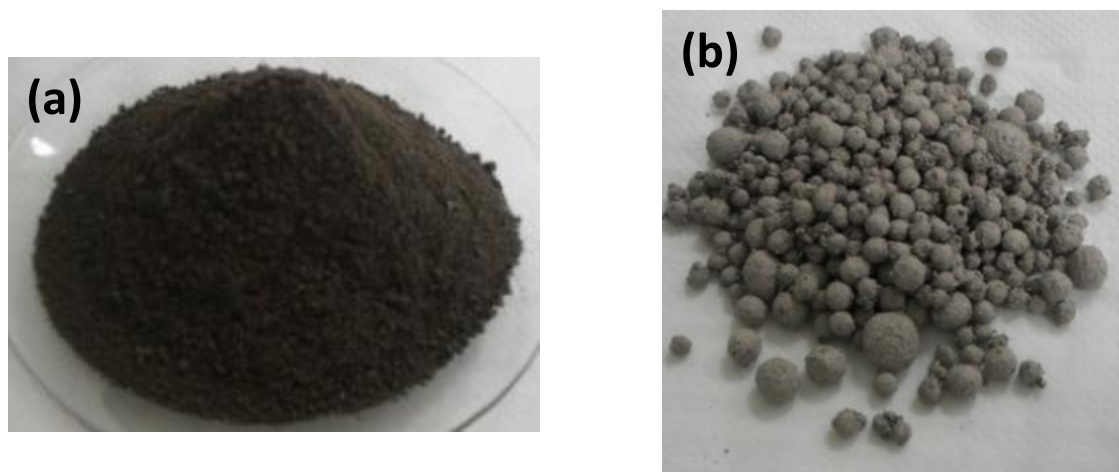


Figure 2.2 Pictures of (a) untreated BOF steel slag and (b) granules obtained from the granulation-carbonation test at a reaction time of 90 minutes.

The ratio between the d_{90} , d_{50} and d_{10} values resulted respectively 1.4, 1.6 and 1. This means that the two granule size distribution curves were almost identical for smaller particle sizes ($d < 1\text{mm}$) while diverged slightly for larger dimensions ($1 < d < 9\text{ mm}$).

In Figure 2.3 , the weight distribution in the 4 particle size classes of the untreated slag is compared with that of the treated material obtained after different reaction times. For the granulation experiments (Figure 2.3a), it can be seen that the content of the finest fraction (class D) decreased from almost 100% in the untreated slag to about 10% in samples collected after 90 minutes. Granules with a size fraction between 2.36 and 4 mm (Class C) were not found after any of the tested reaction times, while a significant decrease of class B granules and a corresponding increase of class A particles was observed for longer treatment times, highlighting the ongoing agglomeration process. The effect of the granulation-carbonation treatment on granule size distribution is reported in Figure 2.3b.

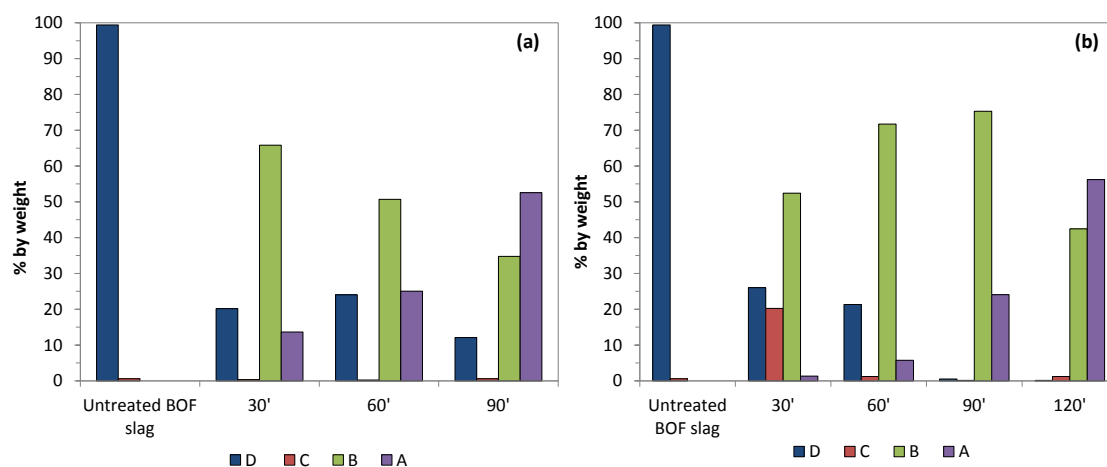


Figure 2.3 Comparison of the weight distribution of the untreated slag and the granules obtained after a) the granulation and b) the granulation-carbonation treatments at different reaction times. Class A ($d > 9.53$ mm); Class B ($4 < d < 9.53$ mm); Class C ($2.36 < d < 4$ mm); Class D ($d < 2.36$ mm).

The content of classes D and C showed to decrease significantly after 90 minutes, while the amount of class B granules, differently from the granulation tests, showed to increase over time up to a reaction time of 90 minutes. As underlined by the trend of the content of the coarser fraction (class A), the kinetics of particle growth in the presence of CO_2 was slower than that resulting under atmospheric air.

The apparent particle density of both the untreated slag ($d > 0.125$ mm) and samples obtained after granulation and granulation-carbonation was evaluated and compared with that of natural gravel (see Figure 2.4). The value found for the untreated slag was quite high (3.75 g/cm^3) if compared to that of natural gravel (2.7 g/cm^3), probably in relation to the significant iron content of the slag. Similar values, ranging from 3.1 to 3.7 g/cm^3 , were reported also in previous studies on this type of residue (Geiseler, 1996; Motz and Geiseler, 2001; Tossavainen et al., 2007; Belhadj et al., 2012). The density of the material obtained after a granulation treatment of 90 minutes (2.9 g/cm^3) was lower than that of the untreated slag, probably owing to the porosity of the granules formed during the process. A slightly higher density was observed for granules obtained after the combined treatment (3.2 g/cm^3), that can be associated to the carbonation reaction occurring in the material, as discussed below. In addition, it can be noted that the

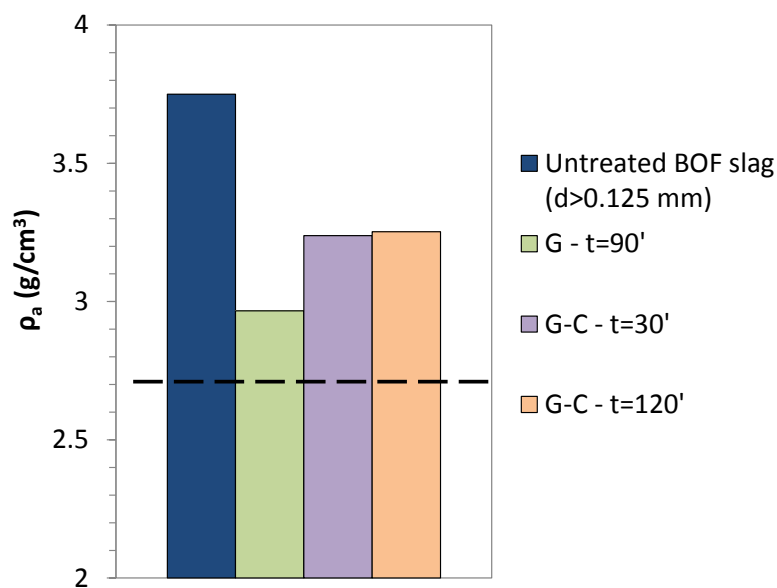


Figure 2.4 Apparent particle density results for: untreated BOF slag; granulated slag after 90 minutes (G granules – t=90’); granulated-carbonated slag after 30 (G-C granules – t=30’) and 120 minutes (G-C granules – t=120’); natural gravel (dotted line).

apparent particle density did not seem to be affected by the reaction time since the values found after 30 and 120 minutes were very similar. The porosity of the granules was hence evaluated as reported in the paper of Wauters et al. (2002) and it ranged between 0.5 for the untreated slag and 0.6 for the granules. The granules obtained after the combined treatment presented a slightly lower value of porosity (0.59) than that of the granules obtained after the granulation treatment (0.63) that could be ascribed to the carbonation reactions, as discussed for the density results.

2.2.2.2. CO₂ uptake of the obtained granules

The extent of carbonation of the slag, resulting from the reaction of the alkaline phases with either atmospheric CO₂ (granulation tests) or pure CO₂ (granulation-carbonation tests), was assessed by measuring the Inorganic Carbon (IC) content of the material before and after each treatment. The IC content of the products of the granulation

treatment ranged between 1.7% and 2%, depending on the reaction time. These values were significantly higher than that of the untreated slag (average IC=0.54%), implying that carbonation occurred also when the material was subjected to the granulation treatment under atmospheric air. However, the IC content of the granulated-carbonated materials that ranged between 3.5 and 4%, was almost twofold higher than that obtained from the granulation tests.

On the basis of the IC content of each treated sample, its CO₂ uptake was evaluated by applying Eq. 2.2, where the IC concentration of the untreated sample (CO_{2 initial}) and of the treated one (CO_{2 final}) is expressed in terms of its CO₂ weight percent.

$$\text{CO}_{2\text{uptake}} (\%) = \frac{\text{CO}_{2\text{final}} (\%) - \text{CO}_{2\text{initial}} (\%)}{100 - \text{CO}_{2\text{final}} (\%)} \cdot 100 \quad (2.2)$$

These data were also used to evaluate the calcium conversion yield, defined as the ratio between the carbonated Ca, proportional to the measured CO₂ uptake, and the amount of potentially reactive Ca phases expressed in terms of Ca content (see Eq. 2.3).

$$R_x (\%) = \frac{\text{CO}_{2\text{uptake}} (\%) \cdot \frac{40}{44}}{\text{Ca}_{\text{tot}} (\%) - \text{CaCO}_{3\text{initial}} (\%) \frac{40}{100}} \cdot 100 \quad (2.3)$$

The CO₂ uptake kinetics observed for each class of granules after undergoing either the granulation or the granulation-carbonation treatment are shown in Figure 2.5a and b, respectively.

For the granulation test, the maximum weighted average uptake value (6%), corresponding to 27% calcium conversion, was already obtained after short reaction times (30-60 minutes) and remained basically constant at increasing reaction times. The slight decrease observed at 90 minutes reaction time can be probably ascribed to the heterogeneity of the material used in the tests. Looking at the carbonation kinetics resulting for each size fraction (see Figure 2.5a) it may be noted that CO₂ uptake

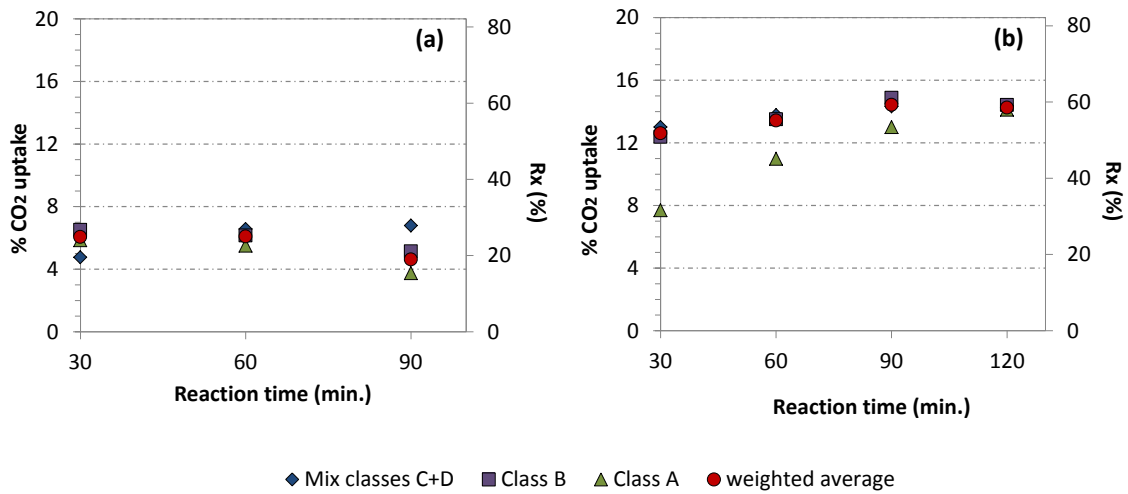


Figure 2.5 Kinetics of CO₂ uptake and Ca conversion obtained from the (a) granulation and (b) granulation-carbonation tests, for mixed classes C and D ($d < 4$ mm), Class B ($4 < d < 9.53$ mm) and Class A ($d > 9.53$ mm) and for the weighted average.

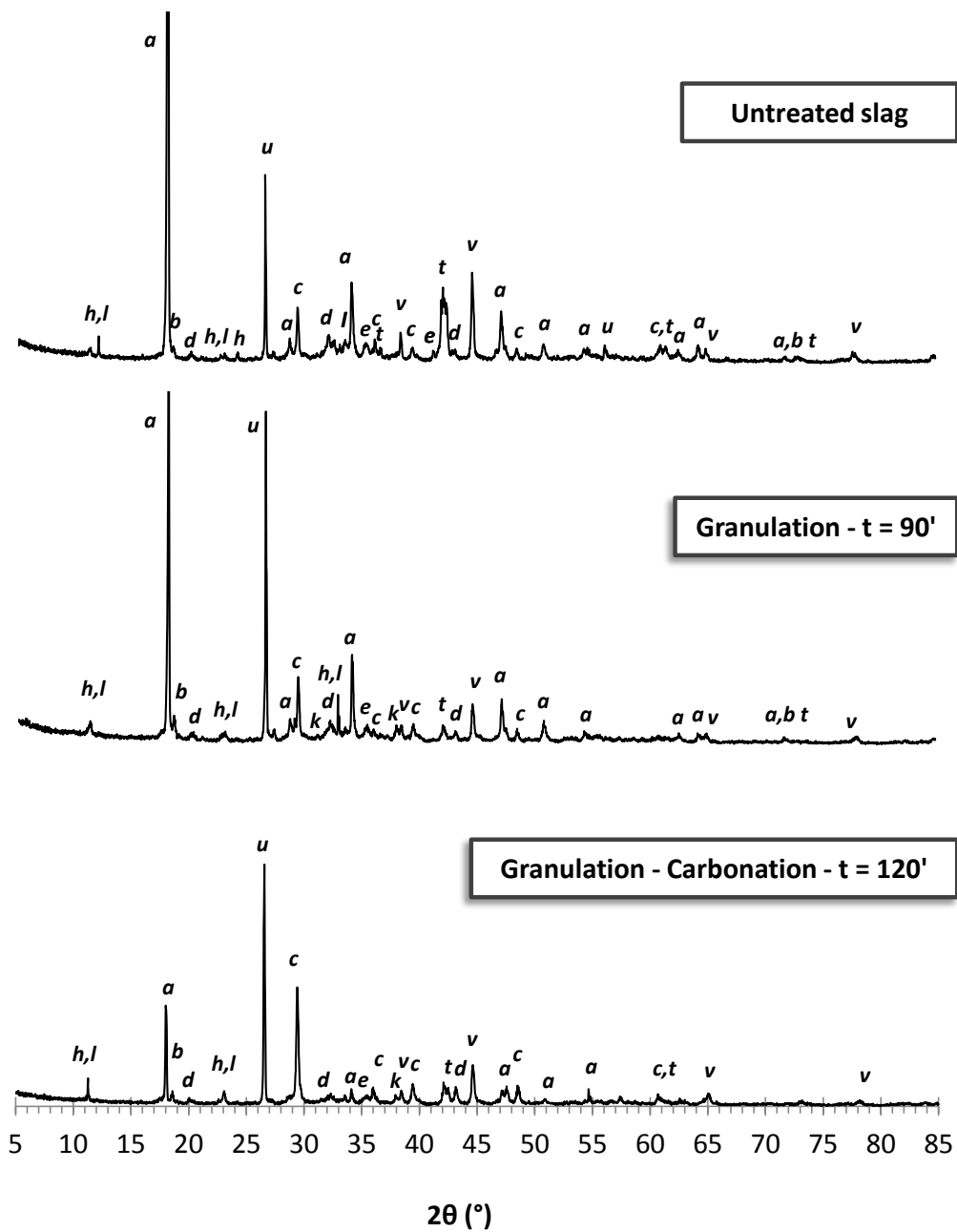
increased with reaction time (from 4% to almost 8%) only for the finest fraction, while it was not notably affected by the reaction time for the other fractions. This suggests that under atmospheric air, apart from the initial CO₂ uptake, only the finest size fraction (class C+D) may undergo some degree of carbonation during the granulation treatment under atmospheric air; this behavior may be related to the higher specific surface available for reaction with CO₂ of the smaller particles compared to the granules belonging to coarser classes (A and B).

The weighted average CO₂ uptake of the granulated-carbonated granules was already above 12% after 30 min, although a large difference could be observed between the coarser fraction (Class A) and the other ones (see Figure 2.5b). The coarser fraction clearly exhibited a much slower carbonation kinetics, although the CO₂ uptake achieved after 120 minutes reaction time was comparable to the one observed for the other dimensional classes. This behavior may be ascribed once again to the larger size of the obtained granules and hence lower specific surface available for the reaction. Nevertheless, under a 100% CO₂ atmosphere, differently from what observed under atmospheric air, carbonation took place also in the coarser particles. Besides, the

average CO₂ uptakes achieved were more than double than those obtained in the granulation tests, with maximum calcium conversions around 60%. The results of the granulation-carbonation tests, achieved with a considerable amount of material (≈500 g) in a dynamic device under ambient T and 1 bar CO₂ pressure, are comparable with those obtained treating 1 g-BOF samples under enhanced operating conditions (T=50 °C and P=3 bar) in a static reactor applying a L/S ratio of 0.3 l/kg (Baclocchi et al., 2012). In addition, differently from the static batch tests, prior to the granulation-carbonation tests, the BOF slag was not subjected to any type of mechanical pre-treatment. Hence, compared to other process routes investigated for accelerated carbonation of residues, i.e. slurry-phase (Huijen et al., 2005) and wet-route process in static conditions (e.g.: Baclocchi et al., 2010a), the tested reaction mode appears to be particularly promising in consideration of the significant CO₂ uptakes achieved and the mild operating conditions applied.

2.2.2.3. Mineralogy of the obtained granules

XRD patterns of the untreated slag and of granules obtained after granulation and granulation-carbonation carried out for a reaction time of 90 and 120 minutes, respectively, are presented in Figure 2.6. The mineralogy of the granulation product was very similar to that of the untreated slag, exhibiting a predominance of Ca phases (Ca hydroxide, Ca-containing oxides, Ca-silicate and calcite) and other oxides, such as coesite, vanadium oxide, magnetite and Mn-Mg oxide. After the granulation-carbonation treatment, the intensity of portlandite peaks decreased significantly while the ratio between calcite and portlandite peaks increased, indicating the reaction of Ca(OH)₂ with CO₂. The only phase for which a noteworthy increase in peak intensity was observed after carbonation was calcite, indicating that, although the peak related to Mn-MgO showed to decrease upon carbonation, only calcium carbonates could be identified. This result is in good agreement with the higher IC value measured in the product of the granulation-carbonation test compared to that of the granulation treatment.



Legend: **a:** portlandite $[Ca(OH)_2]$; **b:** brucite $[Mg(OH)_2]$; **c:** calcite $[CaCO_3]$; **d:** larnite $[Ca_2SiO_4]$; **e:** magnetite $[Fe_3O_4]$; **h:** Ca-Al-Fe oxide $[Ca_2Fe_{1.4}Al_{0.6}O_5]$; **k:** corundum $[Al_2O_3]$; **l:** Ca-Cr-Fe oxide $[Ca_2Cr_{0.5}Fe_{1.5}O_5]$; **t:** Mn-Mg oxide $[(MgO)_{0.725}(MnO)_{0.275}]$; **u:** coesite $[SiO_2]$; **v:** V oxide $[VO]$

Figure 2.6 XRD pattern of the untreated slag and of the granules obtained from the granulation and granulation-carbonation treatments after a reaction time of 90 and 120 minutes, respectively.

Actually, it can be observed that, after carbonation, different peaks of low intensity of portlandite, that has partially reacted with CO₂, were still present in the mineralogy of the granules. This result could be an indication of the irregular diffusion of CO₂ into the aggregates, constituted by different carbonated area. Indeed, depending on the granules' size, the diffusion of CO₂ into the inner core of the granules may result limited by the outer carbonated layer. This outcome will be further investigated in the following paragraphs on the leaching behavior of the aggregates.

2.2.2.4. Effect of the treatment on the leaching behavior of the granules

The results of the EN 12457-2 compliance test carried out on the untreated slag and on crushed material (d<4 mm) obtained from granulation and granulation-carbonation experiments at different reaction times, reported in Table 2.2, indicated that the pH of the untreated slag resulted alkaline (12.4), in good accordance with its high Ca(OH)₂ content detected by XRD. The pH values measured in the treated samples showed to decrease slightly, but remained well above 12, indicating that portlandite was still the solubility controlling phase.

As for the leaching of major slag constituents, Al and Si concentrations showed to increase after both types of treatment, while Ca concentrations did not show to vary significantly after neither type of treatment, in agreement with the pH values that remained above 12. As for Ba, eluate concentrations showed to decrease slightly after the granulation treatment and of over a factor of 2 upon the combined treatment, resulting in any case well below the limit set for non-hazardous waste reuse (1 mg/l). As far as the other trace compounds are concerned, the eluate concentration of Cr, V and Zn, as well as for the untreated material, consistent with the low concentrations detected in other works (Proctor et al., 2000; Tossavainen et al., 2007), were always below the instrumental quantification limit.

These results indicate that the two processes, and in particular the combined one, led to the formation of more soluble Al and Si containing phases probably owing to hydration reactions, while Ba appeared to be more tightly bound to the solid matrix.

Application of the carbonation-granulation treatment on BOF steel slag

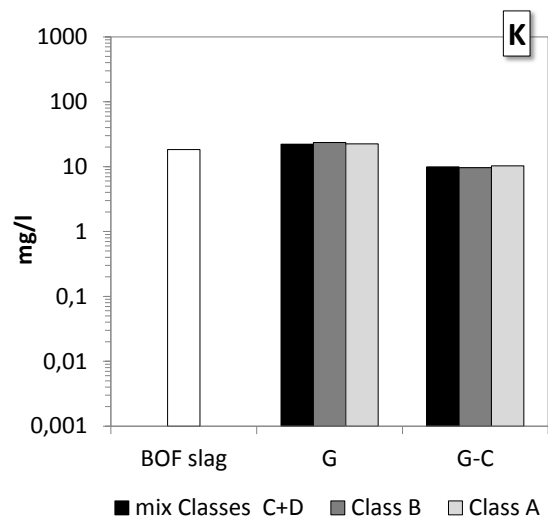
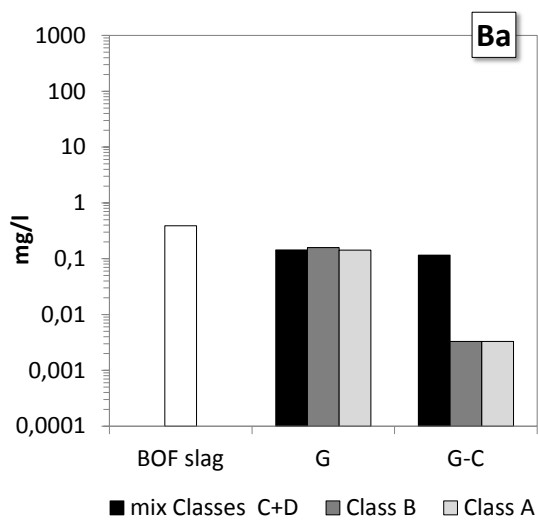
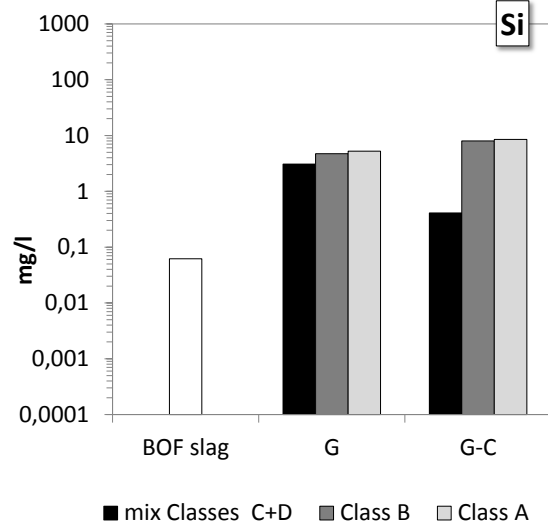
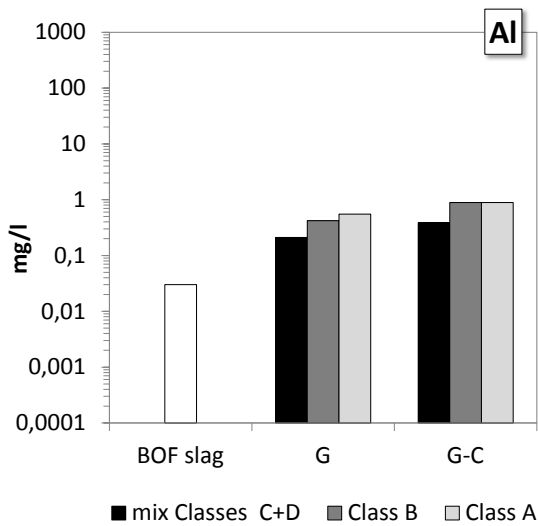
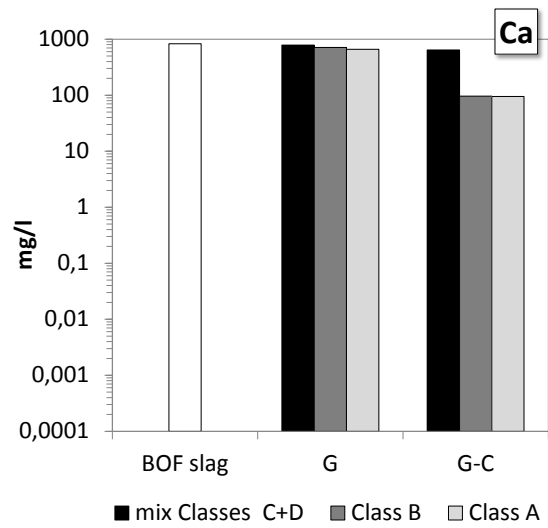
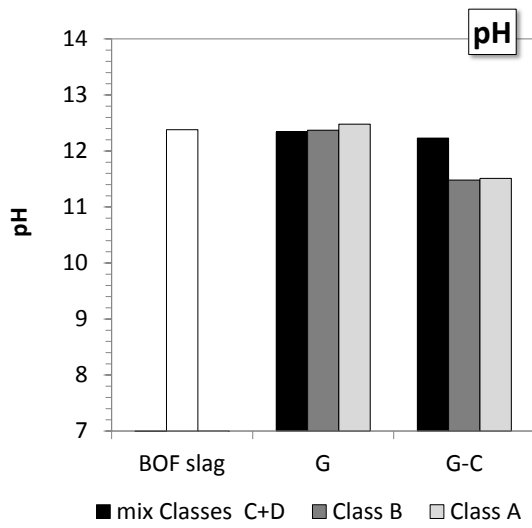
Table 2.2 Results of the EN 12457-2 leaching test on untreated slag and on crushed granules obtained after granulation and granulation-carbonation treatment at different reaction times in terms of: pH and Al, Ba, Ca, Cr, K, Mg, Si, V and Zn concentrations.

	pH	Al mg/l	Ba mg/l	Ca mg/l	Cr mg/l	K mg/l	Mg mg/l	Si mg/l	V mg/l	Zn mg/l
Untreated slag										
	12.38	0.03	0.39	828.77	<0.008	18.34	<0.03	0.05	<0.008	<0.008
Granulation										
30'	12.31	0.10	0.29	829.12	<0.008	8.27	<0.03	0.24	<0.008	<0.008
60'	12.31	0.09	0.30	827.26	<0.008	10.38	<0.03	0.22	<0.008	<0.008
90'	12.34	0.07	0.34	826.65	<0.008	12.69	<0.03	0.15	<0.008	<0.008
Granulation-Carbonation										
30'	12.33	0.13	0.21	806.75	<0.008	8.65	<0.03	0.24	<0.008	<0.008
60'	12.31	0.21	0.17	749.35	<0.008	8.61	<0.03	0.31	<0.008	<0.008
90'	12.30	0.20	0.16	790.60	<0.008	8.13	<0.03	0.31	<0.008	<0.008
120'	12.28	0.19	0.16	828.62	<0.008	9.05	<0.03	0.29	<0.008	<0.008

In order to evaluate the effects of the agglomeration process on the release of major and trace components, leaching tests were also performed on each particle size fraction of the granules obtained after the treatments without grinding. In Figure 2.7, the pH and eluate concentrations of Ca, Al, Si, Ba, V, Cr and Zn resulting for each size fraction of the granules produced after granulation and granulation-carbonation at the highest tested reaction time (90 and 120 minutes, respectively) are reported and compared to the values found for the untreated slag.

After granulation, pH, Ca and V concentrations did not appear to vary significantly for any of the classes compared to the values obtained for the untreated slag. Al and Si release increased of up to one order of magnitude after 90 minutes of the treatment and

Application of the carbonation-granulation treatment on BOF steel slag



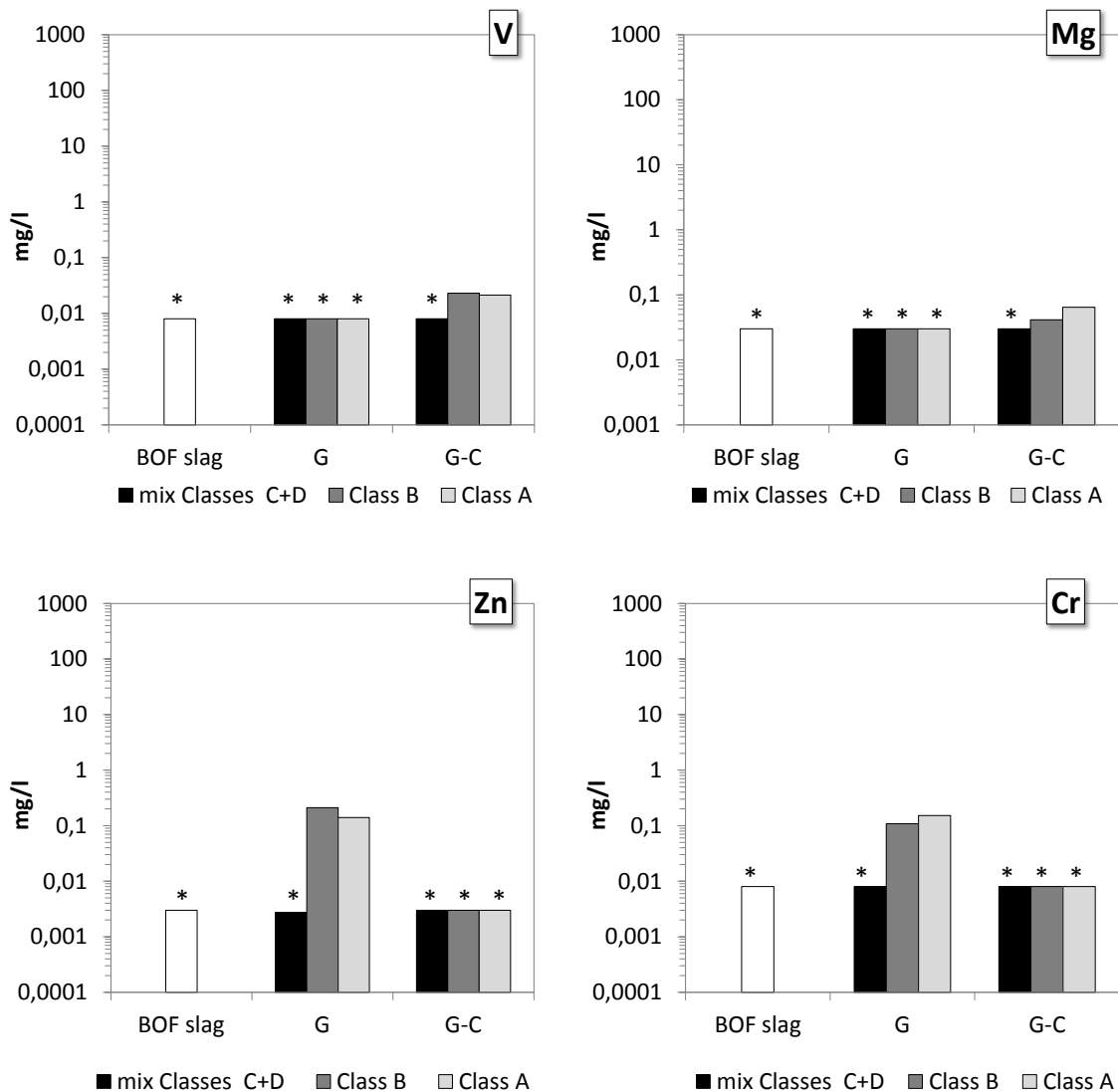


Figure 2.7 EN 12457-2 leaching test results for untreated BOF slag and for the particle size classes obtained after granulation (G) and granulation-carbonation (G-C) (90 and 120 minutes, respectively). The starred bars indicate that the concentrations resulted below the instrumental quantification limit.

the leaching of these elements showed to rise slightly for an increase in granule size. The leaching behavior of Al and Si proved in agreement with the one observed for the crushed samples (Table 2.2) and clearly can be again explained with the formation of more soluble Al and Si containing phases. Also Ba release showed to be affected by the granulation treatment very similarly to the crushed samples, exhibiting an over twofold

decrease for all three size classes. Conversely, both Cr and Zn concentration in the eluate of the coarser fractions increased after granulation well above the values measured for the untreated slag. In this regard, Cr leaching could become critical as its concentration in the eluates of class A and class B particles (0.11 and 0.15 mg/l, respectively) showed to exceed the Italian limit for reuse of waste (0.05 mg/l). Further investigations, such as the performance of the pH-dependent leaching test could be useful in order to better understand the enhancing effect of granulation on the release of chromium and zinc from the coarse particle size fractions formed upon the treatment.

The carbonation-granulation treatment appeared to significantly affect the leaching behavior of the granules obtained after a reaction time of 120 minutes, as can be observed in . Namely, although the pH of the finer fractions (mix classes C and D) was not notably affected, the pH of the coarser ones (class A and class B) decreased from values well above 12 to around 11.4. A similar behavior was observed for Ca and Ba concentrations in the eluate of class A and class B, that were both reduced of at least one order of magnitude with respect to the untreated slags, whereas a much lower effect was observed for the finer fractions (mix classes C and D). Conversely, Si and Al leaching increased upon carbonation mainly for the coarser fractions; Si release in particular proved over two orders of magnitude higher in classes A and B compared to the untreated slag. This trend was similar to that exhibited by the products of the granulation treatment, suggesting that the reaction of silicate phases such as larnite with CO₂ was quite limited, as also indicated by the results of XRD analysis. Upon carbonation, V concentrations in the eluates increased for classes B and A from values below the quantification limit for the untreated slag (<0.008 mg/l) up to almost 0.02 mg/l. Finally, as can be noticed in , the release of Zn and Cr from all three particle size fractions of the granulated-carbonated slags resulted lower than the quantification limit, similarly to what observed for the untreated slag.

The leaching behavior of the treated materials resulting for crushed and uncrushed samples, discussed above with reference to Table 2.2 and Figure 2.7 respectively, was fairly similar for the granulated material, whereas some important differences were noticed for the materials obtained from the granulation-carbonation process. It was hence hypothesized that these differences, mainly concerning the pH value and Ca, Ba

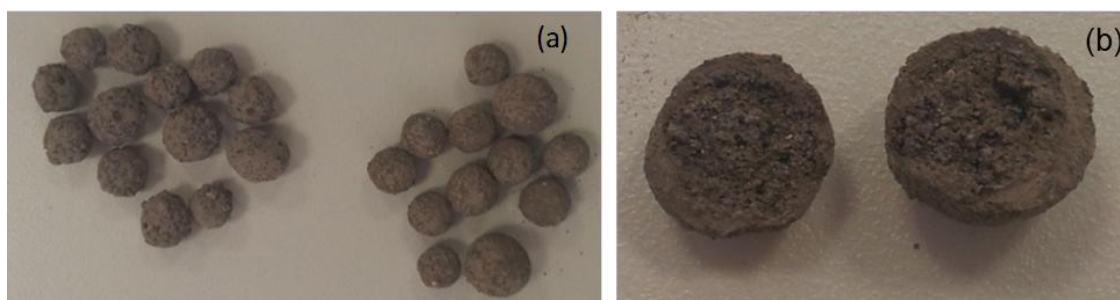


Figure 2.8 a) Granules (Class A) obtained after the granulation-carbonation experiment at a reaction time of 120 minutes and b) the inner section of a granule obtained from the same experiment.

and V leaching, could be associated to the higher extent of carbonation achieved in the external layer of the particles with respect to the internal core, that can be hardly reached by CO_2 once that the product layer is formed (Melton et al., 2008). A higher extent of carbonation in the external layer, that is the one directly in contact with water in the leaching test, could in fact explain the lower eluate pH and calcium and barium concentrations as well as the slight increase of V release. A first confirmation of this hypothesis came from the visual inspection of the granules obtained from the carbonation-granulation experiments, shown in Figure 2.8. This figure shows that the section of the granules belonging to class A is characterized by a dark inner core surrounded by a thin outer layer. In order to further support this finding, the outer layer and the inner core of the particles were separately analyzed for the Inorganic Carbon content (IC). Based on these data, the CO_2 uptake was found to be 4 times larger in the outer layer than in the inner core for class B particles and up to 8 times larger for class A ones. This result suggests that the different extent of carbonation found in the external layer may actually explain the different leaching behavior of the carbonated granules with respect to the crushed materials.

2.2.2.5. Effect of the treatment on the mechanical strength of the granules

One of the goals of the application of the tested treatments on the BOF slag was the production of aggregates to reuse in construction works, in substitution of primary raw materials. Hence, in order to compare the mechanical properties of the treatment products with those of natural gravel, it was decided to perform the Aggregate Crushing Value (ACV) test on both types of materials.

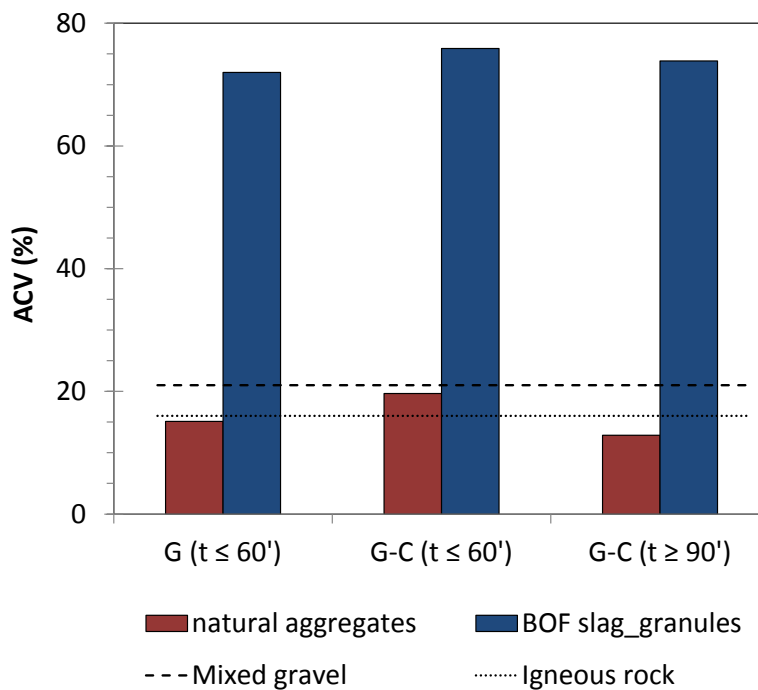


Figure 2.9 Aggregate Crushing Value (ACV) results for the natural aggregates and the granules obtained after the granulation and the granulation-carbonation treatment at different reaction times.

In this section, the test was carried out on the mixed granules retrieved from the granulation tests at reaction times lower than 60 minutes and on the granules obtained from the combined granulation and carbonation experiments at a reaction time lower than 60 and greater than 90 minutes. The tested natural gravel was prepared having the same particle size distribution as the analyzed granules. The results (see Figure 2.9) showed that the amount of fine particles ($d < 2.36\text{mm}$) obtained applying the

standardized confined compressive test on the treatment products was significantly higher (over 70% by weight of the material) than that achieved for natural gravel (20% by weight of the material), that showed values similar to those reported in the British standard BS 812-110 (1990) for the igneous rock (16%). In addition, the ACV obtained for the granules resulting from the combined treatment appeared to be slightly higher than that of the material produced by the granulation test. As an indication, the Indian Roads Congress established that the ACV should not exceed 30% for the aggregates used at the pavement surface, whilst it should be less than 45% for those used as sub-base layers. Hence, it may be concluded that the granules produced using only water or water and CO₂ as binder presented inadequate mechanical properties for reuse in construction applications.

2.3. Further investigation: evaluation of the effects of cement used as binder for the production of granules

The results achieved in the previous section, in which BOF slag was mixed with water, showed that the granulation/carbonation treatment is an effective process for producing granules, although the mechanical strength was lower than that reported for natural aggregates. The low mechanical performance of the granules may be related to the low hydraulic activity of the BOF slag, i.e. poor capacity to react with water and form a hard material (Wang and Yan, 2010). Hence, the BOF steel slag were mixed with cement, a hydraulic material that yields high-strength reaction products immediately upon reaction with water, in order to evaluate if the mechanical resistance of the resulting granules approached that of natural aggregates. In these experiments, it was decided to fix the reaction time of the experiments to 30 min in order to evaluate the effect of the cement in the mixture upon both the granulation and the granulation-carbonation tests. The obtained granules, as well as the untreated slag, were characterized in terms of their particle size distribution, inorganic carbon content and leaching behavior. The granules were then subjected to the ACV test so to analyze their mechanical performance.

2.3.1. Materials and methods

The BOF steel slag sample was collected, after metal recovery, from a different heap of the same slag storage site of the steelmaking plant reported in the previous paragraph. The cement used in the tests was a high resistance Portland cement (CEM I 52.5R), selected as binder also in the work of Scanferla et al. (2009) dealing with the granulation treatment of soil. Moreover, it was decided to use this type of cement because, previous granulation tests carried out in our groups on soil mixed with CEM 42.5R and CEM 52.5R, pointed out that using the latter one allowed to achieve lower ACV, and hence higher strength (Capobianco, 2014).

The granulation and granulation-carbonation experiments were carried out at a set reaction time of 30 min, keeping the same operating conditions adopted in the previous section, i.e. tilt and speed equal to 50° and 24 rpm, respectively. For each experiment, approximately 500 g of material was used and three different compositions were tested: CEM 0%, CEM 10% and CEM 20%, in which 0%, 10% and 20% by wt. of slags were replaced by cement in the total mixture, respectively. The liquid to solid ratio was set equal to 0.12 l/kg for the granulation tests and to 0.13 l/kg for the granulation/carbonation tests. For this set of experiments it was decided to increase the liquid to solid ratio for the granulation-carbonation experiments because preliminary tests (not reported here) showed that the agglomeration with cement is more effective. The granules obtained after the experiments were cured at controlled conditions (RH=100% and T=25 °C) for 28 days, in order to allow the completion of the cement hydration reactions. Subsequently, they were tested through the analysis of the particle size distribution, mechanical strength and inorganic contaminant leaching, employing the same methods reported in the previous section. The extent of carbonation of the granules was also analyzed in terms of the inorganic carbon content, following the same procedure adopted in the previous section.

Furthermore, batch accelerated carbonation tests were performed on the as-received BOF slag sample at mild operating conditions (T=20 °C, p=1 bar,), close to those applied in the granulation tests, but varying the liquid to solid ratio (from 0.1 to 0.4 l/kg), in order to evaluate possible changes in the extent and kinetics of carbonation

resulting from the different reaction mode adopted (batch or granulation-carbonation). In each run, carried out in a pressurized stainless steel reactor equipped with a 150 ml internal Teflon jacket and placed in a thermostatic bath for temperature control, three 1 g slag samples were mixed with water at a set liquid to solid (L/S) ratio and exposed to a 100% CO₂ flow for different reaction times, ranging from 15 to 60 minutes. The humidity of the gas was maintained at 75% using a saturated NaCl solution in the reactor. The carbonated samples obtained from the batch tests were then analysed so to determine the IC content, following the same procedure adopted for the granules.

2.3.2. Results and discussion

2.3.2.1. Effect of the treatment on the particle size distribution of the granules

The particle size distribution of the granules is reported in Figure 2.10, while in Table 2.3 the d_{10} , d_{50} and d_{90} values are reported, in comparison to the untreated slag. It can be seen that after the granulation treatment (see Figure 2.10a), the mean diameter of the granules increased by increasing the amount of cement in the mixture, probably related to the binding properties of cement and to its finer particle size distribution. In particular, it resulted equal to 2.5 mm for the granules without cement, i.e. three times higher than the untreated slag (0.7 mm), whereas it showed to be equal to 5 and 7 mm for the granules containing 10% and 20% by weight of cement, respectively. Moreover, it can be observed that increasing the amount of cement, the amount of obtained granules having a size lower than 2mm, corresponding to the upper diameter of the untreated slags, was also reduced.

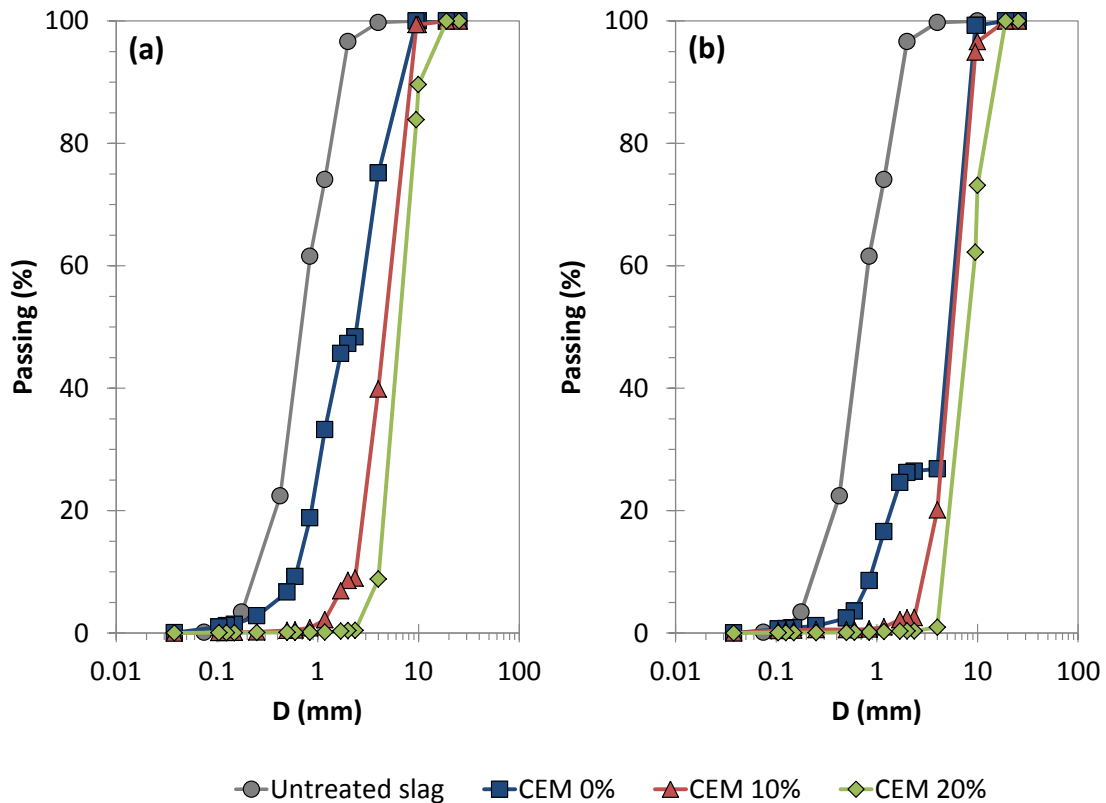


Figure 2.10 Particle size distribution of the untreated slag and of the granules, prepared by replacing the slag with different percentage of cement, obtained after (a) the granulation and (b) the granulation-carbonation treatment.

The effect of the granulation-carbonation treatment on the granule size distribution is reported in Figure 2.10b and it can be seen that, for all the tested mixtures, the size was greater than that achieved without carbonation. However, in this case the mean size of the granules increased less for increasing amount of cement in the mixture. Indeed, similar d_{50} were reached for the granules containing only BOF slags (5.8 mm) and for those containing 10% by wt. of cement (6.2 mm). The mean diameter showed to be slightly higher for the granules made up with 20% by wt. of cement (8.4 mm). Furthermore, it can be seen that the granules without cement were characterized by a higher amount of fine particles, i.e. almost 30% by wt. of the material presented a size lower than 2 mm, with respect to the granules containing cement.

Table 2.3 d_{10} , d_{50} and d_{90} of the untreated BOF slag, and of the granules obtained after the granulation and the granulation-carbonation tests with the BOF blended with 0%, 10% and 20% by weight of cement.

	d_{10}	d_{50}	d_{90}
Untreated BOF slag			
	0.3	0.7	1.8
Granulation			
CEM_0%	0.6	2.5	7.3
CEM_10%	2.4	4.9	8.7
CEM_20%	4.1	7	10.3
Granulation-Carbonation			
CEM_0%	0.9	5.8	8.8
CEM_10%	3.1	6.2	9.2
CEM_20%	4.8	8.4	15.7

2.3.2.2. CO₂ uptake of the obtained granules

The CO₂ uptake achieved after the batch carbonation tests was determined as a function of the CO₂ content after (CO₂ final) and before (CO₂ initial) the treatment, by applying Eq. 2.2, reported in the previous section. The CO₂ uptakes were derived from the results of the inorganic carbon content analysis that for the as received slag was equal to 0.6%. As it can be observed in Figure 2.11, the kinetics of carbonation of the BOF slag did not change significantly with the variation of liquid/solid ratio adopted. In particular, the samples with a l/s equal to 0.4 l/kg showed the lowest kinetics of carbonation, reaching a 3% CO₂ uptake after 60 minutes. However, reducing the amount of liquid showed to slightly increase the uptake of the slag, whose maximum uptake of almost 5% was obtained after 60 min at both l/s ratios of 0.1 and 0.2 l/kg. Actually, although this parameter is highly dependent on the characteristics of the tested residue, also other works reported an l/s equal to 0.125 l/kg as the optimal value for the carbonation of steel slag (Johnson et al., 2003). Moreover, the slight decrease in CO₂ uptake for the

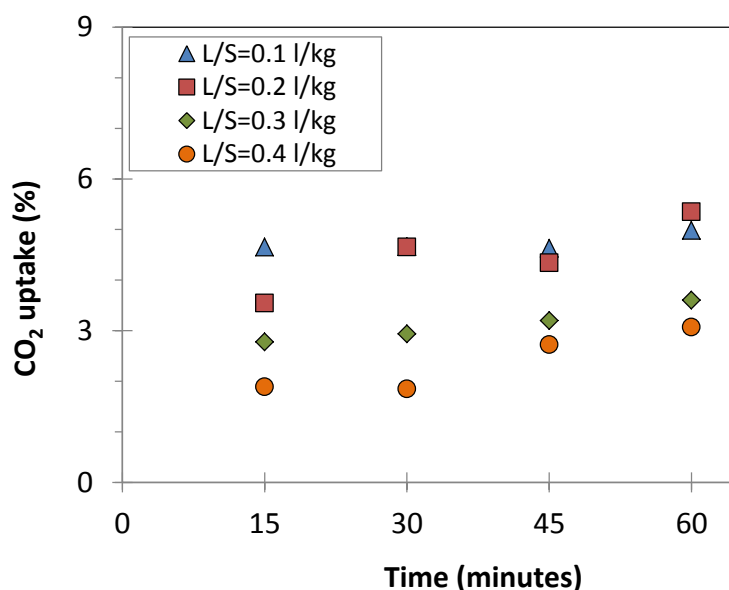


Figure 2.11 CO₂ uptake kinetics of untreated BOF slag as a function of L/S ratio (T=25 °C, p=1 bar CO₂)

highest tested l/s ratio can be likely related to the limited CO₂ diffusion due to the blockage of the pores, filled with water.

The extent of carbonation of the the granules was evaluated as an average value of the obtained sample at three different curing times: immediately after the test and after 7 and 28 days of curing. The IC content of the products of the granulation treatment after 28 days of curing ranged between 1.4% and 0.74%, for the granules obtained by mixing the slag with 0% or 20% of cement, respectively. These values were slightly higher than that obtained for the untreated slag (average IC=0.6%), implying that carbonation occurred, to a larger extent for the samples without cement, also when the material was subjected to the granulation treatment under atmospheric air. The IC content of the granulated-carbonated materials, that ranged between 1.3% and 2.3%, was almost twofold higher than that obtained from the corresponding granulation tests.

On the basis of the carbon content of the treated samples, the CO₂ uptake was evaluated by applying Eq. 2.2, reported in the paragraph 2.2.2.2, and the results are shown in Figure 2.12. For the granulation test (see Figure 2.12a), it can be seen that significant differences of the uptake values, that remained almost stable and negligible, were not retrieved in the first stages of curing (until 7 days) for the granules produced with all the

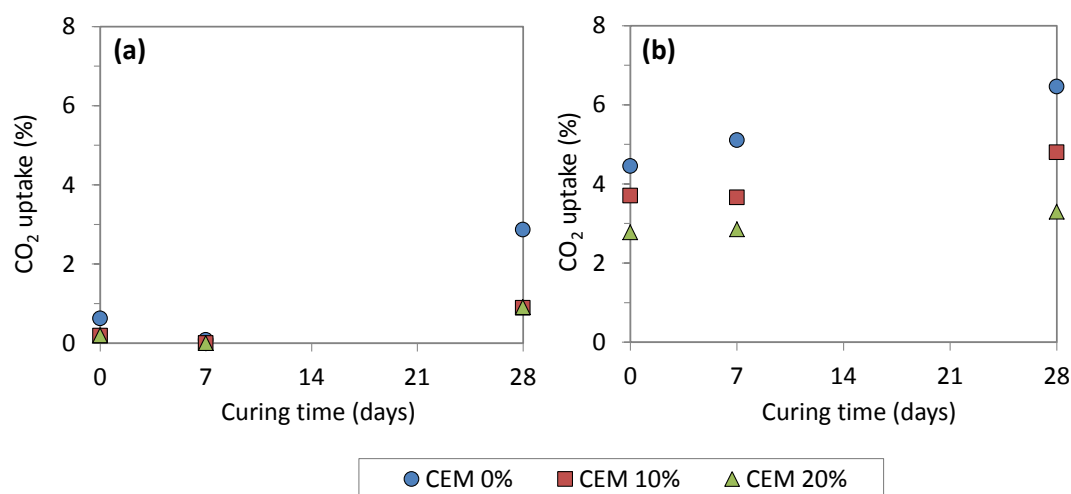


Figure 2.12 CO₂ uptake with curing time obtained from the (a) granulation and (b) granulation-carbonation tests, for the granules obtained by mixing the BOF slag with 0%, 10% and 20% by weight of cement.

different mixtures. The maximum uptake of 3% was achieved after 28 days of curing from the granules constituted of 100% of BOF slag. The CO₂ uptake of the granules obtained after the granulation-carbonation treatment is reported in Figure 2.12b. It can be seen that a higher extent of carbonation was achieved with respect to the granules obtained after the granulation under atmospheric air. Moreover, an increasing trend of the uptake with curing time was observed for all the different mixtures, although it appeared that increasing the amount of cement in the mixture reduced the uptake of the granules. Indeed, faster carbonation kinetics was achieved for the granules without cement (CEM_0%), that reached an uptake of 6% after 28 days of curing. The highest uptake reached from the granules containing 10% and 20% by wt. of cement was equal to 5% and 3%, respectively after 28 days of curing. The value obtained for the granules named CEM_0% resulted lower than that achieved in the previous work (see Figure 2.5), probably because of the different batch of slag used that, in this case, being collected from a different pile outside the storage site of the plant was slightly carbonated than the previous ones.

It can be noticed that, at the tested conditions, the granules constituted of 100% BOF slag showed the highest CO₂ uptake values for all the curing times, that may be ascribed to a higher degree of porosity of these granules with respect to those containing cement. It is likely that the reduced amount of free water, required by the finer cement particles to allow the hydration reactions to occur, may also have exerted an influence on the uptake of the granules based on cement-slag mixtures. Moreover, the addition of cement allowed to produce a more dense granule structure that may have hindered further carbonation with increasing curing times. Indeed, other researchers also found that the total porosity of cement pastes decreased faster with carbonation, due to the reaction of the C-S-H, formed upon hydration of cement with water, and CO₂ (Ngala et al., 1997). However, to confirm this hypothesis, the density and porosity of the granules needs to be further investigated. Moreover, it should be observed that the results of the granulation-carbonation tests, achieved with a considerable amount of material (≈ 500 g) in a dynamic device under ambient T and 1 bar CO₂ pressure, were comparable with those obtained treating 1 g-BOF sample in the static reactor applying the same operating conditions (see Figure 2.11).

2.3.2.3. Effect of the treatment on the environmental behavior of the granules

The leaching behavior of the granules was assessed by following the standard procedure (EN 12457-2), but without previously grinding the material, in order to evaluate the release of the aggregates at conditions similar to their natural use in bound or unbound applications. The pH values of the untreated slag and the granules are reported in Figure 2.13, where it can be seen that the regulatory limit established by the Italian legislation for reuse in simplified procedure (It. MD 186/06), set at 12, was overall exceeded. In particular, after the granulation treatment, the pH value obtained for the granules, regardless the amount of cement in the mixture, showed to be slightly higher than that reported for the untreated slag (12.5).

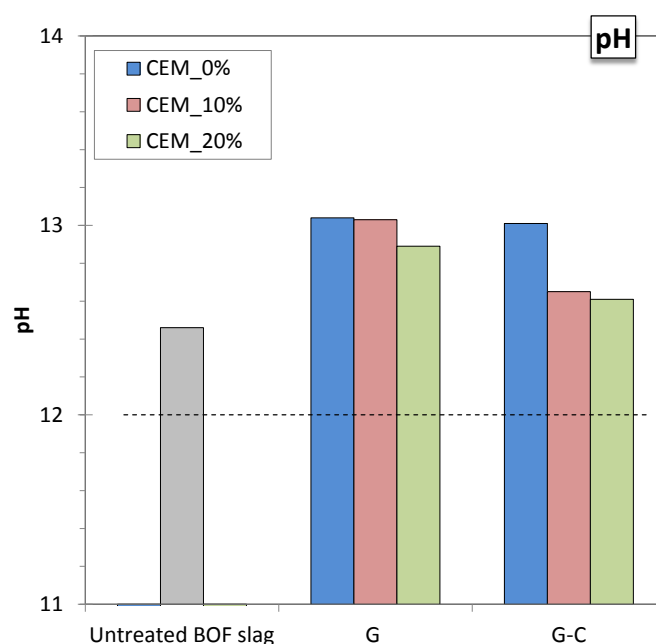


Figure 2.13 pH values obtained for the untreated BOF slag and for the granules after the granulation (G) and granulation-carbonation (G-C) treatments, with different mixtures of cement. The dotted line indicates the limit for reuse as for the It. MD. 186/06

After the carbonation-granulation treatment, the pH of the granules constituted by 100% of BOF slag resulted equal to 13, similar to that obtained without carbonation. Conversely, upon carbonation, the pH of the granules containing cement showed to slightly decrease, passing from almost 13 to 12.6 for both the mixtures. This mild reduction may be ascribed to the carbonation of cement rather than of the BOF slag, since the pH of the granules constituted only by BOF slag showed not to be affected by the carbonation treatment.

The concentrations obtained from the leaching tests carried out on the granules achieved after the granulation and the granulation-carbonation treatments are reported in Figure 2.14, compared to those measured for the untreated BOF slag.

Note that, among the regulatory elements, barium was the only one that presented a concentration higher than the quantification limit of the instrument, but still below the regulatory limit (1 mg/l) established by the Italian legislation for reuse in simplified procedure (It. M.D. 186/06).

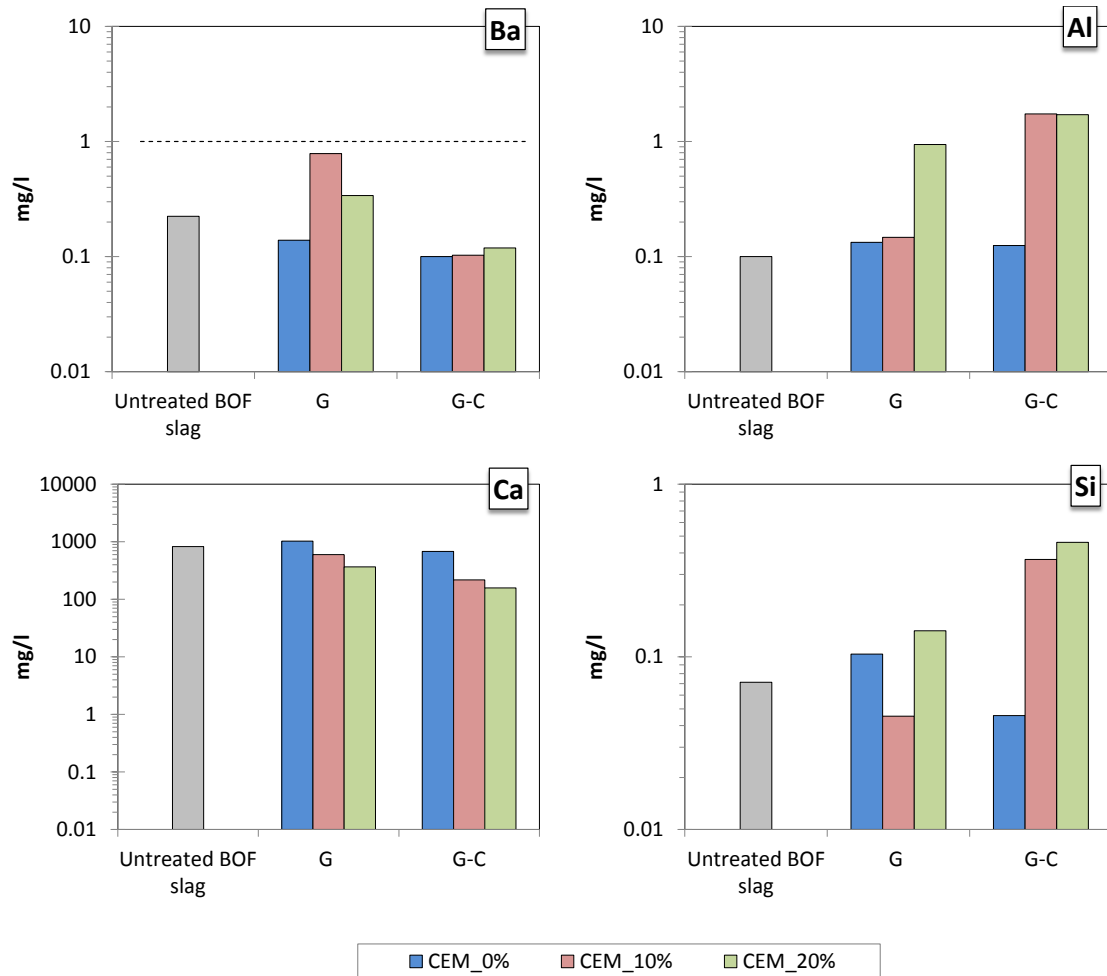


Figure 2.14 EN 12457-2 leaching test results of the untreated BOF slag and of the granules (without crushing the material) after the granulation (G) and the granulation-carbonation (G-C) treatment for different cement mixtures. The dotted line indicates the limit for reuse (It. M.D. 186/06).

The other elements shown in Figure 2.14, i.e. Al, Ca and Si, were selected in order to assess the influence of the carbonation process on the leaching behavior of the aggregates. As for Ba, the concentration obtained for the untreated BOF slag resulted equal to 0.2 mg/l that showed to slightly decrease for the granules obtained from the granulation treatment without using cement in the mixture. On the other hand, the release of Ba showed to increase when the granules were constituted of 10% and 20% by wt. of cement, reaching, in the former case, almost the threshold set for the reuse of the material. This effect is likely correlated to the higher release of Ba from the cement

that in a previous study resulted four times higher than the limit set for reuse (Capobianco, 2014). As for the leaching of major slag constituents, Al concentrations showed to increase after the granulation treatment, and this effect was more evident for the granules with 20% by wt. of cement. The concentrations of Ca showed to decrease for an increased amount of cement in the mixture, passing from 1000 mg/l of the untreated slag to 370 mg/l of the granules with 20% by wt. of cement. Conversely, the release of Si, apart from the lower concentration of the granules with 10% by wt. of cement, resulted almost the same to that obtained for the untreated slag, i.e. 0.1 mg/l.

The carbonation-granulation treatment appeared to affect the leaching behavior of the granules, especially for those containing cement. The concentrations of Ba resulted similar for all of the tested conditions, equal to 0.1 mg/l, and overall lower than those achieved for the untreated slag and for the granules obtained after the granulation treatment. This finding may be related to the formation of Ba carbonates, from either the carbonation of slag or cement (Valls and Vazquez, 2001; Baciocchi et al., 2015b). The leaching of Al showed not to be affected by the carbonation treatment for the granules mixed only with the BOF slag. Conversely, with cement, the release of Al increased of almost one order of magnitude with respect to the non-carbonated granules, probably related to the formation of more soluble phases, like Al (hydro)-oxides. Similarly to aluminum, the release of Si increased after the combined treatment, above all for the granules containing cement, probably owing to the formation of more soluble phases, i.e. SiO₂, derived from either the carbonation of cement (Fernández-Bertos et al., 2004) or of the BOF slag (Baciocchi et al., 2015b). Conversely, upon carbonation, the release of calcium decreased for all of the tested mixtures, although this effect was more evident for the granules containing cement, for which the concentration was halved. This finding may be correlated to the formation of less soluble Ca phases, i.e. calcite, as a result of the reactions of portlandite or of the calcium silicate hydrate like phases with CO₂ (Suzuki et al., 1985; Taylor, 1997).

2.3.2.4. Effect of the treatment on the mechanical strength of the granules

The results of the ACV test performed on the granules obtained after the granulation and granulation-carbonation experiments using different cement mixtures are reported in Figure 2.15 and compared with the values showed in the British standard for the igneous rock (16%), mixed gravel (21%) and blast furnace slag (35%). It can be seen that without cement, the granules were characterized by a low mechanical strength, i.e. an ACV equal to 60%, and the carbonation treatment showed not to exert any effect on the mechanical performance of the aggregates. The poor mechanical properties of these granules were similar to those achieved in the previous section and, once again, they may be ascribed to the low binding potential of this residue when mixed only with water. The use of cement as binder appeared to yield a noteworthy improvement of the mechanical performances of the aggregates, although carbonation showed not to exert any effect on the final strength of the granules. Indeed, the ACV value obtained by replacing 10% by wt. of cement to the initial mixture, resulted equal to almost 25% after both the treatments, ranging between the values reported for blast furnace slag and mixed gravel. Increasing the amount of cement in the mixture of up to 20% by wt. allowed to achieve a lower ACV, comparable with that reported for igneous rocks, i.e. 16%.

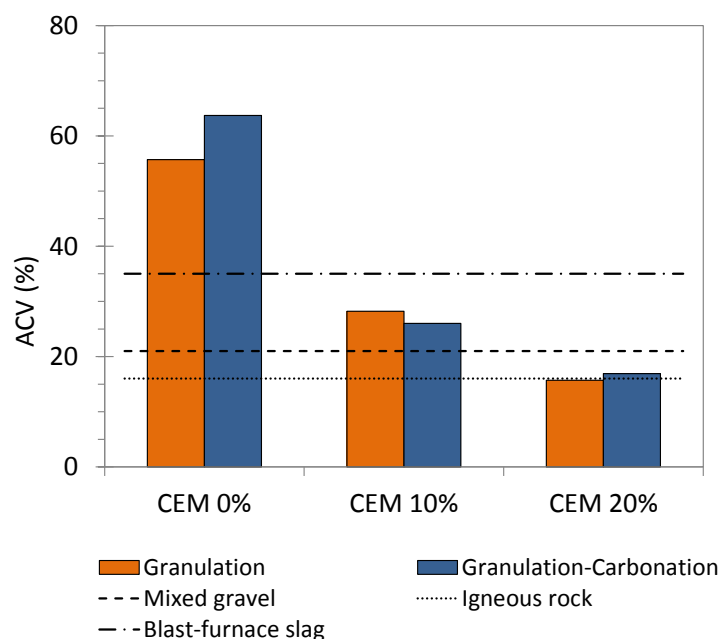


Figure 2.15 Aggregate Crushing Value (ACV) results for the granules obtained after the granulation and the granulation-carbonation treatment blended with different percentage of cement, compared with the values reported in the BS 812-110:1990.

2.4. Main findings

The aim of this chapter was to analyze the effects of a combined granulation-carbonation treatment applied to BOF steel slag. The main physical, chemical and environmental properties of the yielded granules were evaluated and compared to those resulting for the products of granulation tests carried out under atmospheric air. Both tested treatments allowed to produce granules with a tenfold larger particle size compared to the untreated slag. The CO₂ uptake followed a growing kinetics along the reaction time, reaching a maximum of 16% after 90 minutes of treatments. Concerning the mineralogy of the materials, it was found that a very significant conversion of calcium hydroxide to calcite was detected for the granulated-carbonated samples. As for the environmental behaviour of the treated material, relevant differences were observed performing the leaching tests on crushed or uncrushed granules produced by the combined treatment. In fact, the eluates obtained following the EN compliance test (i.e.

crushing the samples), did not exhibit relevant differences in pH and Ba, Ca, V and Zn release compared to the untreated slag; instead, when the leaching tests were performed on the different size fractions of the treated materials without any preliminary size reduction, the coarser fractions of the granulated-carbonated slag exhibited a noteworthy pH reduction, a decrease of Ca and Ba mobility and an increase of V leaching compared to the untreated slag. This result was explained with by differential carbonation of the outer layer of the particles with respect to the inner core, which was confirmed by the relevant differences retrieved in their IC content. Nevertheless, the mechanical strength of the achieved aggregates, measured in terms of ACV, resulted very low compared to that obtained for natural gravel. Hence, with the aim of improving the mechanical properties of the aggregates, both the treatments were applied to slag-cement mixtures, using 10% and 20% by wt. of cement. In this case, the mechanical performance of the granules was greatly improved by combining the slag with cement already for a 10% cement content and reached an ACV similar to that reported in the British Standard for igneous rock, i.e. 16% for the tests carried out using 20% cement. Finally, carbonation seemed not to enhance or hinder the mechanical properties of the obtained granules for all the tested mixtures.

Chapter 3

Effect of coupling alkali activation and CO₂ curing on BOF steel slag

3.1. Introduction

In the previous chapter the effects of a combined granulation- carbonation treatment applied to a BOF steel slag were explored for producing aggregates for civil engineering applications, while also storing CO₂. Besides the effects on the physical and mineralogical characteristics, or the environmental behavior, the obtained granules showed a poor mechanical performance, i.e. not comparable to that reported for the natural aggregates, unless mixing the slag with cement. This result was ascribed to the low binding potential of the residue when mixed with water. Hence, rather than using cement, an alternative and suitable options may be represented by the alkali activation treatment, that could be exploited for enhancing the hardening reactions of the slag. As reported in Chapter 1, the great part of the literature works focused on the application of this process on the amorphous blast furnace slag and fly ash, so to produce alternative binders to cement. However, recent studies (Kriskova et al., 2014; Salman et al., 2014a) were based on the application of the alkali activation treatment to other slag rich in Ca

and Si, also coming from the steel making process (e.g. continuous casting slag or AOD slag) in order to produce a valuable final product. In particular, the work of Salman et al. (2014a) pointed out that treating a crystalline and non-hydraulic slag with an alkali activation treatment coupled with an initial period of steam curing at high temperature allowed to achieve a dense and strong solid, consisting of a calcium silicate hydrate matrix. Actually, besides the alkali activation process, as for all cementitious materials, a curing stage is also needed in order to allow the completion of the hydration reactions. In this regard, the optimization of the different operational curing conditions, such as the relative humidity, the temperature, the time of exposition and the CO₂ concentration, played a prominent role to attain a high quality of the final product (Criado et al., 2010). Different authors have reported that raising up the temperature during the curing phase, regardless the activator used, accelerates the rate of the hydration reactions at early ages, leading to a higher final mechanical strength of the activated-slag mortars (Shi and Day, 1996; Fernández-Jiménez et al., 1999; Bakharev et al., 1999b; Burciaga-Díaz et al., 2013). Moreover, different works have shown that curing blocks of concrete in a CO₂ rich environment allows to achieve similar compressive strength to that obtained for those cured in a steam chamber, that is the most widely adopted and highly energy extensive process in the cement field (Shi et al., 2011; Zhan et al., 2013).

In this light, this chapter reports the investigation carried out on the alkali activation process, coupled with CO₂ curing, on the Basic Oxygen Furnace (BOF) slag in terms of its effects on the mineralogical properties of the obtained material, along with the effects on the mechanical strength and the extent of CO₂ uptake. To this aim, the effects of different parameters were evaluated, which are reported below:

- Activators nature and concentration

The nature of activator exerts a central role in the effectiveness of the activation process. Indeed, the literature studies on the blast furnace slag or fly ash showed that the activation with sodium silicate provided enhanced mechanical strength in a short curing time, while the carbonate-based activators (i.e. Na₂CO₃) were generally responsible for the acquisition of long-term strength (Fernández-Jiménez et al., 1999). The latter finding was ascribed to the lower pH of the alkali solution, that originated a lower

strength development at early curing times. With this type of activator, the mechanical performance proved to increase at later curing time only after the formation of carbonated compounds, due to the high concentrations of CO₃²⁻ ions (Wang et al., 1994). In the current study, two different alkali activators were tested: a mixture of sodium hydroxide and sodium silicate, and a mixture of sodium hydroxide and sodium carbonate, with set molarities and concentrations.

- The combination of alkalis with the CO₂ curing, at either ambient or elevated temperature

The CO₂ curing was carried out in order to assess the effect of carbonation on the slag activated with the different alkali solution. Moreover, the effect of the curing temperature on the extent of carbonation was evaluated, since other works found that increasing the operating temperature exerted a positive effect on the enhancement of the CO₂ uptake of the slag (Bacocchi et al., 2010a).

- The combination of the activated BOF steel slag with other sources of solid silicates, i.e. the blast furnace slag (BFS) at different BOF/BFS ratios (100/0 and 75/25).

The addition of blast furnace slag, which is a residue highly reactive towards alkalis, was tested in order to provide an additional source of silicates into the system for enhancing the production of the resulting main binding phase (calcium silicate hydrate). In this case, the experiments were performed by keeping a constant curing temperature equal to 20 °C.

Hence, this chapter is divided into two main sections: the first one, called materials and methods, that firstly reports in detail the nature of the materials used in this study and the different alkaline compositions used; this first part reports also the methods of characterization of the untreated materials, the experimental techniques used to evaluate the effects of different activators on the early hydration reactions (this phase was called “screening phase”) and on the long-term reactions of hydration and carbonation, and

finally, the preparation of mortar samples, along with the analysis carried out for the evaluation of the strength of the materials.

The second section, after reporting the results of the characterization of the untreated materials, firstly describes the findings achieved in the initial screening phase, obtained by performing a calorimetric study on the BOF slag and on the BOF/BFS mixture, with the aim to select the alkaline solutions able to provide the faster rate of hydration. Afterwards, the alkaline solutions that showed to accelerate the hydration reactions of the slag were selected for the further investigations of the reactions occurred at later curing time. In this case, the effects on the BOF slag, in terms of mineralogy, of the alkali activator, the different curing conditions and the mixture with the blast furnace slag, are presented. Finally, in the last part of the chapter, the extent of carbonation of the samples and the mechanical performance of mortars prepared with either the BOF slag or the blended slag were assessed after curing the samples in a CO₂ rich environment.

3.2. Materials and methods

3.2.1. Materials and alkaline solution composition

The slag analyzed in this study was collected at the outlet of the basic oxygen furnace (BOF) of an Italian steel plant employing the integrated steelmaking process, after crushing and magnetic separation for iron and metal recovery, different to that used in the previous chapter. The blast furnace slag used in the blended mixtures with BOF slag were collected from a Belgian steelmaking plant.

The slags were activated by using two different solutions:

- i) a mixture of sodium hydroxide (NaOH) and sodium silicate (Na₂SiO₃)

Two sodium hydroxide solutions of 2M and 4M, prepared by dissolving the pellets (fisher scientific, 99.4% purity) in the deionized water, were mixed in a 50:50 and 75:25

weight ratio with a commercial solution of sodium silicate (ABCR GmbH Co. KG, 39-40% silicates in water). The silica modulus of the four solutions, expressed as the molar ratio of SiO₂ and Na₂O, is reported in Table 3.1.

ii) a mixture of sodium hydroxide (NaOH) and sodium carbonate (Na₂CO₃)

Two sodium hydroxide solutions of 2M and 4M, prepared as reported for the previous mixture, were mixed in a 50:50 and 75:25 weight ratio with two sodium carbonate solutions of 1M and 2M, respectively. The molarities of the sodium carbonate solution were set in order to achieve the same sodium oxide content of the sodium hydroxide solutions, that resulted equal to 5% and 10.5% for the lowest and the highest molarity, respectively.

A summary of the adopted alkali solutions, as well as the code employed to identify them in the results, is presented in Table 3.1.

The molarity of sodium hydroxide was set below 5M, since other works observed the presence of efflorescence on specimens activated with a NaOH solution equal or higher than 5M and cured in the humidity chamber (Salman, 2014b). This effect is related to the high concentration of activator in the slag that, in combination with the moist curing conditions (RH>90%), may leach out the sodium ions. The latter are more able to react with the atmospheric CO₂ to form the corresponding carbonate (Na₂CO₃•nH₂O) which can hydrate, giving rise to the efflorescence phenomenon. Other works also showed that increasing the amount of alkali-activators in the specimens increase the severity of efflorescence (Allahverdi et al., 2008).

In this study, the nature and concentration of the activator and the BOF/BFS ratio, along with the curing conditions, were evaluated to assess their influence on the BOF slag. Table 3.2 reports the identification code of the slag mixtures that will be further adopted in the discussion of the results.

Table 3.1 Activator type and the corresponding molarity, weight ratio, silica modulus and code of identification of the alkaline solutions adopted.

Activator type and molarity	Weight ratio	Silica modulus	Code
NaOH (2M) + Na ₂ SiO ₃	50:50	2.3	NH (2M) + NS_50:50
NaOH (2M) + Na ₂ SiO ₃	75:25	1.4	NH (2M) + NS_75:25
NaOH (4M) + Na ₂ SiO ₃	50:50	1.7	NH (4M) + NS_50:50
NaOH (4M) + Na ₂ SiO ₃	75:25	0.85	NH (4M) + NS_75:25
NaOH (2M) + Na ₂ CO ₃ (1M)	50:50	-	NH (2M) + NC (1M)_50:50
NaOH (2M) + Na ₂ CO ₃ (1M)	75:25	-	NH (2M) + NC (1M)_75:25
NaOH (4M) + Na ₂ CO ₃ (2M)	50:50	-	NH (4M) + NC (2M)_50:50
NaOH (4M) + Na ₂ CO ₃ (2M)	75:25	-	NH (4M) + NC (2M)_75:25

Table 3.2 Composition of the slag mixtures used.

Code	Amount of BOF slag (% by wt.)	Amount of BF slag (% by wt.)
BOF100	100	0
BOF75	75	25

3.2.2. Methods

3.2.2.1. Characterization of the untreated sample

The particle size of the air-dried BOF slag sample was determined by applying the ASTM D422 standard procedure. The as-received BF slag sample was dried, milled and the particle size distribution was measured by using the laser scattering method (MasterSizer Micro Plus, Malvern), where the samples were dispersed in ethanol. The

chemical characterization of both slags was obtained with the alkaline fusion method, consisting of mixing the milled material with Li₂B₄O₇, heating at 1050 °C in a muffle and dissolving the material in a solution of nitric acid, at concentration of 4%; thus, it was obtained a solution analyzed by the ICP-OES analyzer. The mineralogical compositions was evaluated by powder X-ray diffraction (XRD) analysis with Cu Ka radiation using a Philips Analytical PW 1710 diffractometer, operating at 45 kV and 35 mA, with an angular step of 0.02° held for 2s over a range of 5°-75° 2θ. The Inorganic Carbon (IC) content was evaluated by using a Shimadzu TOC VCPH analyser equipped with a SSM-5000A solid sampler.

3.2.2.2. Screening phase: calorimetric test to evaluate the early-age hydration reactions

The early hydration kinetics was investigated through isothermal conduction calorimetry, carried out in a TAM Air device (TA instrument), on the BOF slag pastes (slag + activator) obtained by using the BOF slag fraction below 0.25 mm, which corresponds to 41% by weight of the total amount of the sample. The BOF slag pastes were prepared by mixing the slag either with water or with the alkali solutions, reported in Table 3.1, by keeping the liquid to slag ratio equal to 0.3 l/kg. The calorimetric tests performed on the BOF100 were carried out at two temperatures, i.e. 20 °C and 50 °C, in order to assess the effect of the temperature on the rate of the heat of hydration. Besides, pastes prepared by using the BOF75 mixtures were mixed with the different alkali solution reported in Table 3.1, at a liquid to solid ratio of 0.4 l/kg, and placed in the calorimetry at 20 °C. The different liquid to solid ratio used for the previous mixtures was due to the different workability of the different materials with the alkali solutions. Moreover, before the insertion in the calorimeter, the material was mixed by hand for three minutes and this operation lead to a loss of information regarding the initial heat of wetting, that corresponds to the first high peak detected in the calorimetric curves,

which was not considered in the calculations of the cumulative heat flow curves (Garcia-Lodeiro et al., 2013).

Based on the results achieved from the calorimetric test, the mixtures of sodium hydroxide/sodium silicate and of sodium hydroxide/sodium carbonate that yielded the higher degree of hydration were selected for testing the effect of the process on the long-term reactions, at different curing conditions.

3.2.2.3. Evaluation of the effects of the combined process (alkali activation and CO₂ curing) on the long-term reactions

Paste preparation and curing conditions

The slag pastes were prepared in a plastic mould of 2.5 x 2.5 x 2 cm³, using about 15g of the as-received material.

The BOF100 pastes were prepared by using a alkali solution to slag ratio equal to 0.2 l/kg; after having mixed the slag with the activator solution for three minutes, the pastes were cured for 3, 7 and 28 days in the curing chambers at the following conditions:

- a humidity chamber (HC), RH=98% and T=22 °C, used as reference.
- two carbonation chambers at set CO₂ concentration (5%) and relative humidity (75%), but kept at two different temperatures: 20°C (CC20) and 50 °C (CC50). The relative humidity of both the carbonation chambers was kept constant by using a saturated K₂CO₃ solution.

The long term reactions were also assessed on the blended mixture consisting of 75% by wt. of BOF slag and 25% by wt. of BFS (BOF75). The solution to slag ratio was set equal to 0.4 l/kg, that showed to be the optimal value to ensure the workability, and the blended pastes were cured in the humidity chamber and in the carbonation chamber at 20 °C, at the same conditions reported for the BOF100 pastes.

During the curing period, the pastes were demoulded at the same time when a suitable consistency was achieved, and replaced in the same chamber, in order to allow the overall exposure of the surfaces of the samples to the atmosphere of the chambers. After

the curing time, the pastes were powdered in an agate mortar and dried in a vacuum-drier (Alpha 1-2 LD, Martin Christ) for 2 hours at 0.011 mbar, according to the sublimation curve of the water, in order to remove the free water content and stop further hydration reactions.

Methods of characterization of the pastes

The crushed pastes were analyzed in terms of their mineralogy, in order to identify the reaction products obtained with the different alkali solutions and curing conditions adopted.

The mineralogical compositions of both untreated material and slag pastes was evaluated by powder X-ray diffraction (XRD) analysis with Cu Ka radiation using a Philips Analytical PW 1710 diffractometer, operating at 45 kV and 35 mA, with an angular step of 0.02° held for 2s over a range of 5-75 2θ.

The thermogravimetric analysis (TGA) was carried out with a Netzsch STA 409 PC DSC-TGA equipment in an atmosphere of pure N₂ at 60 ml/min, over a temperature range of 20-1000 °C, at a heating rate of 10 °C/min and the differential thermal gravimetry (DTG) data were used to identify the reaction products. The bound water content was calculated from the mass loss up to about 450-500 °C by applying the method described in Marsh and Day (1998) and Taylor (1997).

The carbonate content was evaluated also by Inorganic Carbon analysis using a Shimadzu TOC VCPH analyser equipped with a SSM-5000A solid sampler. The degree of carbonation of the samples, assessed by measuring the inorganic carbon content (IC), was calculated by applying the following equation:

$$\text{CO}_{2\text{uptake}} (\%) = \frac{\text{CO}_{2\text{final}} (\%) - \text{CO}_{2\text{initial}} (\%)}{100 - \text{CO}_{2\text{final}} (\%)} \cdot 100 \quad (3.1)$$

where the IC concentration of the untreated sample (CO_{2 initial}) and of the treated one (CO_{2 final}) is expressed in terms of its CO₂ weight percent.

3.2.2.4. Mortars preparation and compressive strength analysis

The mortar samples for the compressive strength analysis were prepared following the EN 196-1 standard method. Firstly the material was mixed with 0-2 mm sand river at a 1:3 slag to sand ratio, and then the activator was added, at a liquid to slag ratio set equal to 0.9 in order to maintain the workability of the mortars. Uniformly, each alkali activated mixture was cast in three steel molds (4 x 4 x 16 cm³) and compacted for 3 minutes in a jolting machine so to remove air bubbles. It was decided to cure the slag mortars in the two carbonation chambers, keeping the same curing conditions and time as for the slag pastes. Furthermore, once achieved the suitable consistence, the mortar beams were cut in four cubes (4 x 4 x 4 cm³), and then placed back into the CO₂ chambers to complete the curing. The mechanical strength of the mortar cubes was assessed in duplicate by using the Schenck-RM 100 compression testing machine, with a loading rate set equal to 2 mm/min.

The mechanical strength was evaluated on the mortar samples prepared with the BOF100 composition, activated with both the alkali solutions and cured in both the carbonation chambers, i.e. CC20 and CC50. It was decided to test only the samples cured in the carbonation chamber, since based on the crushing resistance of the slag pastes, it was expected that the mortar specimen would not acquire a suitable mechanical resistance for the test if cured in the humidity chamber. Moreover, it was also decided to test the BOF75 composition, activated with the sodium hydroxide/sodium silicate solution and cured in the carbonation chamber at 20 °C (CC20) in order to figure out the effects of this composition on the mechanical strength

3.3. Results and discussion

3.3.1. Characterization of the untreated materials

The particle size distribution of the untreated BOF slag sample, reported in Figure 3.1, showed a material characterized by particles smaller than 2 mm with a mean diameter equal to 0.35 mm. The milled blast furnace slag showed a mean diameter equal to 5 μm.

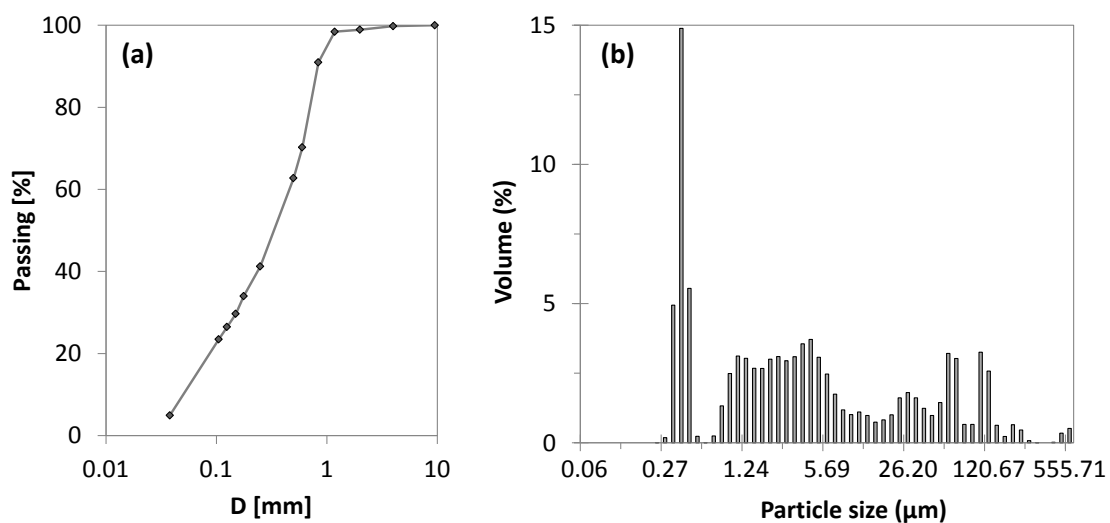


Figure 3.1 Particle size distribution of (a) the BOF slag sample and (b) the BFS sample

The main chemical constituents of the BOF slag sample, reported in Table 3.3, were Ca (265 g/kg) and Fe (221 g/kg), as also reported in Santos et al. (2012), followed by Mg (45.7 g/kg) and Mn (41.5 g/kg). Such constituents slightly differ from the ones reported for the BOF slag sample described in the previous chapter, as this BOF slag sample was collected from a different pile. With respect to the BOF slag, the BF slag showed a slightly higher content of calcium (301.8 g/kg), as well as of Si (164.3 g/kg) and Al (49.1 g/kg), which constituted the main element. These latter values are close to those reported in other literature studies (Escalante et al., 2001).

Table 3.3. Elemental composition of the as-received BOF slag and of the BF slag sample, expressed as % on a dry weight basis.

Element (%wt.)	BOF slag	BF slag
Al	0.97	4.91
Ba	0.006	0.04
Ca	26.5	30.18
Cr	0.13	0.001
Cu	0.03	0.01
Fe	22.12	0.29
K	0.06	0.82
Mg	4.6	5.17
Mn	4.15	0.11
Na	0.19	0.25
Si	2.2	16.43
V	0.05	0.01
Zn	0.03	0.003

The XRD pattern of both the as received materials are reported in Figure 3.2. It is evident that the BOF slag are characterized by a crystalline nature, with the main phases detected being dicalcium silicate (larnite), wuestite (FeO), Ca-Al-Fe oxide (Ca₂Fe_{1.4}Al_{0.6}O₅), srebrodolskite (CaFeO₄) and traces of portlandite. In this case, the mineralogy of this batch of slag was different from the one reported in Chapter 2, where also peaks of portlandite and coesite characterized the mineralogy of the slag. On the contrary, the blast furnace slag displayed an amorphous character, with two humps and only one peak that could be ascribed to merwinite (Ca₃Mg(SiO₄)₂).

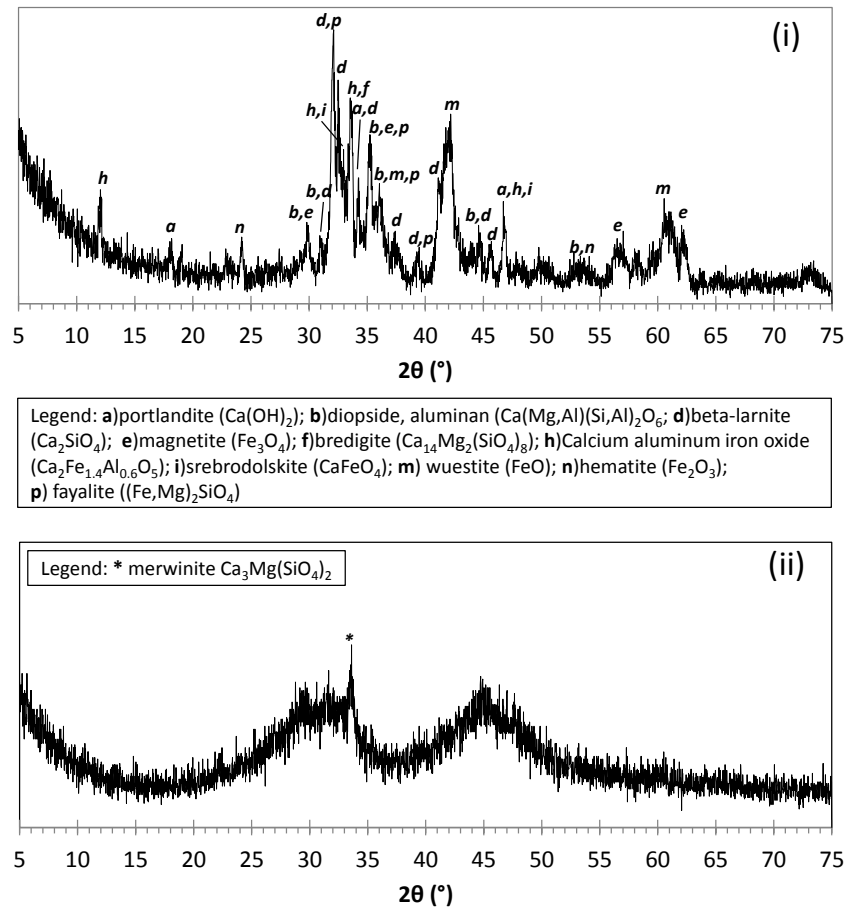


Figure 3.2 XRD patterns of as-received (i) BOF slag and (ii) BF slag.

3.3.2. Screening test: evaluation of the short-term reactions by heat of hydration

3.3.2.1. Hydration rate of BOF slag mixed with water

The evaluation of the heat flow produced by the hydration reactions as a function of time has been widely employed to understand the mechanism that governs the hydration of cement (Bullard et al., 2011). In this work, the calorimetric study was performed to gain insight on the rate of the hydration reactions of the material mixed with different alkaline solutions and with water, used as reference.

Figure 3.3 reports the isothermal conduction calorimetry results of the BOF slag mixed with water. It shows the presence of an initial narrow peak, probably associated with the phases reactive to water contained in the BOF slag, e.g. C₂S, or to the disturbance of the isothermal conditions while the sample is placed in the calorimeter. Along the reaction time, the cumulative heat flow gave evidence of a slow hydration reactivity of the BOF steel slag mixed with water, probably related to the hydration of C₂S forming C-S-H like phases, in accordance with the findings of Wang and Pan (2010) and Wang et al. (2011).

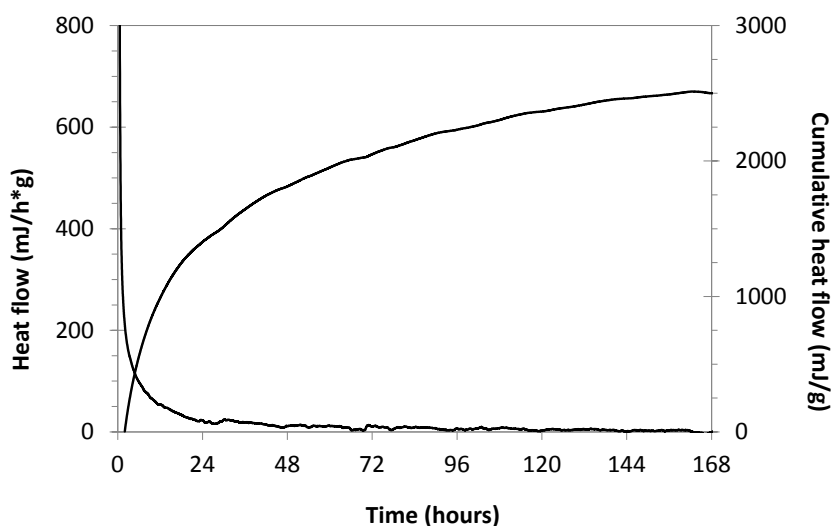


Figure 3.3 Heat flow and cumulative heat flow at 20 °C of BOF slag hydrated with deionized water.

3.3.2.2. Effect of alkali activation on BOF slag at 20 °C

The results of the isothermal conduction calorimetry for the BOF slag activated with different combination of sodium hydroxide/sodium silicate are reported in Figure 3.4a and b. In terms of the cumulative heat flow pattern (Figure 3.4b), the results showed that as the molarity of the sodium hydroxide decreases, the final heat value increases and the highest heat value (almost 45 J/kg) was observed for the solution named NH (2M) + NS_{50:50}, also characterized by the highest silica modulus. Hence, as the heat

release is assumed to be associated with the hydration of the minerals, the BOF slag shows the fastest reaction kinetics with this solution. Also Krizan and Zivanovic (2002) reported that, for the blast furnace slag, there is a correlation between the silica modulus of the solution and the release of heat, and the authors attributed this finding to the faster hydration rate of the calcium silicate hydrates. On the other hand, it is possible to see in Figure 3.4b that the mixtures containing sodium hydroxide with a molarity of 4M showed the lowest cumulative heat flow values, regardless the hydroxide content. However, for all the tested solutions, it is evident that the cumulative heat flow curves did not reach a final stable trend even after 15 days of reaction, highlighting a slow hydration kinetics of the activated samples.

The heat flow patterns are reported in Figure 3.4a and were characterized by different peaks at different time intervals. First of all, as previously reported for the hydration curve of the material mixed with water, an initial very early sharp peak was obtained, that can be associated to the initial heat of wetting, which is in turn associated to the initial dissolution of the material (Fernández-Jiménez et al., 1998). This intense initial peak was followed, for all the solutions considered, by a delay period of slow reaction rate, which can be identified by the lack of peaks. After this phase, whose extent depends on the alkali solution used, different exothermic peaks were observed, associated to the precipitation of the reaction products. The longest delay period and the highest peak were observed for the activating solution containing NaOH 4M at 75% by wt., while no peaks were detected when the BOF slag was activated with a solution containing the same molarity (4M) but lower amount (50% by wt.) of the sodium hydroxide. Conversely, two early consecutive peaks were observed when the BOF slag was activated with the solution containing NaOH 2M at 75% by wt., while two broad exothermic peaks, with a slow kinetics of depletion, were observed for the mixture containing sodium hydroxide 2M at a 50% by wt.

Other works dealing with blast furnace slag found that a long induction period is usually related to the C-S-H precipitation (Shi and Day, 1995). Shi et al. (1995) observed the presence of large peaks for a blast furnace slag activated with a sodium silicate solution, which were related to the polymerization reactions of the available silica ions present in

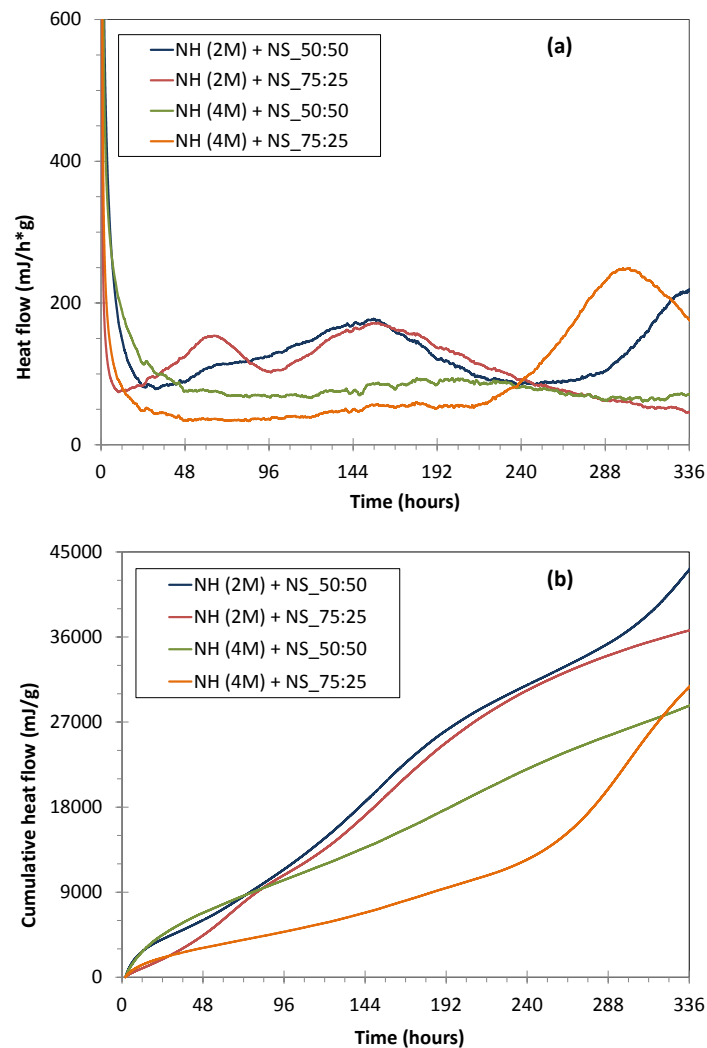


Figure 3.4 (a) heat flow and (b) cumulative heat flow of the BOF100 at 20 °C, mixed with different molar concentrations and weight ratios of a mixture of NaOH and Na₂SiO₃

the solutions. However, it should be underlined that most of the relevant literature on alkali activation has been carried out on blast furnace slag, which contrary to steel slag, is a glassy and amorphous residue. Recently, the work of Salman et al. (2015) focused on the effects of alkali activation on crystalline stainless steel slag, by testing different solutions based on silicates. The calorimetric results at 80 °C revealed that the higher cumulative heat was obtained for the highest amount of silicate in the activating

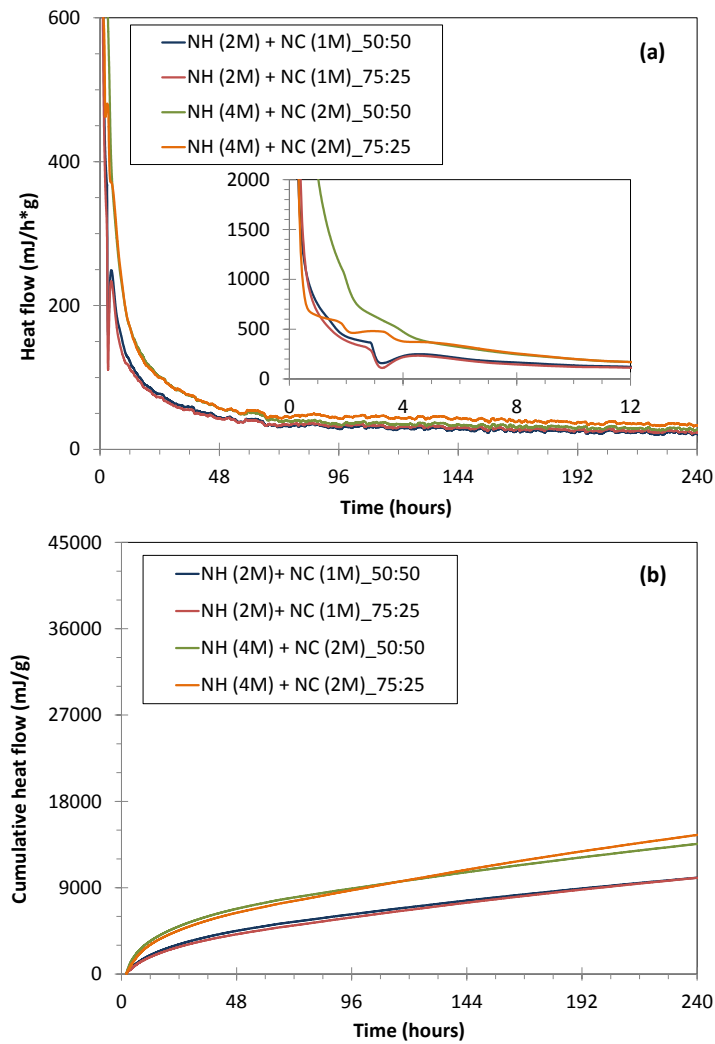


Figure 3.5 (a) heat flow and (b) cumulative heat flow of BOF100 at 20 °C, mixed with different molar concentrations and weight ratios of a mixture of NaOH and Na₂CO₃

solution, while the earliest heat release peak was achieved for the lowest content of silicates in the activating solution. These trends were similar to those obtained in this study, although at 20 °C the process showed to be highly delayed, as shown by the time (more than ten days) required to activate the hydration reactions.

The findings of the calorimetric study carried out at ambient temperature obtained for the pastes activated with the sodium carbonate/sodium hydroxide solutions are reported in Figure 3.5. The cumulative heat flow curves, reported in Figure 3.5b, showed an

overall intensity lower than that observed for the pastes mixed with the sodium silicate/sodium hydroxide solution (see for comparison Figure 3.4). Indeed in this case, the final highest cumulative heat value resulted equal to almost 15 J/g, three times lower than the highest one reported in Figure 3.4b for the sodium hydroxide/sodium silicate solution. After the first 72 hours of reaction, no meaningful heat exchange of the cumulative heat curves with time occurred and the higher heat release was achieved for the samples activated with a solution of sodium hydroxide 4M and sodium carbonate 2M (mixed at a 75:25 % by wt). Actually, only a slight difference can be observed between the trend of this curve and the other ones, which can be correlated to the slight initial curvature observed in the heat flow curves (see Figure 3.5a). Indeed for the latter, beyond the initial intense peak associated once again to the heat of initial wetting, small or not appreciable peaks were observed in the first hours of the reaction, as reported in the small panel into the Figure 3.5a. Afterwards, it seemed that the hydration reactions occur slowly since the formation of peaks was not observed along the reaction time. Garcia-Lodeiro et al. (2013), working on a mixture of cement and fly ash activated with a sodium carbonate solution, associated the calorimetric peaks of low intensity detected in the early hours of reaction to the precipitation of carbonates (calcite and gaylussite).

3.3.2.3. Effect of alkali activation on BOF slag at 50 °C

Although exothermic peaks were observed upon the activation of BOF slag at 20 °C, it can be seen from Figure 3.4 and Figure 3.5 that the cumulative heat release, mainly for the sodium carbonate solution, showed rather low values. This may be attributed to the slow reaction rate at ambient temperature (20 °C), which does not give sufficient dissolution of the silicates and, subsequently, precipitation of the main reactive and hardening phases of the slag, as reported in other studies (Shi and Day, 1996). Therefore, the effect of alkali activation on the early hydration reactions was also evaluated at a temperature equal to 50 °C, by performing the calorimetric measurements on the BOF steel slag with the alkali solution reported in Table 3.1. The results of the

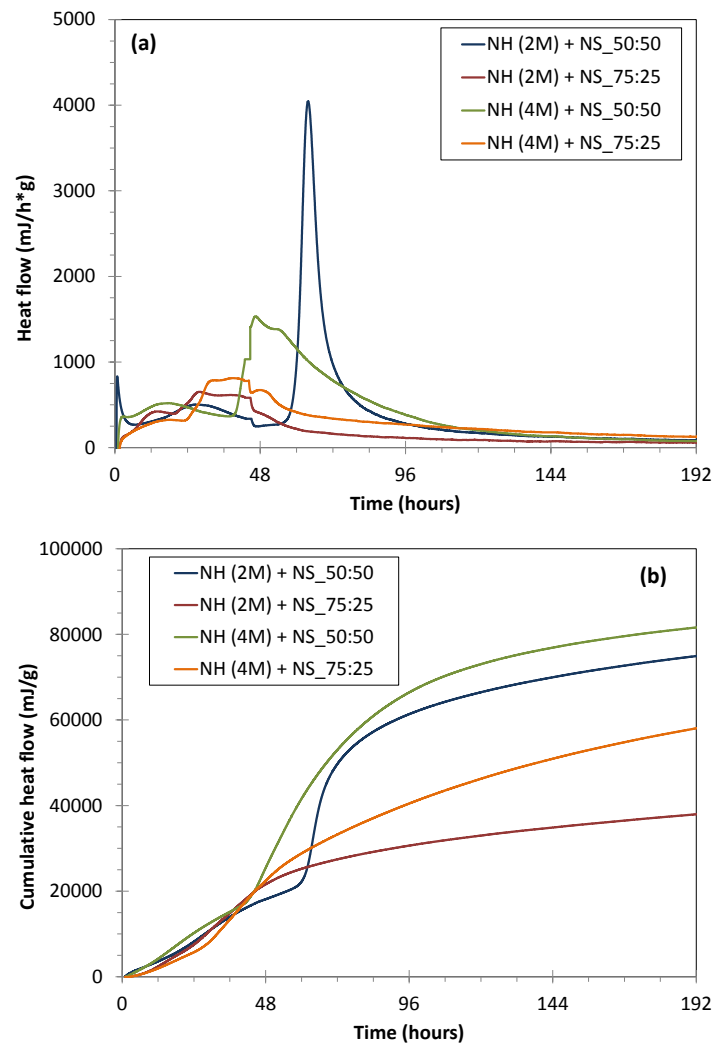


Figure 3.6 (a) heat flow and (b) cumulative heat flow of BOF100 at 50 °C, mixed with different molar concentrations and weight ratios of a mixture of NaOH and Na₂SiO₃

study carried out at higher temperature are shown in Figure 3.6 and Figure 3.7 and it can be observed that, for all of the tested solutions, the yielded heat or cumulative heat flow values showed to be higher than those achieved at 20 °C, suggesting an acceleration of the reaction kinetics at this enhanced temperature.

As far as the sodium silicate/sodium hydroxide solutions are concerned (see Figure 3.6a and b), it can be observed that, in terms of cumulative flow, the highest amount of heat release was obtained for the mixtures containing the same amount of sodium hydroxide

(50% by wt.), regardless the molarity. Hence in this case, the greater heat release was correlated to the amount of hydroxides present in the solution, rather than to the molarity, conversely to what observed in the calorimetric curves obtained at 20 °C. The highest cumulative heat flow value obtained after nine days of reactions resulted equal to 80 J/g for the solution containing NaOH 4M at 50% by wt., showing to be double than the greater one obtained at 20 °C. This behavior may be attributed to the enhanced slag dissolution rate for higher NaOH content, since, at this temperature, it is likely that the amount of NaOH directly influence the rate of reaction, leading to an enhancement of the breakdown of the CaO or MgO bonds in the slag and to a subsequent faster precipitation of the reaction products (Altan and Erdogan, 2012).

The heat flow patterns, displayed in Figure 3.6a, were characterized by two main peaks: the first one occurs in the first days of the reaction and has an extent dependent on the type of activator and the second one showed, in any case, an intensity higher than the first one. The highest peak was achieved after three days of reaction with the activator solution composed of a sodium hydroxide concentration of 2M at 50% by wt. and was characterized by a height equivalent to 4 J/gh. Therefore, comparing these results with those obtained at 20 °C, it can be concluded that the main effect of the temperature increase is to accelerate the hydration reactions, since the formation of two peaks, only hinted at 20 °C, already occurred in five days of reaction. Moreover, these results are in agreement with the findings achieved in Salman et al. (2015), since setting the molarity of the solution, it resulted that the higher cumulative heat was obtained for the highest amount of silicate in the activating solution, while the earliest heat release peak was achieved for the lowest content of silicates in the activating solution.

Concerning the sodium hydroxide and sodium carbonate activator, the general shape of both the heat flow and cumulative heat flow curves at 50 °C (see Figure 3.7a and b) was considerably similar to that reported at lower temperature (see Figure 3.5), although in the former case a heat intensity five times higher was retrieved, indicating the fast dissolution of the reactive phases. The small panel present in Figure 3.7a shows a particular of the heat flow patterns in the first hours of the reaction. For the pastes mixed with the solutions containing the highest concentrations of both the activators,

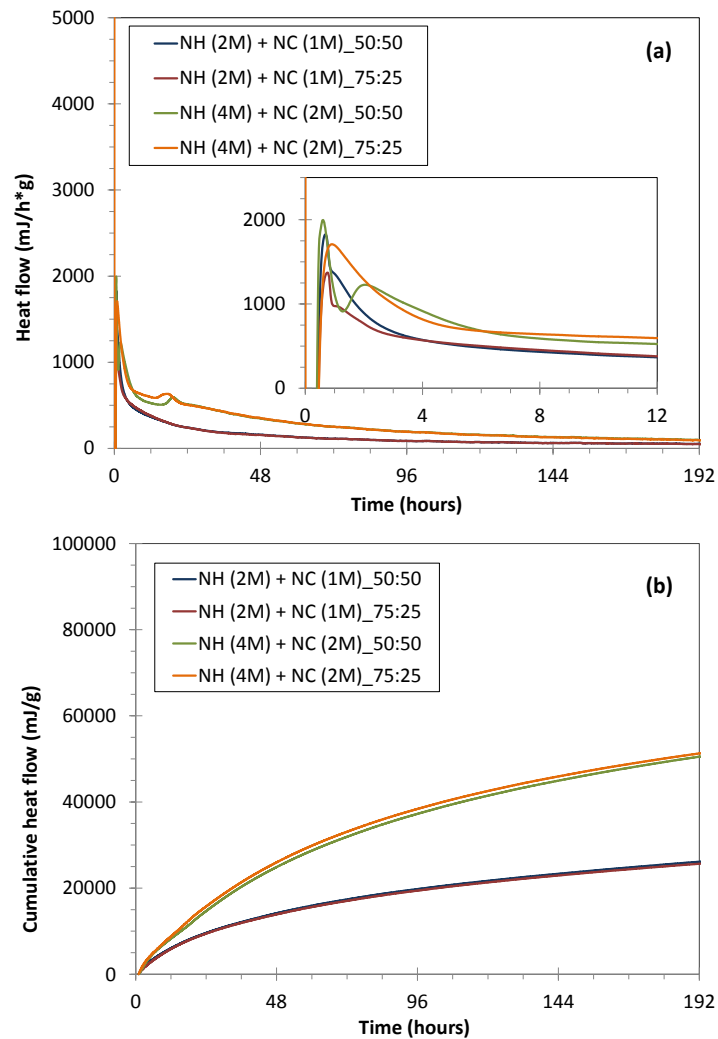


Figure 3.7 (a) heat flow and (b) cumulative heat flow of BOF100 at 50 °C, mixed with different molar concentrations and weight ratios of a mixture of NaOH and Na₂CO₃

along with the first initial tight peak, a small shoulder was observed in the first hour of reaction, meaning that a fast second dissolution step occurred at higher temperature. These mixtures showed also the same highest cumulative heat flow values (equal to 40 J/g), followed in pairs by the ones with lower concentrations, as obtained also for the samples analyzed at lower temperature.

3.3.2.4. Effect of alkali activation on BOF/BFS mixture at 20 °C

The results obtained by performing the calorimetric analysis on the slag pastes made up with 75% by weight of BOF slag and 25% by weight of BFS (labelled as BOF75), mixed with different concentrations of sodium hydroxide and sodium silicate (see Table 3.1), are reported in Figure 3.8.

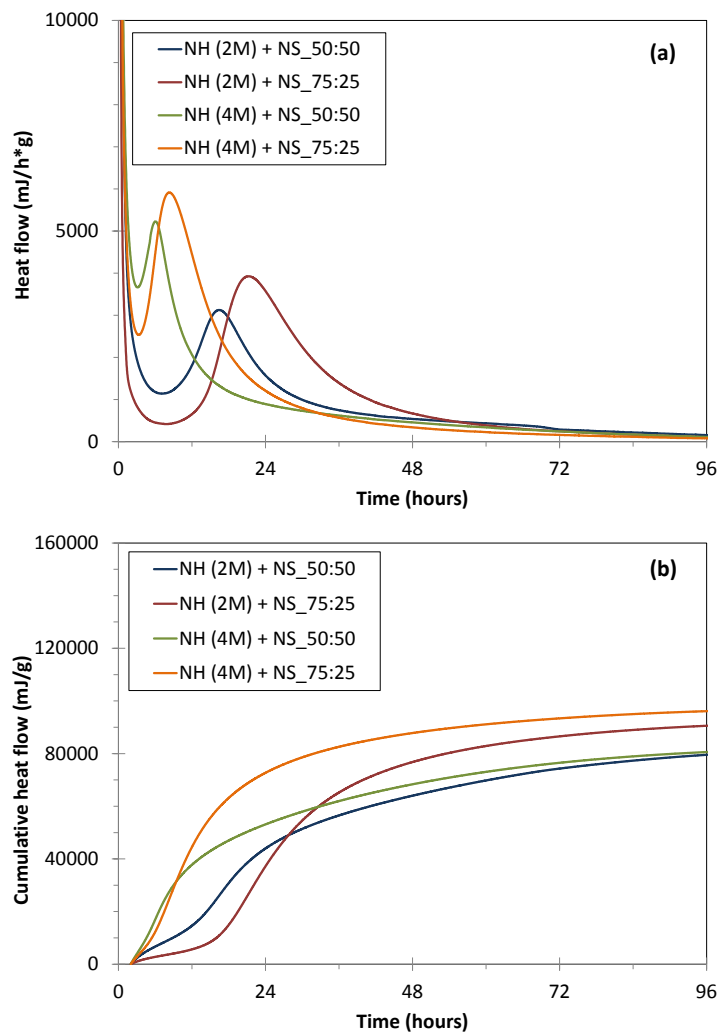


Figure 3.8 (a) heat flow and (b) cumulative heat flow of BOF75 at 20 °C activated with different molar concentrations and weight ratios of mixtures of NaOH and Na₂SiO₃

In the early time (up to 36 hour), the cumulative heat release pattern (see Figure 3.8b) showed a trend slightly different to that achieved in the late hours, probably related to a different degree of the hydration reaction of the material with the different solutions along the time. In particular, after 96 hours of reaction, the highest cumulative heat flow values were retrieved for both the solutions containing 75% of the sodium hydroxide, even if the one with NaOH 2M presented the slowest initial hydration kinetics. Making reference to the silica modulus of the silicate activators (see Table 3.1 for comparison), it can be observed that increasing this value (from 0.8 to 2.3) led to a slight decrease of the final cumulative heat flow values. Krizan and Zivanovic (2002) displayed a different result for the blast furnace slag pastes, since for the authors the presence of a higher amount of silicates in the activating solution (and so higher values of the silica modulus) should result in a higher total cumulative heat release due to an acceleration of the formation and hence precipitation of the reaction products.

As for the heat flow trend (see Figure 3.8a), two main peaks were observed, for all the tested conditions, in the first hours of reaction. The initial peak, occurred in the first minutes, was related to the initial dissolution of the material after mixing, while the second one, detected in the first 48 hours of reaction, showed an intensity and extent depending on the activator nature. Indeed, it can be observed that the solution with a molarity of NaOH equal to 4M allowed to achieve the peaks within less than one hour, while reducing the concentration of NaOH to 2M led to a delay in the peak formation and hence to a longer initial induction period. According to Krizan and Zivanovic (2002) and to Garcia-Lodeiro et al. (2013), the precipitation of C-S-H gel resulted in a longer induction period. In this case, the molarity of the sodium hydroxide in the alkaline mixture exerts the main effect on the initial rate of the reaction, regardless its amount in the solution. This finding was also reported in the work carried out by Altan and Erdogan (2012) on the blast furnace slag, where, setting the amount of water-glass in the activator, the heat evolution peak and the cumulative heat flow showed to increase when the NaOH concentration increased.

When the mixture of Na-hydroxide and Na-carbonate at different molarities was used as activator (see Figure 3.9a and b), the highest peak was the one associated to the highest

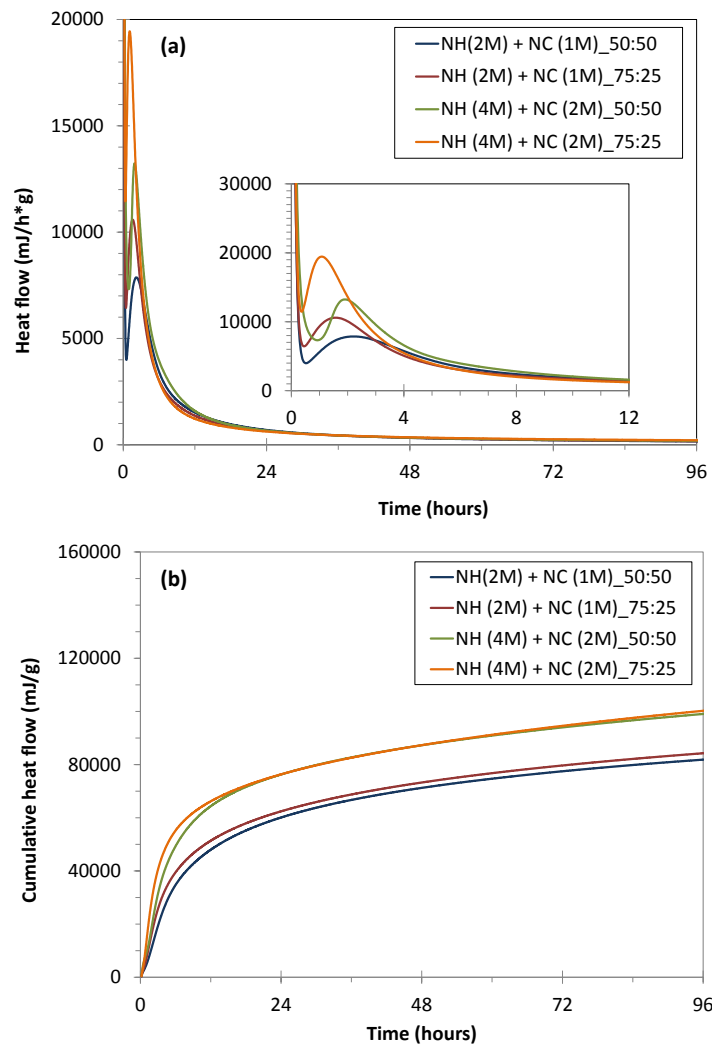


Figure 3.9 (a) heat flow and (b) cumulative heat flow of BOF75 at 20 °C activated with different molar concentrations and weight ratios of mixtures of NaOH and Na₂CO₃

molarity adopted for both the compounds and with 75% of NaOH in the solution, while, conversely, the lower one was obtained for the solution containing the lowest molarities and 50% of NaOH. The cumulative heat curves showed that the blended slag had similar values when activated with solutions containing the same concentration of both the compounds that constitute the activator solution, regardless the amount of each one. This finding was actually similar to that obtained for the BOF100 composition, which may be correlated to the fact that changing the concentrations of this type of activator

did not exert a relevant effect on the slag reactivity. However, it is interesting to notice that, when the alkaline solution with the sodium carbonate is employed, an overall higher intensity of the peaks, as well as a faster precipitation of the reactive products (occurring in the first 6 hours of reaction) was obtained with respect to the sodium silicate activator. These earlier peaks could be associated to the fast precipitation of calcium carbonate and calcium-sodium carbonate, as reported also in other works (Garcia-Lodeiro et al., 2013).

Thus, summarizing, the alkali activator mixtures that provided the highest reactivity for the BOF100 slag in the calorimetry tests at 20 °C were the following:

- NaOH (2M) and Na₂SiO₃, 50:50
- NaOH (4M) and Na₂CO₃ (2M), 75:25.

On the other hand, the BOF75 composition showed to be more reactive with the following alkaline solutions:

- NaOH (4M) and Na₂SiO₃, 75:25
- NaOH (4M) and Na₂CO₃ (2M), 75:25.

These solutions were hence used to further investigate the effects of the alkali activation process on both the slag composition (BOF100 and BOF75) on the long-term reactions, as will be discussed in the following section.

3.3.3. Long-term reactions: effect of the process on the mineralogy of the BOF slag

The effects of the alkali activation process, in combination with the CO₂ curing, on the BOF100 and BOF75 slag composition, were investigated through thermal and mineralogical analysis, with the aim to identify the reaction products and to assess the degree of hydration or carbonation of the samples. In particular, in the following paragraph, the results are shown in terms of the total mass loss and the bound water

content, along with the differential thermo-gravimetric (DTG) plot, calculated from the TG analysis. The bound water content is usually associated to the structural and chemically bound water of the hydration product (e.g. C-S-H, Ca(OH)₂) and its evaluation allowed to assess the extent of the hydration reactions of the activated samples. Moreover, to support the information achieved from the thermal analysis, the XRD of the samples are discussed.

Hence, the following paragraphs firstly show the results obtained for the BOF100 slag mixed with water; then, the effects of the two alkali solutions and the different curing conditions adopted, either on the BOF100 slag or the BOF75 slag compositions, are discussed.

3.3.3.1. Results obtained for the BOF slag mixed with water

Figure 3.10 reports the results of the thermal analysis carried out on the BOF100 slag pastes, mixed with water and cured in the humidity chamber, carbonation chamber at 20 °C and 50 °C. As shown in the graphs reported in column A, the total mass loss of the samples cured in the humidity chamber and in the carbonation chamber at 20 °C showed to be very similar, although in the former curing condition it appeared to be slightly higher. Increasing the temperature of the carbonation curing chamber up to 50 °C showed to increase the total mass loss value and the bound water content of the samples for the different curing times. In addition, for the latter curing condition, it can be seen that, at all the curing times, the difference between the total mass loss and bound water content was more marked than the other two curing state. Thus, it can be ascribed to the higher amount of formed carbonates in these samples already at early curing time, since this parameter corresponds to the CO₂ release.

The DTG plot, reported in Figure 3.10B, were characterized by three main peaks for all the curing times and conditions. An initial one, almost negligible and described by a very low intensity, was observed at around 100 °C and it may be referred to a calcium

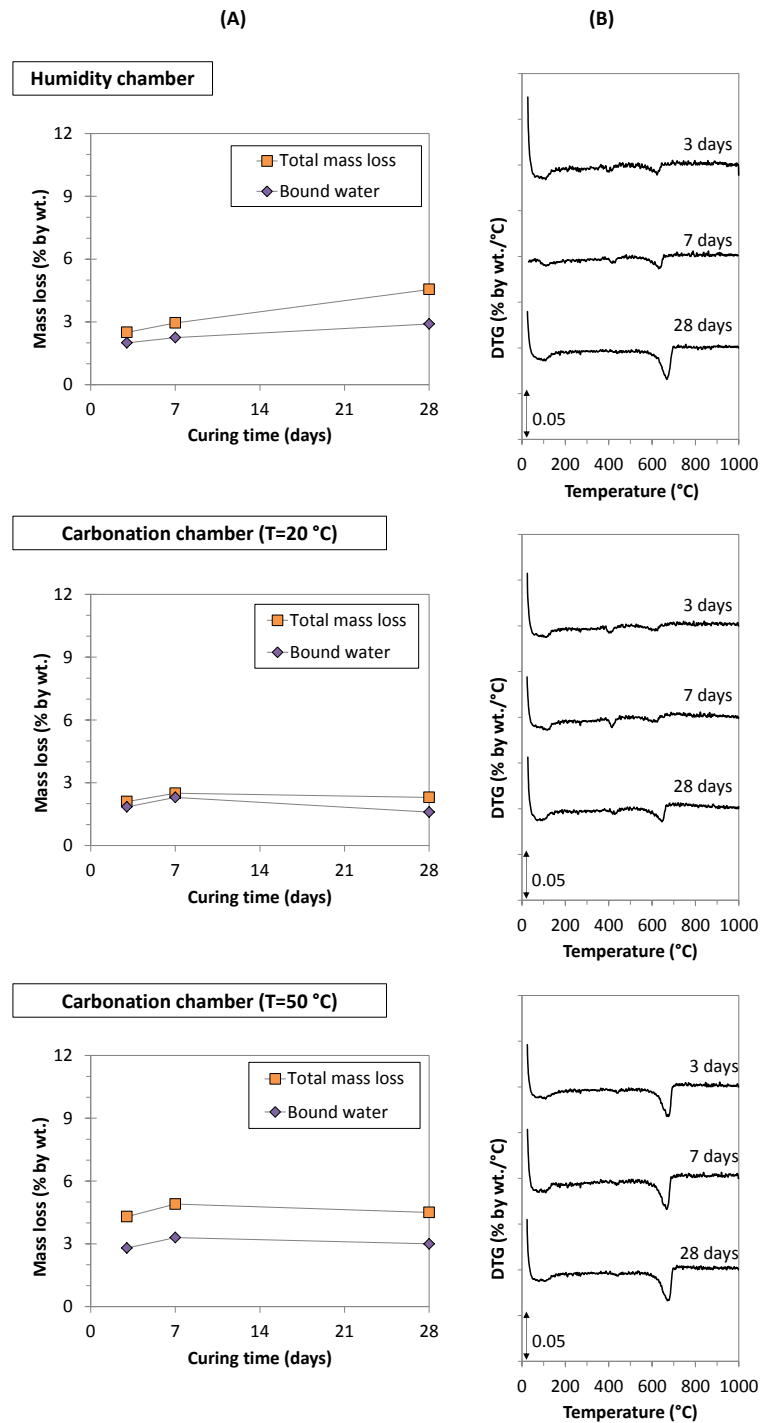


Figure 3.10 Comparison of the (A) total mass loss and bound water content from TGA analysis and (B) DTG plot of BOF100 pastes mixed with **water** and cured in the humidity chamber and carbonation chamber at a temperature of 20 °C and 50 °C.

silicate hydrate like phase. The formation of this phase was identified also in other studies (Wang et al., 2010; Wang et al., 2011), as the product of the BOF slag hydration reactions, where however it was observed as an impure form containing also other elements, such as Fe, Al and Mg. However, further investigation, as the analysis of the microstructural properties of the slag, are required to confirm this finding. A second peak was observed at around 400 °C at early curing time for the samples cured in the humidity chamber and in the carbonation chamber at 20 °C and it corresponds to the decomposition temperature of portlandite. The disappearance of this peak after 28 days of curing was matched by the increasing intensity of the third main peak at 650 °C, clearly related to the formation of calcite. However, for the samples cured in the carbonation chamber at 50 °C, this peak showed a similar intensity for all the curing times and higher than the other curing conditions, proving that the main effect of increasing the curing temperature in a CO₂ rich environment was the quickly occurrence of calcium carbonate, already after 3 days of curing.

3.3.3.2. Effect of the alkali activator and different curing conditions

The effect of the sodium hydroxide/sodium silicate solution on the samples cured in the humidity chamber and in the carbonation chamber at 20 °C and 50 °C, is reported in Figure 3.11, in which the thermal analysis results are shown.

The graphs in column A report the total mass loss and the bound water content along the curing time for the tested curing conditions. It can be observed that the highest amount of total mass loss was achieved when the samples were cured in the carbonation chamber at 20 °C. At this curing condition, the trend observed along the curing time showed to slightly increase between three and seven days of curing and then it settled until 28 days, similarly to the samples cured in the humidity chamber. Conversely, for the samples cured in the carbonation chamber at 50 °C, the total amount of the reaction products, associated to the total mass loss, showed a steady trend with time.

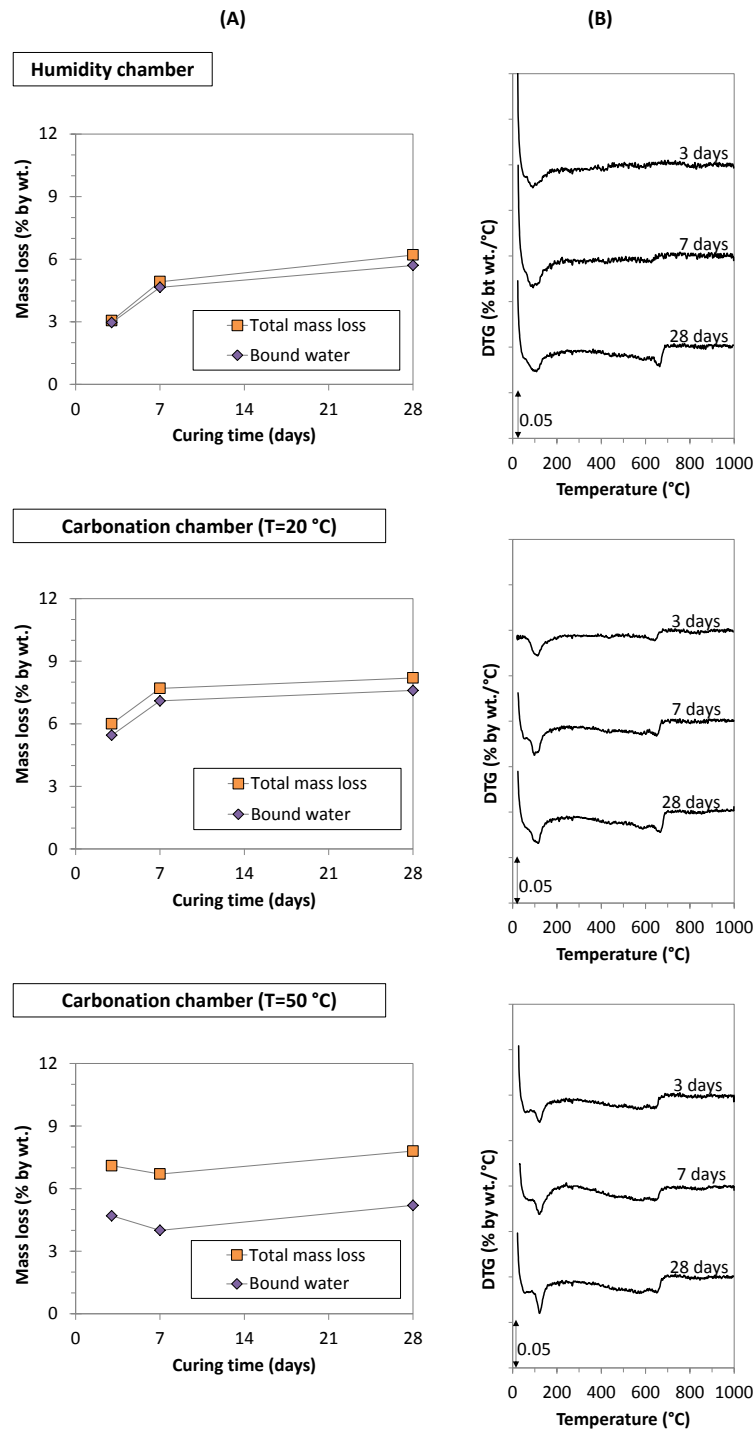


Figure 3.11 Comparison of the (A) total mass loss and bound water content from TGA analysis and (B) DTG plot of BOF100 pastes mixed with the NaOH 2M + Na₂SiO₃_50:50 solution and cured in the humidity chamber and carbonation chamber at a temperature of 20 °C and 50 °C.

Moreover, the amount of CO₂ release, associated to the formed carbonates and correlated to the difference between the total mass loss and the bound water content, was more relevant for the carbonated samples cured at higher temperature. Making reference to the DTG plot (see column b), at all curing times and conditions it can be observed a peak at around 100-120 °C, which may either correspond to the decomposition of C-S-H type reaction products (Taylor, 1997) or to gaylussite. A peak at around 650-700 °C, representing the decomposition temperature of CaCO₃, was more evident at the later curing time (28 days) for the samples cured in the humidity chamber and at all curing times for those cured in a CO₂-rich atmosphere, regardless the temperature adopted. Nevertheless, it was observed that, with the alkali solution and in the carbonation chamber at 20 °C, the intensity of the peaks associated to the C-S-H like phase resulted higher and to CaCO₃ lower than that achieved for the slag mixed with water (see Figure 3.10). This may suggest that the main reactions product of the BOF slag mixed with this activator is a calcium silicate hydrate phase, along with calcium carbonate, while in the presence of water the main product may result only the latter one.

The thermal analysis results obtained for the samples prepared using 100% of BOF slag and mixed with the sodium hydroxide/sodium carbonate solution are reported in Figure 3.12 for all the curing conditions. It can be observed that the total mass loss and the bound water content increased along the curing time when the samples were cured in the humidity chamber. This increasing trend was observed also for those cured in the carbonation chamber at 20 °C, although it showed to settle between 7 and 28 days. Raising the temperature in the carbonation chamber up to 50 °C accelerated the initial formation of the reaction products, since the total mass loss value, as well as the bound water content, retrieved after 3 days resulted higher than the other curing conditions and almost equal to that obtained after 28 days of curing. The DTG plot, reported in the column B of Figure 3.12, showed that most of the mass loss from the samples cured in the humidity and in the carbonation chamber at 20 °C occurred at temperatures below 200 °C. For these curing conditions, an evident narrow peak was observed at around 100-120 °C, whose intensity showed to be highly similar along the curing times.

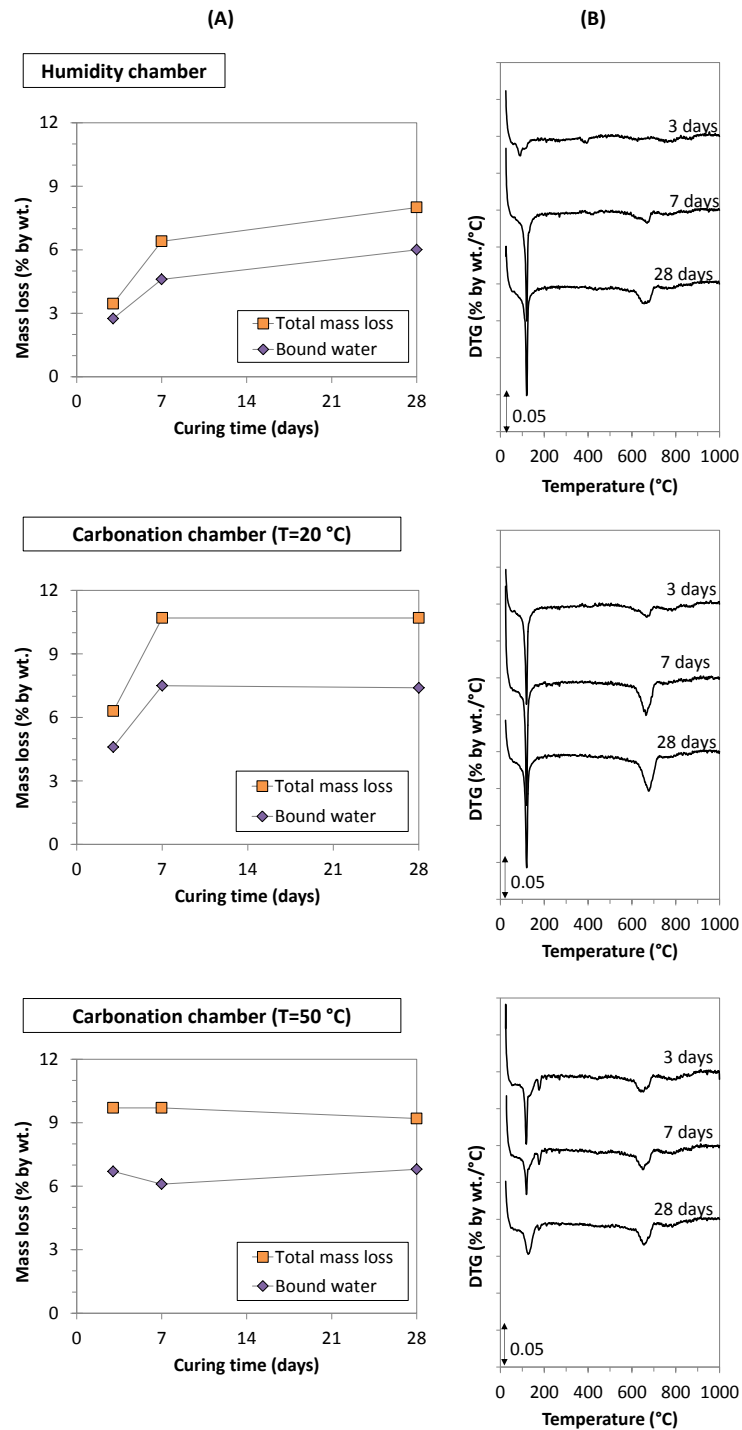


Figure 3.12 Comparison of the (A) total mass loss and bound water content from TGA analysis and (B) DTG plot of BOF100 pastes mixed with the NaOH 4M + Na₂CO₃ 2M_75:25 solution and cured in the humidity chamber and carbonation chamber at a temperature of 20 °C and 50 °C.

The shape of this peak, and hence the nature of the associated reaction product, resulted highly different from that obtained from the analysis of the samples activated with the other alkali solution, or water. Indeed, it could be related either to the decomposition of a C-S-H like phase (Taylor, 1997) or to that of gaylussite (Na₂Ca(CO₃)₂•5H₂O), a hydrated sodium carbonate that dehydrates at this temperature (Johnson and Robb, 1973). There is evidence on other literature studies of the occurrence of this latter phase as hydration product of alkali slag, mainly blast furnace or fly ash, activated with a sodium carbonate solution (Garcia-Lodeiro et al., 2013; Bernal et al., 2013). Its formation may be ascribed to the additional supplying of carbonate ions, resulting from the dissociation of Na₂CO₃, along with those obtained from the hydration of atmospheric CO₂, that, in combination with the Ca²⁺ obtained from the solid dissolution, forms such carbonate phase (Garcia-Lodeiro et al., 2013). However, at the higher tested curing temperature, it was observed that the intensity of the peak associated to gaylussite was lower than that reported for the other two curing conditions at the same curing time. Moreover, for all the curing times, a small shoulder on the edge of these peak, at around 180 °C, was noticed and it can be associated also to the loss of water from the hydration of the sodium-calcium carbonate (Johnson and Robb, 1973). Finally, for all the tested curing conditions, a second main peak at around 650 °C was observed, which is related to the decomposition temperature of calcium carbonate, whose intensity showed to vary depending on the curing condition. In particular, it resulted highly comparable for all the curing times for the pastes cured at higher temperature in the CO₂ curing chamber.

In conclusion, the findings obtained from the thermal analysis displayed in this section showed that different carbonate phases may form upon alkali activation, whose nature depends on the type of the activator solution and on the curing conditions. A peak of different intensity associate to a C-S-H like phase was detected for all the alkali solutions used, while a tight one associated to gaylussite was particularly evident in the presence of the sodium hydroxide/sodium carbonate solution, mainly for slag pastes cured in the humidity or in the carbonation chamber at 20 °C. The highest intensity of the peaks associated to calcium carbonate was observed at later curing time for the

carbonated paste at 20 °C activated with the sodium hydroxide/sodium carbonate solution. Raising the carbonation curing temperature to 50 °C probably accelerated the formation of this phase, as peaks were detected already after three days of curing and showed to settle up to 28 days. This effect could be ascribed to an initial faster rate of carbonation, that may have led to the formation of a carbonate layer, which has hindered further CO₂ diffusion through the pores of the material and hence further carbonation for increasing curing time.

The mineralogy of the samples activated with the sodium hydroxide/sodium silicate solution, cured for 7 and 28 days at all the curing conditions, is reported in Figure 3.13i, and compared with the untreated BOF slag. Firstly, it can be observed that the alkali activated samples exhibited different peaks of Ca phases, like Ca-containing oxides and Ca-silicate, along with other oxides, such as iron oxide and Ca-Al-Fe oxide, with an intensity lower than that retrieved for the untreated BOF sample. However, upon the alkali activation, it was noticed the occurrence of calcite, whose intensity showed to increase with the curing times only when the samples were cured in the humidity chamber. On the other hand, for the samples cured in the CO₂ chamber, regardless the temperature, the intensity of the calcite peak was similar for both the curing times and its formation occurred already after 7 days, as also suggested by the DTG graphs. It can be also observed that the XRD plots, at all curing times and conditions, are characterized by a broad hump (44°-52° 2θ), which may be attributed to an amorphous formation, likely a C-S-H type reaction product, as also reported in the DTG results. Finally, the peaks of gaylussite, that based on the DTG plots seemed to form as well in the samples cured in the carbonation chamber at 50 °C, were not retrieved in the XRD plots. This result was tentatively ascribed to the detection limit of this analysis, probably related to the fact that for these samples, the low intensity of the peak of gaylussite can be hardly detected by the XRD.

The mineralogy of the samples activated with the sodium hydroxide/sodium carbonate solution, cured for 7 and 28 days at all the curing conditions, is reported in Figure 3.13ii and also compared with the untreated BOF slag.

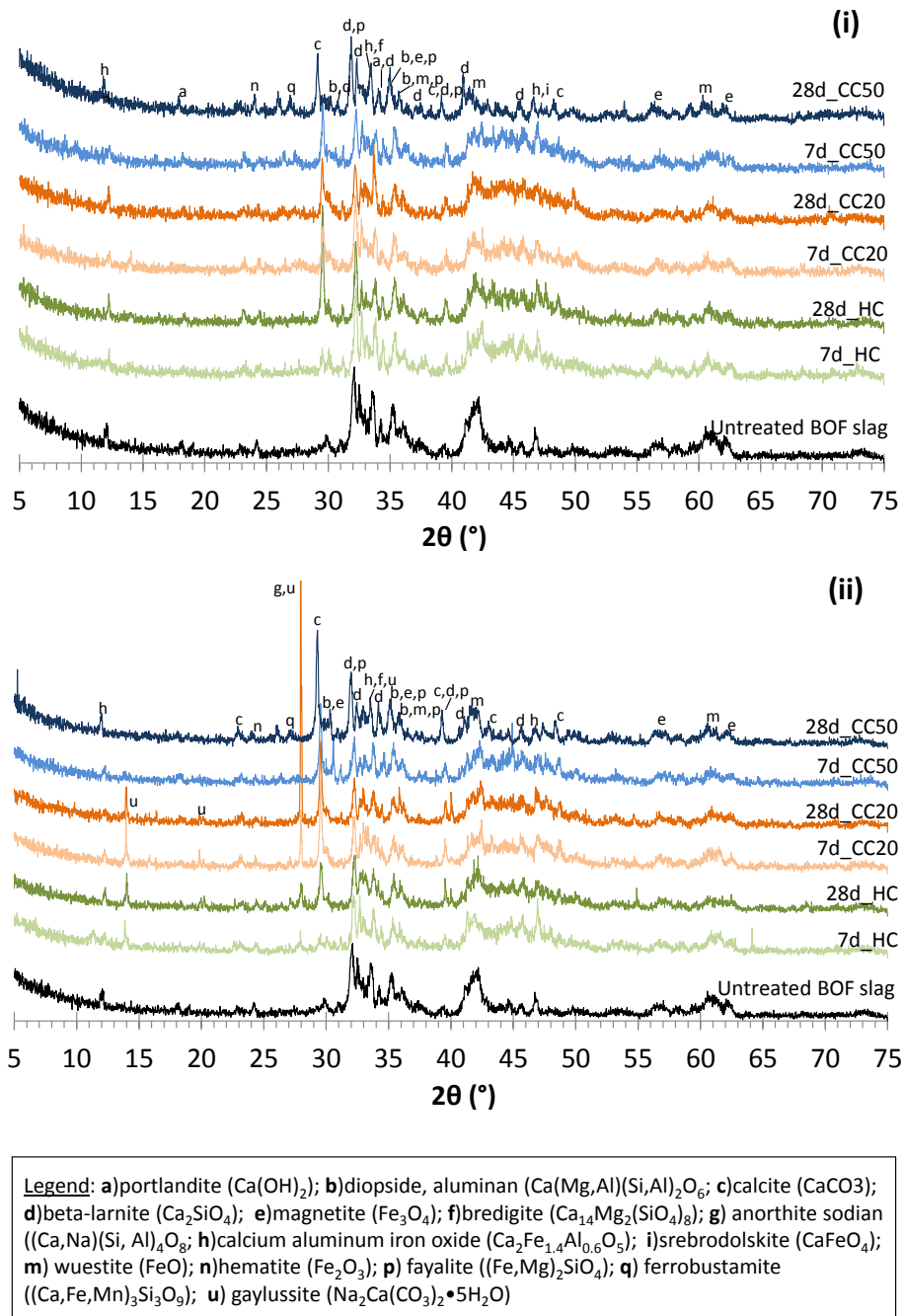


Figure 3.13 XRD pattern of the untreated BOF slag and the BOF100 pastes mixed with (i) the **NaOH 2M + Na₂SiO₃_50:50** solution and (ii) the **NaOH 4M + Na₂CO₃ 2M_75:25** solution, cured in the humidity chamber (HC), carbonation chamber at 20 °C (CC20) and 50 °C (CC50).

As also reported in the previous discussion, the mineralogy of the alkali activated samples was very similar to that of the untreated slag. However, upon the alkali activation, the occurrence of calcite was noticed, whose intensity showed to be higher upon 28 days of carbonation curing. Furthermore, in addition to calcite, the mineralogy of the activated samples showed also the presence of a peak of sodian anorthite, a calcium-aluminum silicate with inclusion of sodium, and different peaks of gaylussite, in agreement with the results obtained from the DTG analysis. It is worth noting that the peaks of gaylussite appeared only for two curing conditions, i.e. humidity and carbonation chamber at 20 °C. Moreover, in the latter condition, it resulted that the ratio between the intensity of the peaks of gaylussite and calcite was higher after 28 days of curing than 7 days, indicating that in the former case gaylussite represented the main carbonate phase. Conversely, the main and newly formed peak detected upon activation and curing in the carbonation chamber at 50 °C was calcite rather than gaylussite, consistent with the DTG results.

3.3.3.3. Effect of alkali activation and different curing conditions on the BOF/BFS mixture

The results of the thermal analysis performed on the samples containing 75% by wt. of BOF slag and 25% by wt. of BFS, activated with the solutions selected after the calorimetric tests, are reported in this section.

The results obtained for the samples activated with the sodium hydroxide/sodium silicate solution are shown in Figure 3.14, where in the column A the total mass loss and the bound water content are reported at different curing time and for the two tested curing conditions. It can be seen that the formation of reaction products, associated to the total mass loss, increased slightly along the curing time, and that the amount of total mass loss coincided with that of the bound water content for all the curing times and conditions.

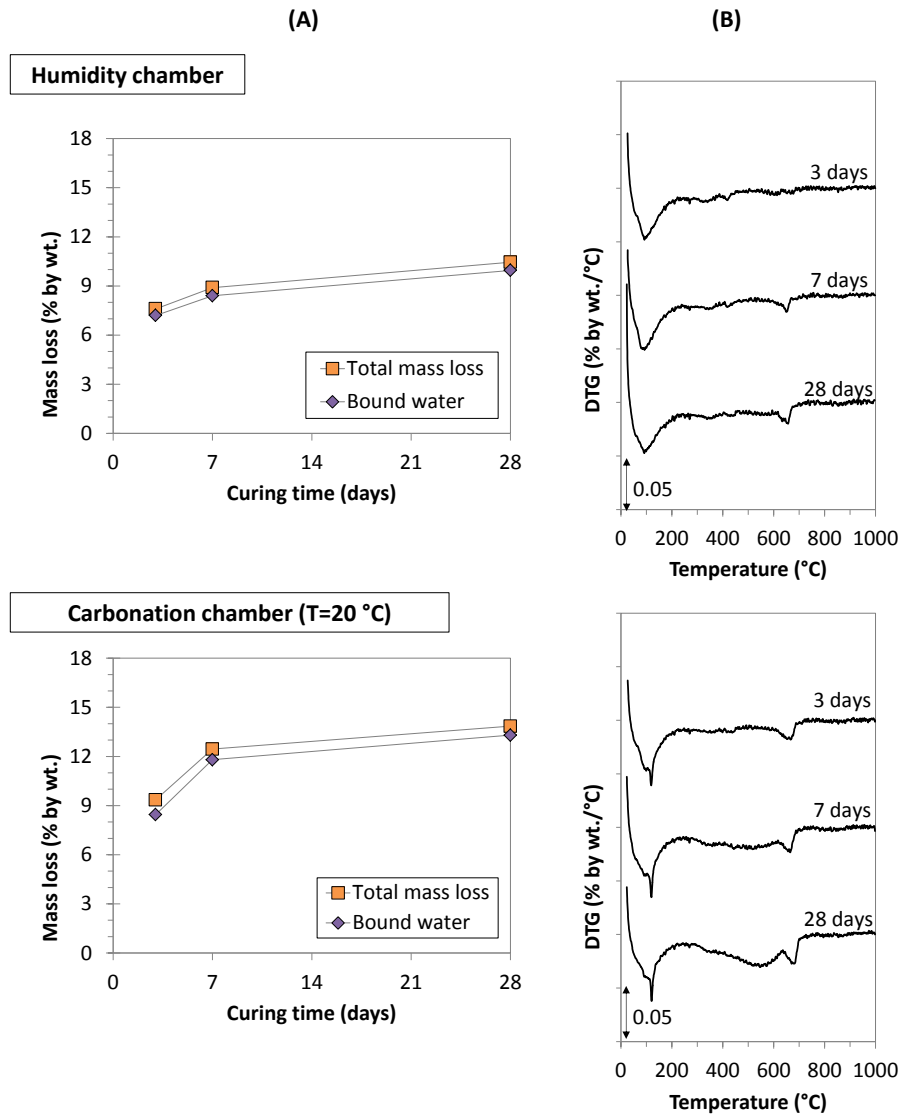


Figure 3.14 Comparison of the (A) total mass loss and bound water content from TGA analysis and (B) DTG plot of BOF75 pastes mixed with the NaOH 4M + Na₂SiO₃ 75:25 solution and cured in the humidity chamber and carbonation chamber at a temperature of 20 °C.

The DTG plot (see Figure 3.14 column B) showed that for the samples cured in the humidity chamber, a broad initial peak at around 100 °C, ascribed to the decomposition temperature of the C-S-H gel, was observed, with an intensity similar for all the curing ages. The second peak, detected at around 650-700 °C, which corresponds to the formation of calcium carbonate phase, showed an increasing intensity along the curing

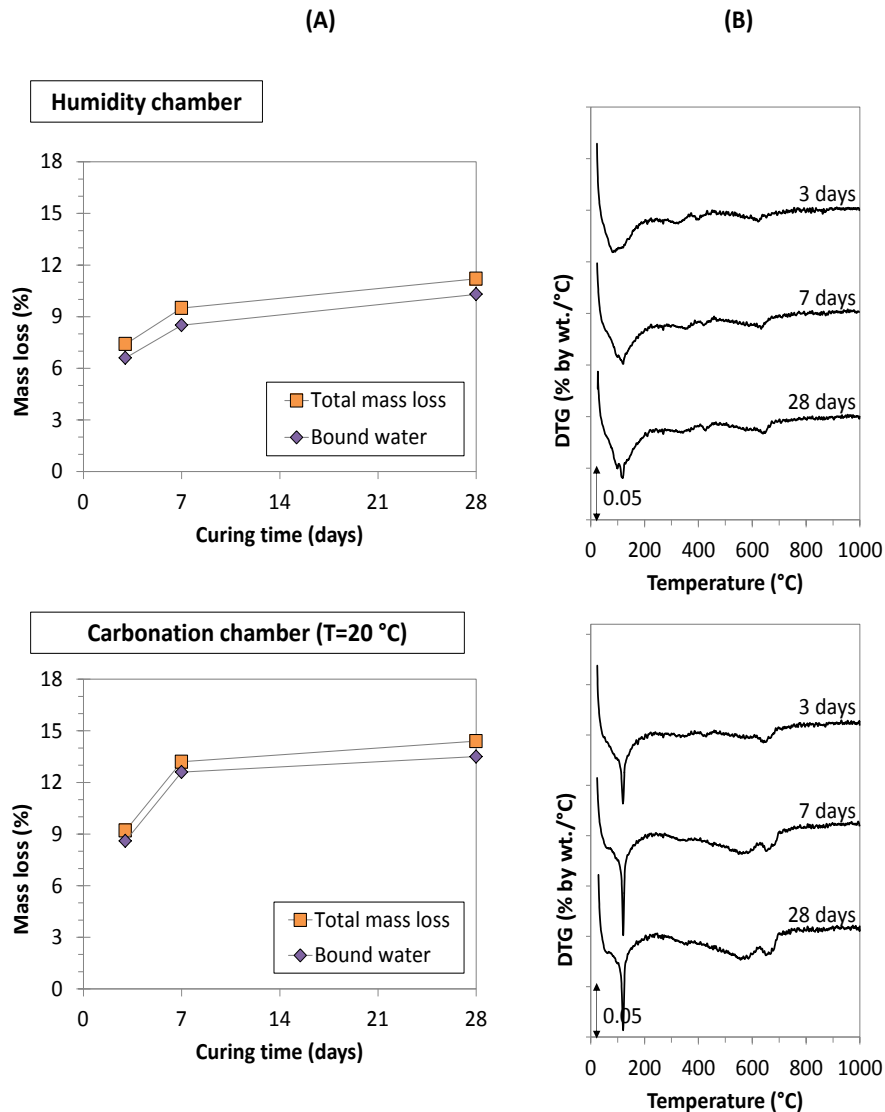


Figure 3.15 Comparison of the (A) total mass loss and bound water content from TGA analysis and (B) DTG plot of BOF100 pastes mixed with the **NaOH 4M + Na₂CO₃ 2M_75:25** solution and cured in the humidity chamber and carbonation chamber at a temperature of 20 °C.

time. Upon curing in the carbonation chamber at 20 °C, the DTG graphs of the samples showed the formation of peaks at the same decomposition temperature observed for those cured in the humidity chamber. Nevertheless, the first peak was located at 100-120 °C and showed a sharper shape than that observed for the not-carbonated samples, which is probably related to the decomposition temperature of gaylussite.

The degree of the long-term reactions of the BOF75 samples activated with the sodium hydroxide/sodium carbonate solution, cured at the tested conditions for all the times, is reported in Figure 3.15. It can be seen that the trend of the total mass loss and the bound water content (column A of Figure 3.15) was similar to that observed for the samples activated with the sodium hydroxide/sodium silicate solution. Making reference to the DTG plot (column B of Figure 3.15), for the samples cured in the humidity chamber it can be observed a broad peak, which remained constant for increasing curing time, at around 100 °C, probably corresponding to the C-S-H-like phase. For this curing condition, two peaks of low intensity were also observed at around 400 °C and 650-700 °C, which correspond to the decomposition temperatures of portlandite and calcite, respectively. On the other hand, the samples cured in the carbonation chamber showed a narrow and sharp peak at 120 °C at all curing times, which has already been related to the decomposition temperature of gaylussite. Moreover, as for the samples cured in the humidity chamber, a second peak corresponding to the calcite was also observed, with an intensity that showed to slightly increase along the curing time.

The XRD patterns of the activated BOF75 slag, at the two tested curing conditions after 7 and 28 days of curing, are shown in Figure 3.16 and compared with that of the untreated material. Firstly, it can be observed that, with both the activators, the mineralogy of the samples has a more marked amorphous character than the untreated BOF slag, which can be correlated to the nature of the BFS present in the mixtures (see Figure 3.2). The patterns of the samples activated with the two different solutions resulted very similar.

The peaks of dicalcium silicate and merwinite present in the untreated slag samples (see for comparison Figure 3.2) showed to decrease upon activation and curing in the humidity chamber or in the carbonation chamber at 20 °C. the formation of different Ca-containing phases were observed in the treated samples, e.g. calcite, ranchinite, grossular or earlandite. In particular, the most predominant peak for all the operating conditions was that associated to calcite and ranchinite. The formation of different peaks of low intensity of grossular and earlandite was observed for all the samples upon

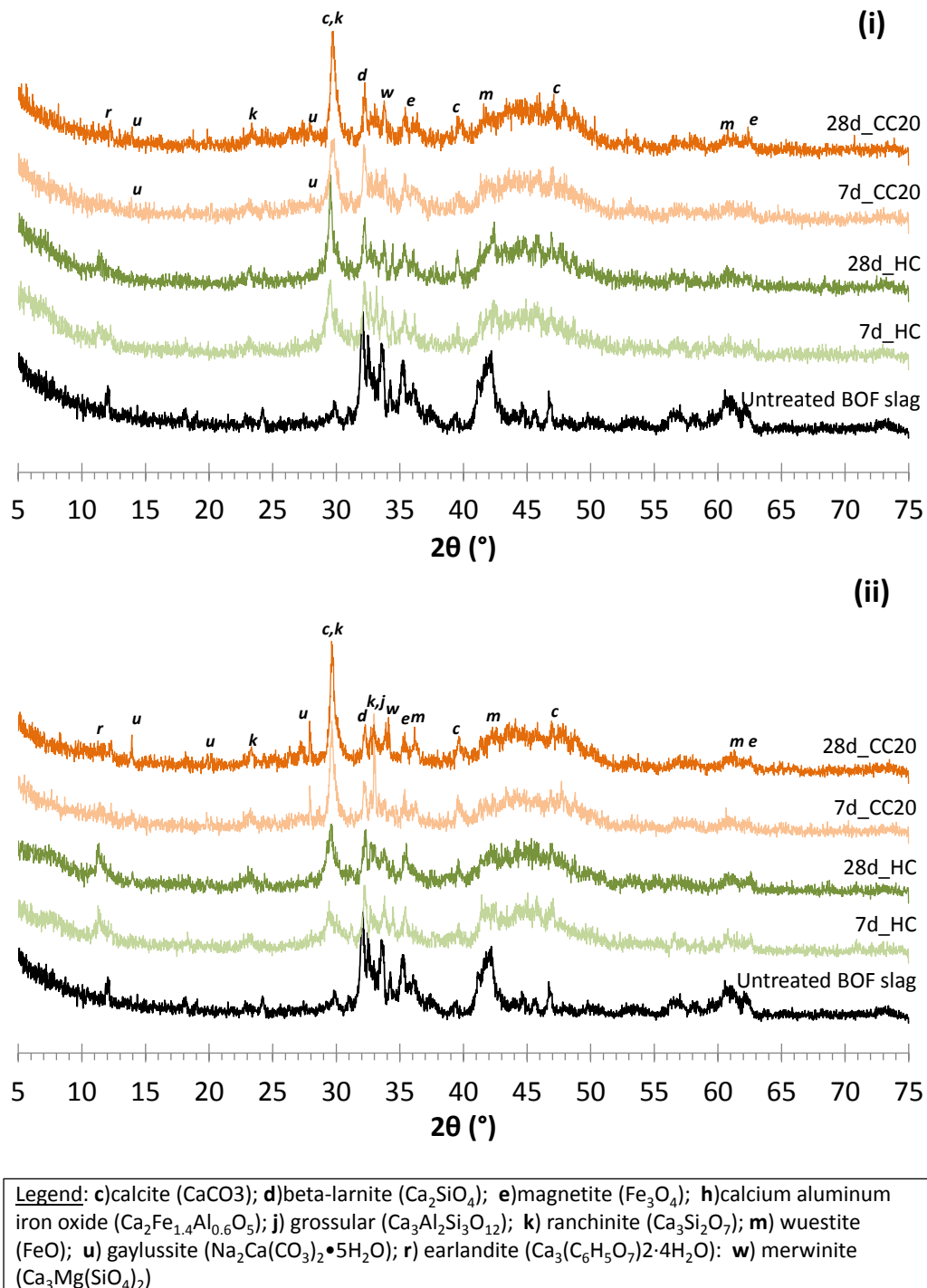


Figure 3.16 Comparison of the XRD pattern of the untreated BOF slag and the BOF75 pastes mixed with (i) the NaOH 4M + Na₂SiO₃ 75:25 solution and (ii) the NaOH 4M + Na₂CO₃ 2M 75:25, cured in the humidity chamber (HC) and carbonation chamber at 20 °C (CC20).

the combination of alkalis and carbonation. Grossular was also found in the study of Puertas et al. (2004) after the activation of blast furnace slag with waterglass cured in a humidity chamber.

Finally, it is interesting to notice that the peaks of gaylussite appeared mainly when the material was activated with the sodium hydroxide/sodium carbonate solution and cured in the carbonation chamber, confirming the TGA results. The intensity of these peaks resulted slightly lower in the XRD plots related to the pastes activated with sodium hydroxide and sodium silicate after curing in the carbonation chamber. Gaylussite, found also for the pastes prepared with 100% of BOF slag and activated with the same alkali solution, is a hydrated sodium carbonate phase that has been reported as one of the main reaction products of the carbonation reactions of the activated blast-furnace slag. Its formation was mainly related to the reactions of the activator with the calcium ions dissolved from the solid, in the presence of a high availability of water (Bernal et al., 2012).

3.3.4. Extent of CO₂ uptake

The CO₂ uptake of the BOF100 and BOF75 pastes, subjected at the different tested curing conditions, was assessed by measuring the Inorganic Carbon (IC) content of the samples. In particular, it was analyzed for the samples mixed with water and with the tested alkali solution reported in the previous section.

The results obtained for the slag mixed with water, adopted as reference, are reported in Figure 3.17. It appeared that the extent of carbonation increased steadily with time in the humidity chamber, while it showed to be almost steady for the samples cured in the carbonation chambers. It resulted that the lowest amount of CO₂ uptake was obtained for all the curing times for the samples cured in the carbonation chamber at 20 °C, whose maximum CO₂ sequestration resulted equal to 0.3%. Increasing the temperature in the carbonation chamber up to 50 °C allowed to achieve an uptake of 2%, already after 3 days of curing.

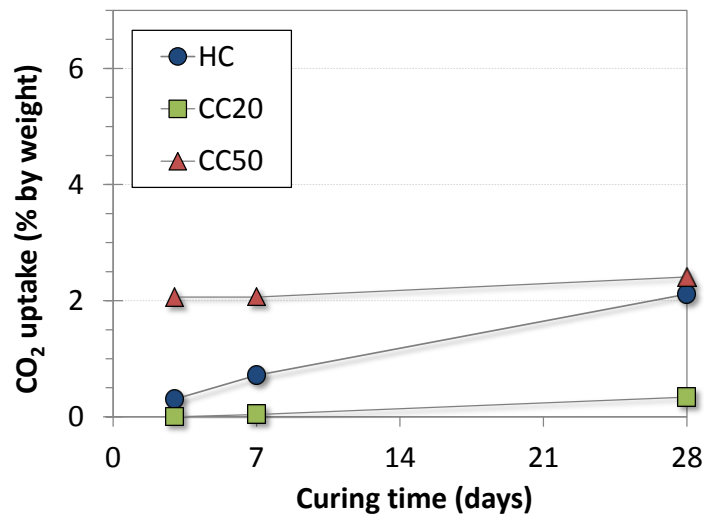


Figure 3.17 CO₂ uptake, along the curing time, of BOF100 pastes mixed with **water** and cured in the humidity chamber (HC), the carbonation chamber at 20 °C (CC20) and at 50 °C (CC50).

A direct comparison of these findings with those obtained in the literature could not be achieved due to the different operating conditions adopted. Other studies (Baciacchi et al., 2015b) using this type of BOF slag, in which 1 gram of milled BOF slag, humidified with water and exposed to a flux of 100% of CO₂ at T= 50 °C and P=10 bar, achieved a maximum CO₂ uptake value, after 24 hours of treatment, equal to 20 % by wt. Beyond the different operating conditions adopted, the results obtained in this study may be highly ascribed to the lower surface area exposed to the CO₂ atmosphere, since the samples were prepared as square moulds to allow the curing.

When the BOF100 slag was activated with both the alkali solutions (see Figure 3.18), the degree of carbonation of all the samples showed to increase linearly with the curing time in the humidity chamber, for which the maximum uptake was reached after 28 days and resulted almost equal to 4%. This value showed to be two times higher than the maximum obtained under the same curing conditions for the pastes mixed with water. Upon CO₂ curing, the CO₂ uptake values showed to slightly increase, regardless the temperature, with respect to those retrieved in the humidity chamber. In particular, the maximum CO₂ sequestration achieved for the sodium hydroxide/sodium

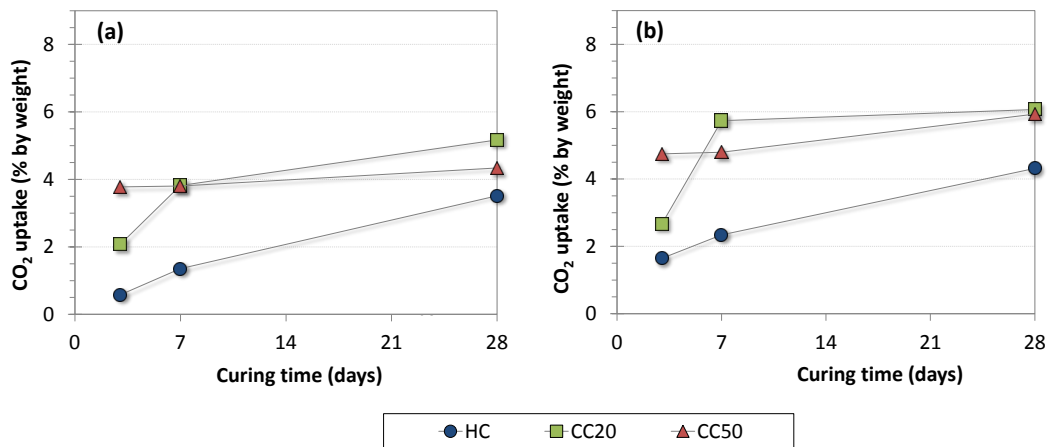


Figure 3.18 CO₂ uptake, along the curing time, of BOF100 slag pastes mixed with (a) NaOH 2M + Na₂SiO₃ 50:50 solution and (b) NaOH 4M + Na₂CO₃ 2M 75:25 solution, cured in the humidity chamber (HC), the carbonation chamber at 20 °C (CC20) and at 50 °C (CC50).

silicate solution resulted equal to 5.2% in the carbonation chamber at 20 °C after 28 days of curing, and similarly for the sodium hydroxide/sodium carbonate solution it resulted equal to 6% by wt. after 28 days of curing in the carbonation chamber, at both tested temperatures. It is interesting to notice that the samples mixed with both the alkali solutions and cured in the carbonation chamber at 50 °C showed a constant trend along the curing time. This may be probably due to the rapid formation of carbonates at the outer edge of the specimens, that may limit the further diffusion of CO₂ into the core of the slag pastes, leading to a settled CO₂ uptake of the material, as previously observed in the DTG plot for the peaks associated to calcite. Moreover, in both cases, only the value achieved after 3 days of curing resulted higher than that obtained from the CO₂ curing at 20 °C, likely due to the initial enhancement of the dissolution rate of the reactive minerals (e.g. silicates) at higher temperature. Increasing the temperature of the reaction leads to two opposite effects on the carbonation reaction: on the one hand, it favours the dissolution of Ca from the solid, while on the other one, it reduces the solubility of CO₂ (Huijens et al., 2005). Nevertheless, Liu et al. (2001) found that, at atmospheric pressure, the second effect is the rate-limiting step only when the carbonation is carried out at temperatures above 60°C.

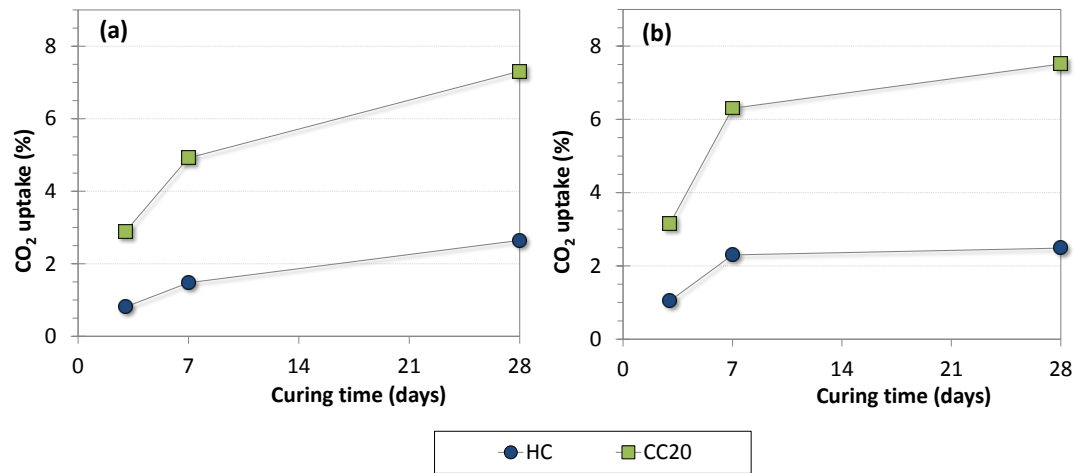


Figure 3.19 CO₂ uptake, along the curing time, of BOF75 pastes mixed with (a) NaOH 4M + Na₂SiO₃_75:25 solution and (b) NaOH 4M + Na₂CO₃ 2M_75:25 solution, cured in the humidity chamber (HC) and the carbonation chamber at 20 °C (CC20) and at 50 °C (CC50).

The CO₂ uptake obtained from the pastes prepared with 25% by wt. of BF slag, activated with the sodium hydroxide/sodium silicate and the sodium hydroxide/sodium carbonate solutions, at different curing conditions, are reported in Figure 3.19. In general, it can be seen that the degree of carbonation of the samples increased along the curing time, and this effect was even more evident for those activated with the sodium hydroxide/sodium silicate solution. The highest uptake achieved in the humidity chamber was equal to 2.5% for both activators and after 28 days of curing. Higher CO₂ uptake values were observed upon curing in the carbonation chamber at 20 °C and, at earlier curing times (3 and 7 days), they showed to be slightly higher for the samples mixed with the sodium hydroxide/sodium carbonate solution than those mixed with the other one. It may be related to the initial precipitation of carbonates, formed by the combination of the ions Ca²⁺, dissolved from the solid, and the carbonate ions derived from the dissociation of Na₂CO₃ and from the hydration of CO₂.

Thus summarizing, for the BOF100 slag the maximum uptake resulted equal to 60 gCO₂/kg of slag and was achieved in the carbonation chamber at both 20 and 50 °C after 28 days of curing with the sodium hydroxide/sodium carbonate solution. This

value resulted slightly lower than the maximum attained for the BOF75 slag, that resulted equal to 80 gCO₂/kg of slag and was yielded after 28 days of curing in the carbonation chamber at 20 °C by using both the alkali solutions.

3.3.5. Mechanical strength of the slag mortars

The compressive strength results of the slag mortars prepared with 100% of BOF slag, mixed with the two types of activators and cured in the carbonation chamber at a temperature of both 20 and 50 °C, are reported in Figure 3.20 and compared with those obtained from the mortars prepared using 75% of BOF slags and 25% of BF slag activated with the sodium hydroxide/sodium silicate solution and cured in the carbonation chamber at 20 °C.

Making reference to the BOF100 samples, the lowest strength, resulted negligible in the first days of curing, was achieved with the sodium hydroxide/sodium carbonate solution in the carbonation chamber at 20 °C. Using this activator, it was possible to achieve a maximum strength of 1 MPa after 28 days of curing only increasing the curing temperature up to 50 °C. This value showed to be similar to that achieved by using the sodium hydroxide/sodium silicate activator, but curing the mortars at lower temperature, i.e. 20 °C. On the other hand, with this latter activator, increasing the curing temperature up to 50 °C allowed to obtain a strength of almost 2 MPa after 7 days of curing, that remained constant until 28 days.

The mortars prepared by mixing the BOF slag with 25% of blast furnace slag showed in general higher mechanical strength at all curing times with respect to the samples prepared with 100% of BOF slag. Indeed, the compressive strength showed to increase along the curing time, with a maximum value of 4 MPa achieved after 28 days of curing, that resulted two times greater than that retrieved for the mortars prepared with 100% of BOF slag, under the same curing conditions.

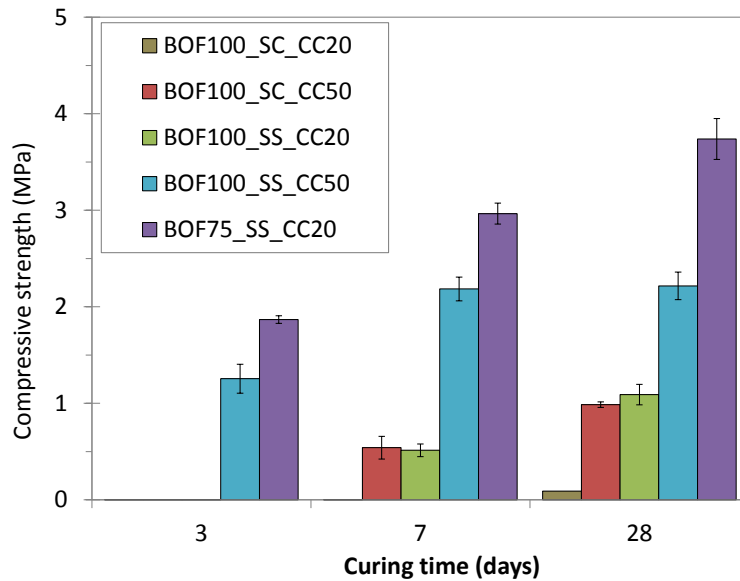


Figure 3.20 Compressive strength of mortar beams prepared with BOF100 and BOF75, activated with different alkali solutions and cured in the carbonation chamber at 20 °C (CC20) and 50 °C (CC50).

This findings was expected, since a better response was already observed for this type of mixture in terms of heat flow release, which can be correlated to the precipitation of highly reactive reaction products (i.e. C-S-H gel) that lead to a higher mechanical performance of the material (Mounanga et al., 2011). In general, the achieved mechanical strength resulted lower in comparison with the typical values reported in the literature for other blended slag. This fact may be highly related to the particle size of the treated BOF slag used in the mixture composition, since the study of Shi (2002) reported that the increases of the mechanical strength of blended ladle slag with 40% of BFS should be ascribed mainly to the different fineness of the material. Nevertheless, the aim of this analysis was to understand which one between the two type of activators, along with the curing conditions, allowed to acquire the highest mechanical strength.

Finally, it can be observed that the BOF100 sample showed a different behavior with respect to the activator used and to the curing conditions adopted, showing a higher strength at higher curing temperature in the carbonation chamber with the sodium hydroxide/sodium silicate solution. This finding was mainly ascribed to the activator

nature, as also other work on the blast furnace slag (Puertas and Torres-Carrasco, 2014), showed that at fixed curing condition, the lowest strength values were retrieved for the pastes prepared with a solution of NaOH and Na₂CO₃, rather than with sodium silicate. The authors associated this result to the nature of the reaction products related to the different type of the alkaline activator, and found that the presence of a C-S-H like phase when the slag were activated with a sodium silicate solution, showing a more condensed structure leading to a lower porosity in the slag system, exerted the main influence on the final mechanical strength of the mortars. In this study, similar findings were also observed, as probably the mechanical performances associated to the BOF slag mortars may be highly associated to the C-S-H like phase, whose formation was reported in the DTG analysis of the samples.

3.4. Main findings

This chapter reports the investigation carried out to exploit the alkali activation process on BOF slags, through the analysis of the effects of such a treatment on early-stage and long-term reactions. Firstly, isothermal calorimetric study was carried out for investigating the short-term hydration reactions of the BOF slag (at 20 °C and 50 °C) and a mixture consisting of 75% by wt. of BOF slag and 25% by wt. of blast furnace slag (at 20 °C), mixed with different sodium hydroxide/sodium silicate and sodium hydroxide/sodium carbonate solutions. The results showed that the BOF slag were reactive at T=20 °C, although the completion of the hydration reactions resulted quite long (more than ten days). The highest cumulative heat flow was obtained for the sodium hydroxide (2M) /sodium silicate (50:50) solution with the highest silica modulus of 2.3, and for the solution containing NaOH (4M) and Na₂CO₃ (2M), 75:25. Increasing the temperature of the reaction up to 50 °C, or mixing the slag with the blast furnace slag, showed to accelerate the initial reactivity of the BOF slag, as the formation of exothermic peaks associated to the precipitation of the reaction products occurred already after 5 days of reaction. The evaluation of the long-term reactivity of the

samples mixed with the alkali solutions that provided the highest earlier reactivity at room temperature, was carried out by thermal analysis after curing in the humidity chamber and in the carbonation chamber (CO₂ at 5%) at 20 °C and 50 °C. The results indicated the formation of calcium carbonate with both type of solutions after carbonation, while the probably formation of a calcium silicate hydrate like phase was observed for the samples activated with the sodium hydroxide/sodium silicate solution. Formation of gaylussite was observed mainly for the BOF slag or BOF/BFS samples cured in either the humidity or the carbonation chamber at room temperature and containing the sodium hydroxide/sodium carbonate alkali binder. In terms of CO₂ uptake, the maximum value, equal to 6%, was achieved for the BOF slag samples mixed with the sodium hydroxide/sodium carbonate solution after 28 days of curing in the carbonation chamber, regardless the temperature adopted. Under the same curing condition, the mixture of BOF slag and blast furnace slag showed a CO₂ uptake only slightly higher, i.e. 8%. Finally, the BOF slag samples activated with the sodium hydroxide/sodium silicate solution and cured in the carbonation chamber at 50 °C showed the highest mechanical strength. Anyway, a mechanical strength of 4 MPa, two-fold higher than the maximum obtained for the samples containing only BOF slag, was achieved by mixing the BOF slag with the blast furnace.

Chapter 4

Investigation of the effects of alkalis on the granules produced by carbonation-granulation treatment

4.1. Introduction

The granulation-carbonation process was discussed in the previous sections as an option for the valorization of the BOF steel slags. This process, when applied directly to BOF slags without any kind of amendment, was found to be effective in producing granules, also allowing to achieve significant CO₂ uptakes. Nevertheless, suitable mechanical properties able to reuse these granules as aggregates in civil engineering applications could not be obtained, unless the slags were mixed with different proportions of cement. Clearly, mixing the slags with cement, although effective in improving the mechanical properties of the obtained granules, would have a detrimental effects in terms of the

GHG reduction, as its production is characterized by high CO₂ emissions. For this reason, alternative options to increase the mechanical performance of the granules obtained after the granulation-carbonation treatments need to be developed.

To this aim, it is in principle possible to exploit the alkali activation process of BOF slags, also investigated previously in this thesis. In Chapter 3, it was reported that the activation of this residue with a solution of sodium silicate and sodium hydroxide showed to be effective for increasing its original low rate of hydration. Based on these findings, this solution has been used in the current work to investigate the effect of combining the granulation-carbonation treatment with alkali activation, with the aim of enhancing the mechanical properties of the obtained aggregates. The tests were carried out using the same set-up employed for performing the experiments discussed in Chapter 2 and the effects of the treatment were assessed in terms of the particle size distribution, CO₂ uptake, leaching behaviour and mechanical properties of the obtained granules, evaluated applying the Aggregate Crushing Value (ACV) test.

4.2. Material and methods

4.2.1. Materials

The sample used in this study was obtained by mixing two residues collected downstream two different Basic Oxygen Furnaces (BOF) employed in an integrated steelmaking plant, after crushing and magnetic separation for iron and metal recovery. The particle size distribution of the untreated material was determined by the ASTM D422 standard procedure. The material size was lower than 1 mm, with a mean diameter equal to 0.2 mm, as reported in Figure 4.1.

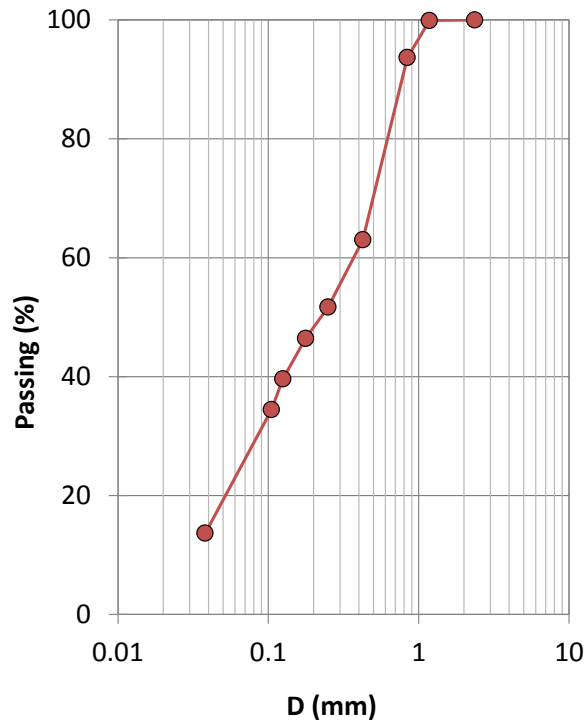


Figure 4.1 Particle size distribution of the untreated BOF slag sample

The elemental composition was determined by alkaline fusion (in triplicate) of slag samples with $\text{Li}_2\text{B}_4\text{O}_7$ in platinum melting pots at 1050 °C for 1 h, followed by dissolution of the molten material with 4% HNO_3 and subsequently ICP-OES analysis of the obtained solution, employing an Agilent 710-ES spectrometer. The chemical composition of the slag, reported in Table 4.1, displayed that Ca and Fe were the main constituents, with concentrations equal to 268 g/kg and 223 g/kg, respectively, followed by Mg (43 g/kg), Mn (31.3 g/kg) and Si (16 g/kg).

The activating solution used in this study was a 50:50 by weight mixture of sodium hydroxide (NaOH) 2M, prepared by dissolving the pellets (fisher scientific, 99.4% purity) in the deionized water, and a commercial solution of sodium silicate (Sigma-Aldrich) whose concentration of silicates in water, evaluated by ICP-OES analysis, resulted equal to 36%.

Table 4.1 Elemental composition of the untreated BOF slag sample expressed as % on a dry weight basis.

Element	% (by wt.)	Element	% (by wt.)
Al	0.8	Fe	22.3
Ba	0.01	Mg	4.3
Ca	26.8	Mn	3.13
Cd	0.02	Si	1.6
Cr	0.07	V	0.05
Cu	0.01	Zn	0.02

4.2.2. Applied treatments

The granulation and carbonation-granulation experiments were carried out following the procedure reported in the second chapter. Air-dried slag (approximately 500 g) was premixed in a plastic bag with either deionized water or the alkaline solution, at two different liquid to solid ratios. Table 4.2 reports a general overview of the experiments carried out in this section, with the code adopted to identify them in the discussion of the results.

In order to obtain a homogeneous initial particle size distribution for all the experiments, the mixture of slag and binder was pushed through a 2 mm sieve, following the procedure widely adopted in other studies on granulation (Iveson et al., 1996; Wauters et al., 2002). The reaction time of each experiment was set equal to 30 or 60 minutes and the product of each test was cured in a controlled environment (room temperature and 100% relative humidity) for 28 days, in order to allow the completion of the hydration reactions. The cured samples were then analysed for assessing their particle size distribution, carbonate content, environmental and mechanical behavior. The particle size distribution of the granules was determined by applying the ASTM D422 standard procedure. The carbonate content, evaluated by Inorganic Carbon (IC) analysis using a Shimadzu TOC VCPH analyser equipped with a SSM-5000A solid sampler, was assessed immediately after the test and on the granules cured for 7 and 28 days, so to follow the carbonation kinetics along the curing time.

Investigation of the effects of alkalis on the granules produced by carbonation-granulation treatment

Table 4.2 Summary of the main parameters adopted for the experiments (W/S: water to slag ratio; AA/S: alkali activation solution to slag ratio).

Code of the experiments	Reaction time (min.)	Binder type	W/S ratio (l/kg)	AA/S ratio (l/kg)
Granulation tests				
G30'_W	30	Deionized water	0.12	-
G30'_AA_W/S=0.12	30	Alkaline activator	0.12	0.16
Granulation-Carbonation tests				
GC30'_W	30	Deionized water	0.12	-
GC60'_W	60	Deionized water	0.12	-
GC30'_AA_W/S=0.12	30	Alkaline Activator	0.12	0.16
GC60'_AA_W/S=0.12	60	Alkaline Activator	0.12	0.16
GC30'_AA_W/S=0.14	30	Alkaline Activator	0.14	0.18
GC60'_AA_W/S=0.14	60	Alkaline Activator	0.14	0.18

The leaching behaviour was assessed by following the EN 12457-2 standard compliance test that involves grinding of the material presenting a grain size above 4 mm. In addition, the leaching behaviour of the unground granules obtained from each treatment was also assessed by applying a L/S ratio of 10 l/kg and a contact time of 24 hours, followed by ICP-OES analysis of eluates, employing an Agilent 710-ES spectrometer. Leaching tests were carried out in duplicate. The mechanical strength of the granules was evaluated by performing the Aggregate Crushing Value (ACV) test, applying the British standard BS 812-110. Batch accelerated carbonation tests were performed on as-received BOF slag samples at mild operating conditions ($T=20\text{ }^{\circ}\text{C}$, $p=1\text{ bar}$, $L/S=0.3\text{ l/kg}$), close to those applied in the granulation tests, in order to evaluate possible changes in the extent and kinetics of carbonation resulting from the different reaction mode adopted (batch or granulation-carbonation). Moreover, two batch carbonation tests were carried out on the as received slag and on a milled sample, at

enhanced operating conditions ($T=50\text{ }^{\circ}\text{C}$, $p=10\text{ bar}$, $L/S=0.3\text{ l/kg}$) that, according to previous studies, were found to improve the steel slag carbonation reaction (Baclocchi et al., 2010a; Baclocchi et al., 2015a). In this case, the aim of the test was to assess the maximum reactivity of this residue towards CO_2 , comparing this finding with the uptake achieved in the granules obtained from the granulation-carbonation treatment. In each run, carried out in a pressurized stainless steel reactor equipped with a 150 ml internal Teflon jacket and placed in a thermostatic bath for temperature control, three 1 g slag samples were mixed with water at a set liquid to solid (L/S) ratio and exposed to a 100% CO_2 flow for different reaction times, ranging from 0.5 to 8 h. The humidity of the gas was maintained at 75% using a saturated NaCl solution in the reactor. The carbonated samples obtained from the batch tests were then analyzed so to determine the IC content, following the same procedure adopted for the granules.

4.3. Results and discussion

4.3.1. Effect of the treatment on the particle size distribution of the obtained granules

The particle size distribution of the produced granules, of which are provided some pictures in Figure 4.2, is reported in Figure 4.3 and compared with the untreated BOF slag. Generally, it is evident that the treatment, with either water or the alkaline solution, exerted a relevant effect on the particle size distribution of the material. Indeed, for the granulation treatment (see Figure 4.3a), the granules showed a mean diameter equal to 10 and 13 mm, with water or sodium silicate solution as binder, respectively, which resulted almost two order of magnitude higher than that reported for the untreated slag. Although the particle size distribution after both the experiments resulted highly comparable, a slightly increased amount of the coarser granules was obtained when the activator was used as binder.

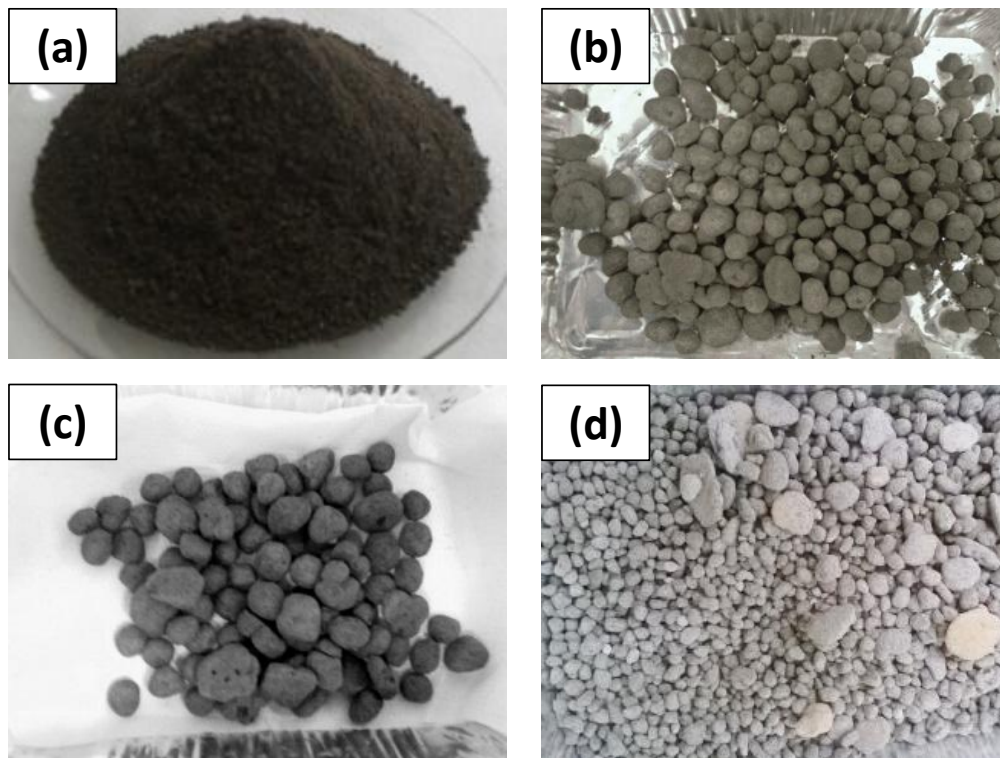


Figure 4.2 Pictures of (a) untreated BOF steel slag, granules obtained from (b) G30'_W, (c) G30'_AA_W/S=0.12 and (d) GC30'_AA_W/S=0.14

The effect of the granulation-carbonation treatment on the size distribution of granules, mixed with water and alkali activator at two different reaction times, is reported in Figure 4.3b. It can be observed that increasing the reaction time from 30 to 60 minutes, resulted in a lowering of the mean diameter of the water-based granules, passing from 3 to 2 mm, differently to what found in the previous chapter. However, since the key mechanism for increase in granule size is the coalescence process (Liu et al., 2000), the slight decrease of the mean particle size may be tentatively ascribed to a breakage phenomenon occurring during the granulation process. Conversely, mixing the slag with the activator produced smaller granules, with a mean diameter slightly above 1 mm and with a comparable particle size distribution for both the tested reaction times. Moreover, since the activator presented a higher viscosity compared with water, this behavior is

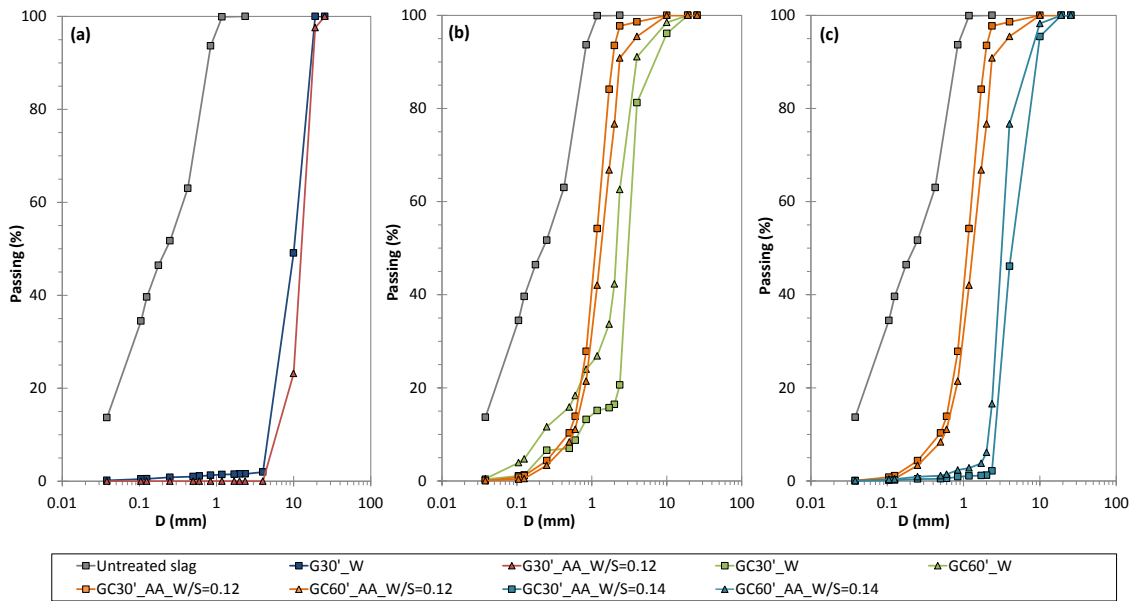


Figure 4.3 Particle size distribution of the untreated slag and of the granules obtained after the tested treatments

consistent with the results of a previous study (Iveson et al., 1996) that indicated that a more viscous binder generally produces stronger granules that tend to deform less during the granulation process leading to a reduction of the consolidation rate and subsequently of their growth. Finally, at the same reaction time, the particle growth in the presence of CO_2 showed to be slower than that resulting under atmospheric air, similarly to what reported in chapter 2; probably this effect may be ascribed to the established conditions in the reactor (e.g. different temperature and relative humidity) under a continuous flux of CO_2 , rather than to the nature of the binder.

The influence of the amount of solution on the particle size distribution of carbonated and activator-based granules is reported in Figure 4.3c. As expected, increasing the w/s ratio value from 0.12 l/kg to 0.14 l/kg accelerated the granules growing rate, leading to a maximum final mean diameter of 4.5 mm, almost four times higher than the maximum obtained at lower liquid content (1.4 mm). Moreover, in both cases, the granule size

distribution showed to be highly uniform, with no appreciable modification when the reaction time increased.

4.3.2. CO₂ uptake kinetics

The degree of carbonation of the slag was expressed in terms of the CO₂ content of the untreated sample (CO₂_{initial}) and of the treated one (CO₂_{final}), by applying the following equation:

$$\text{CO}_{2\text{uptake}} (\%) = \frac{\text{CO}_{2\text{final}} (\%) - \text{CO}_{2\text{initial}} (\%)}{100 - \text{CO}_{2\text{final}} (\%)} \cdot 100 \quad (4.1)$$

The CO₂ contents were defined from the results of the inorganic carbon analysis; in particular, the initial inorganic carbon content of the slag resulted equal to 0.03%, which corresponds to an initial CO₂ concentration of 0.1%. The main results of the batch carbonation tests, carried out at on the as-received slags at mild and enhanced operating conditions, and in the latter case also on a milled slag sample, are reported in Figure 4.4. The CO₂ uptake of the as-received slags was characterized by a rather slow kinetics, regardless the other conditions adopted. However, as reported in other studies (Baclocchi et al., 2010a), increasing the temperature and pressure of the reaction allowed to achieve a higher uptake, leading to a value of 8% after 8 hours of reaction. Other than temperature and pressure, grain size was also the parameter that seemed to most affect slag reactivity towards CO₂ (Baclocchi et al, 2009). Indeed, the carbonation test at enhanced conditions on milled slags allowed to achieve a maximum uptake of almost 15% already after 2 hours of reaction, comparable to that obtained in Baclocchi et al. (2015b).

The CO₂ uptake obtained for the granules mixed with water or the alkali solution after the granulation and the granulation-carbonation tests are reported in Figure 4.5, as a function of the curing time. Making reference to Figure 4.5a, it can be observed that, regardless the type of binder used, the CO₂ uptake of the granules achieved after the

granulation treatment was very low, reaching a maximum of 0.6% after 7 and 28 days of curing. The average CO₂ uptake of the granules showed to increase after the granulation-carbonation treatment, with values equal to almost 2.3% and 3% for the granules containing water and the alkali activator, respectively.

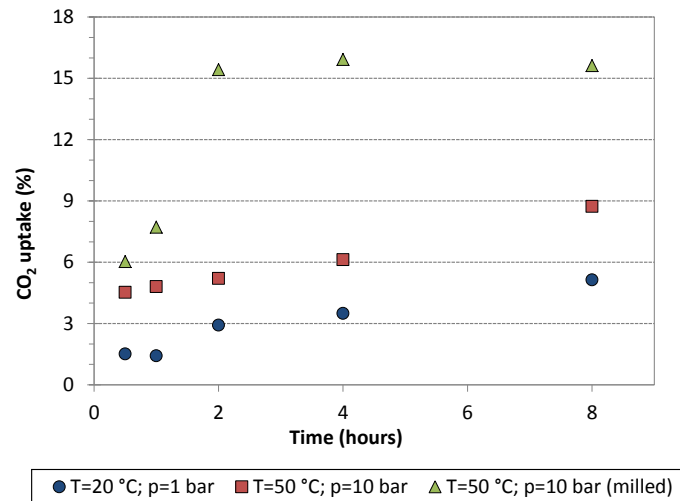


Figure 4.4 CO₂ uptake kinetics of BOF slag mixed with water.

The effect of the reaction time of the granulation-carbonation treatment on the CO₂ uptake of the alkali activated granules is reported in Figure 4.5b. It can be observed that increasing this parameter from 30 to 60 minutes exerted a negligible effect on the uptake of the granules mixed with water. On the other hand, the effect was slightly more evident for the granules based on the alkali solution, that showed a growing kinetics of CO₂ uptake with the curing time and a maximum uptake of 4% achieved for 60 minutes of treatment after 28 days of curing.

The influence of the amount of water on the uptake of the alkali-activated granules achieved after the granulation-carbonation treatments at both the reaction times is reported in Figure 4.5c. In this case, it appeared that, at a fixed reaction time, increasing the amount of binder from 0.12 to 0.14 l/kg reduced the CO₂ uptake of the granules.

Investigation of the effects of alkalis on the granules produced by carbonation-granulation treatment

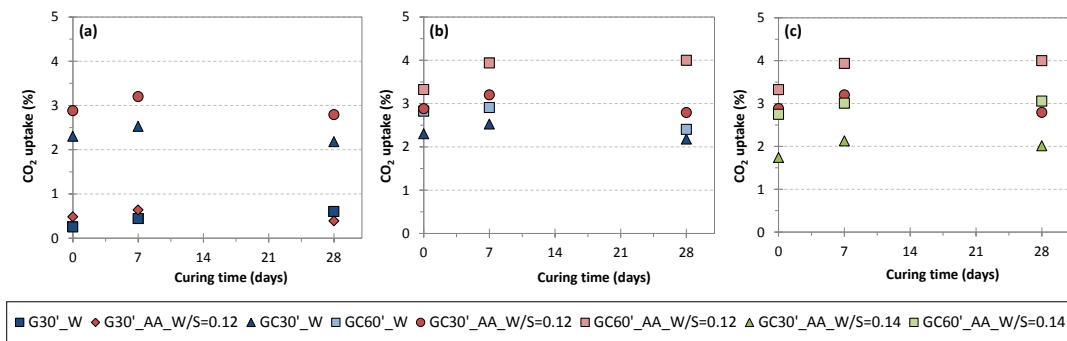


Figure 4.5 CO₂ uptake kinetics along the curing time of the granules mixed either with water or the alkali solution, obtained after the granulation and granulation-carbonation treatments, at (a) set reaction times and different binders; (b) at different reaction times and (c) at different water to solid ratio.

Namely, the highest uptake of 4% was achieved for the granules at a w/s ratio of 0.12 l/kg after 60 minutes of treatment. Furthermore, the CO₂ uptake of the granules with water obtained after the granulation-carbonation tests, achieved with a considerable amount of material (≈ 500 g) in a dynamic device under ambient T and 1 bar CO₂ pressure, are comparable once again with those obtained treating 1 g-BOF samples in the static reactor applying the same operating conditions (see Figure 4.4). A direct comparison of these results with those achieved with the granules based on the slag-cement mixture, reported in Figure 2.12, is difficult to realize, as the steel slag samples used in these tests derived from two different batches. Nevertheless, considering that activation provides an alkaline environment that should promote further carbonation by enhancing CO₂ uptake, the low values achieved in this case may be related to the limited solubility of Ca and Mg minerals phases present in the BOF steel slag. The scarce presence of portlandite in this BOF slag sample (see Figure 3.2) can also explain the lower uptakes obtained for the water-based and carbonated granules (GC30'_W and GC60'_W), in comparison with those reported in Figure 2.5.

4.3.3. Effect of the treatment on the leaching behavior of the material

In Chapter 2 it was reported that the leaching behavior of the granules was affected by the grinding process applied to the material, in order to comply with the specifications of the standard test EN 12457-2. Hence, in this chapter, with the same aim, the leaching test was carried out on the crushed and uncrushed granules obtained after the experiments, and the results of the test were also compared with those obtained for the untreated material. Furthermore, in this case, it was decided to perform the standard leaching test, that involves grinding of the material with a size higher than 4 mm, only on the samples that presented an amount of granules with a $d > 4\text{mm}$, greater or equal to 10%.

4.3.3.1. Leaching behavior of the uncrushed granules

The main results of the leaching test carried out on the untreated slag and on the uncrushed granules obtained after the experiments are reported in Figure 4.6. In terms of pH values, it can be observed that the untreated material (sample A) was characterized by an alkaline pH (13.1), slightly higher than that reported in the literature for this kind of slag (Geiseler, 1996). After the granulation treatment, the pH values showed to slightly decrease, with similar values for both the granules based on water (sample B) or alkali activator (sample C), i.e. 12.7 and 12.6, respectively. The influence of the carbonation-granulation treatment on the pH values was not relevant, except for the test carried out for 60 minutes (sample E), for which the pH was reduced to 11.9, i.e. one unit lower than the untreated slag and also complying with the threshold value set by the Italian legislation for reuse ($\text{pH} < 12$).

The regulatory elements showed in Figure 4.6 were the only ones that could be detected in the eluates of the leaching test and among those, barium and zinc were the only one that presented a concentration below the regulatory limit established by the Italian

legislation for reuse in simplified procedure (It. M.D. 186/06) for all the tested conditions. In particular, as for Ba, the alkali activated granules obtained from both the treatments (samples C, F, G, H and I), displayed a content more than one order of magnitude lower than the corresponding granules obtained at the same conditions by mixing the material with water (samples B, D and E); this effect appeared to be more remarkable for higher reaction time (60 minutes). As far as Cr is concerned, it can be observed that the combination of alkali activation and carbonation (sample F, G and I) led to concentrations twice the limit for reuse (0.05 mg/l). A similar behavior was observed also for the release of vanadium, with the exception of the granules obtained from the test named GC30' _AA_ W/S=0.14 (sample H).

The major elements shown in Figure 4.6, i.e. Al, Ca, Na and Si, were selected in order to assess the influence of the carbonation and alkali activation treatments on the leaching behavior of the aggregates. The release of Al showed to increase after all the treatments with respect to the untreated slag, probably related to the formation of more soluble phases, like Al-containing hydroxide (Huijgens et al., 2005). Moreover, it can be observed that after the carbonation-granulation treatment, the release of aluminum showed to decrease for increasing reaction time, regardless the binder used. With regard to the leaching of Ca, similarly to what obtained for barium, the alkali-based carbonated granules were characterized by a concentration one order of magnitude lower than the granules mixed with water; besides, increasing the content of the alkaline binder reduced the concentration of calcium in the eluates. The lower solubility of Ca retrieved for the carbonated granules, regardless the nature of the binder, may be ascribed to the formation of less soluble phases (e.g. calcite) in the treated material (van Zomeren et al., 2011).

The release of Na is expected to be highly affected by the leaching of the hydroxide constituting the alkali activator and, as a matter of fact, as reported in Figure 4.6 there was a difference of more than two order of magnitude between the concentrations obtained for the alkali-based granules and that of the water-based ones. Indeed, the release was quite similar for the granules based on water and obtained through both

Investigation of the effects of alkalis on the granules produced by carbonation-granulation treatment

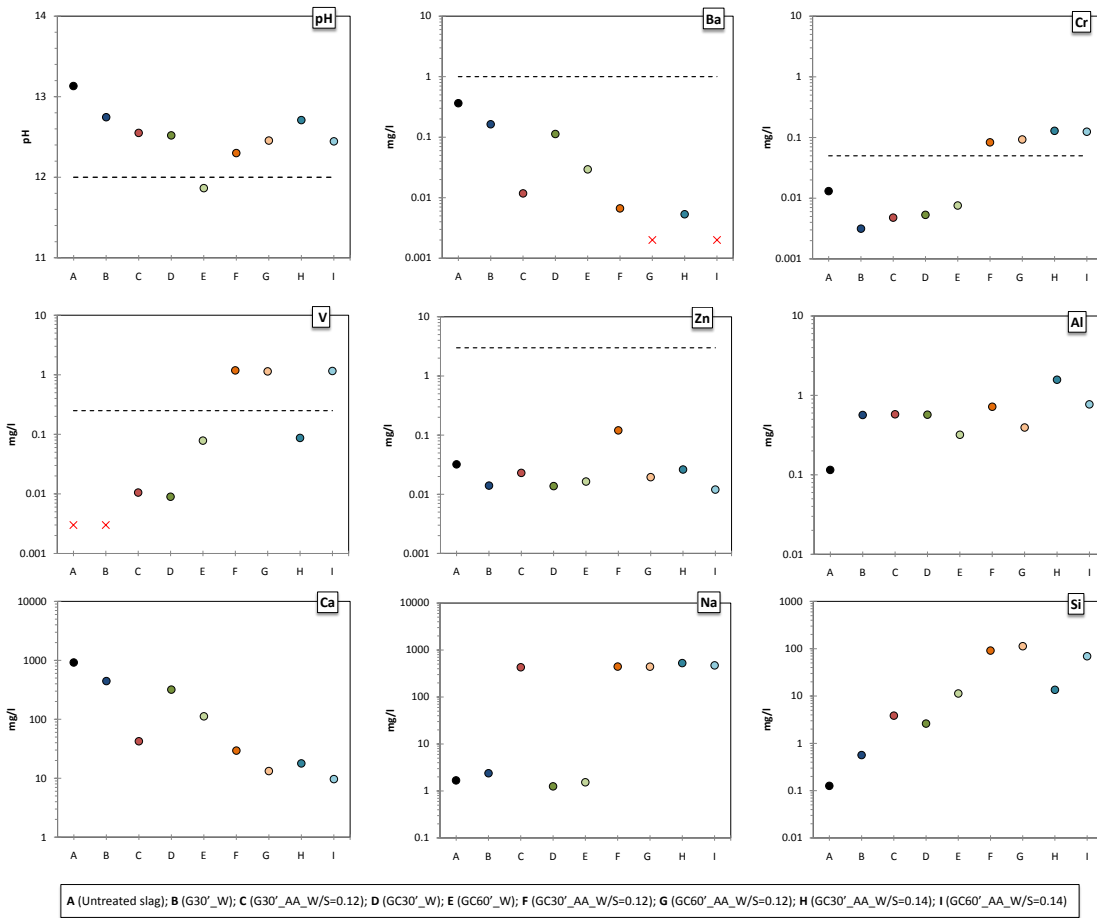


Figure 4.6 Results of the EN 12457-2 leaching test for the untreated slag and for the granules (without grinding the material) obtained after each experiment. The cross indicates that the concentration is below the quantification limit of the instrument, while the dotted line reports the limits for reuse, as for the It. MD 186/06.

granulation and granulation/carbonation treatment, with respect to the untreated material, whose concentration was equal to 1.7 mg/l. A considerable increase of the sodium release was detected for the alkali activated granules, for which the maximum value of almost 530 mg/l was achieved for the test named GC30'_AA_W/S=0.14 (sample H). Moreover, considering the granules based on the alkali activator, it was observed that either carbonation, at different reaction times, or the water to solid ratio exerted a negligible effect on the leaching of this element.

The concentration of Si of the granules obtained from the granulation treatment in the presence of the alkali activator (sample C) resulted equal to 4 mg/l, almost one order of magnitude higher than the untreated slag (0.13 mg/l) and than the granules based on water (0.5 mg/l). After the carbonation treatment, the leachability of Si increased and this was more evident for the alkali-activated granules (samples F and G) obtained after 30 and 60 minutes of treatment, whose silicon concentration resulted equal to 92 mg/l and 113 mg/l, respectively. These values showed to be 45 times and 10 times higher than the concentration obtained for the corresponding non-carbonated granules (sample C). It is worth noting that, following the different experimental conditions, the release of Si showed an increasing trend in opposition with what observed for the leaching of Ca. This finding may suggest that the combined effect of carbonation and alkali activation led to a layer covering the granules constituted of less soluble Ca-containing phase, as calcite, and more soluble Si-phases, as amorphous SiO₂, already suggested as the solubility control phase of the Ca and Si release in carbonated steel slag (Huijgen et al., 2006; Baciocchi et al., 2015b). In addition, it is interesting to notice that, for the different experimental tests, the leaching pattern of Si and V was very similar, likely suggesting that the release of these two elements from the granules treated at the same conditions may be associated to similar mineralogical changes, as reported in other studies dealing with the carbonation of steel slag (van Zomeren et al., 2011).

4.3.3.2. Leaching behavior of the crushed granules

The environmental behavior of the granules was assessed also by the standard EN 12457-2 leaching test, that involves grinding part of the material with a particle size above 4 mm. As already reported, based on the particle size distribution of the granules, it was decided to perform the standard leaching test only on those samples with at least 10% by wt. of granules having a size greater than 4 mm (see Figure 4.7).

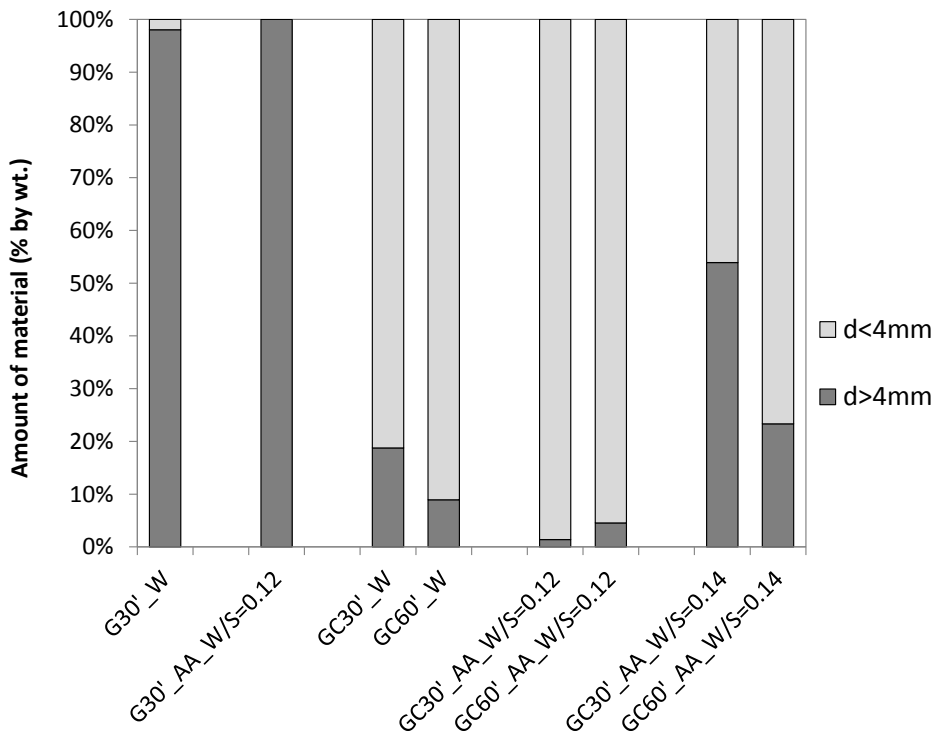


Figure 4.7 Distribution of the amount of granules (% by weight) obtained after each experiment with a diameter higher or lower than 4 mm.

The results of the compliance test, carried out on the crushed samples, is reported in Table 4.3 where the concentrations obtained for the untreated material and for the un-crushed granules are also shown and compared with the limit set for waste reuse.

The pH values obtained for the crushed granules were found to be close or slightly higher than those reported for the un-crushed ones, but always exceeding the Italian limit set for the reuse (pH=12).

As for the regulatory elements reported in Table 4.3, whose concentration was detected in the eluates of the leaching test, it can be seen that their release was not highly affected by the crushing process, applied in order to comply with the standard test. Indeed, among the others, the concentrations of Cr and V were always below the limit

Investigation of the effects of alkalis on the granules produced by carbonation-granulation treatment

Table 4.3 Results of the EN 12457-2 leaching test for the untreated slag and for the crushed and un-crushed granules, obtained after each experiment, compared with the Italian limit set for the reuse (It. MD 186/06).

		pH	Ba mg/l	Cr mg/l	V mg/l	Zn mg/l	Al mg/l	Ca mg/l	Na mg/l	Si mg/l
<i>Untreated slag</i>										
		13.13	0.36	0.01	<0.003	0.03	0.11	915.2	1.67	0.13
<i>Granulation</i>										
G30'_W	Crushed	13.09	0.4	0.01	<0.003	0.03	0.07	1001.3	2.97	0.24
	Un-crushed	12.75	0.2	0.003	<0.003	0.01	0.57	444.35	2.39	0.57
G30'_AA _W/S=0.12	Crushed	12.85	0.18	0.003	<0.003	0.02	0.11	480.62	510.2	0.35
	Un-crushed	12.55	0.01	0.005	0.01	0.02	0.58	42.39	429.2	3.86
<i>Granulation-Carbonation</i>										
GC30'_W	Crushed	12.75	0.17	0.004	<0.003	0.02	0.48	401.39	2.02	1.11
	Un-crushed	12.52	0.11	0.01	0.01	0.01	0.57	318.91	1.25	2.62
GC30'_AA _W/S=0.14	Crushed	12.89	0.03	0.05	<0.003	0.03	0.48	69.17	667	2.49
	Un-crushed	12.71	0.01	0.13	0.09	0.03	1.58	17.83	527.5	13.51
GC60'_AA _W/S=0.14	Crushed	12.29	0.003	0.11	1.26	0.07	0.52	14.59	503	101.8
	Un-crushed	12.45	<0.002	0.12	1.16	0.01	0.77	9.67	472.1	69.36
Limit for reuse	It. D.M. 186/2006	5.5-12	1	0.05	0.25	3	-	-	-	-

for reuse except for the crushed and un-crushed carbonated granules, obtained after 30 and 60 minutes by mixing the slag with the alkali solution.

Among the major slag constituents shown in Table 4.3, it can be observed as follows:

- After granulation, a higher concentration of Ca was observed for the crushed granules with respect to the uncrushed ones, and a lower release of Si and Al as well. This effect was more apparent for the granules based on the alkali

activator. It seemed also that the release of Na was not affected by the crushing process.

- After the granulation-carbonation treatment, it was observed that the concentrations of Ca and Al resulted higher for the crushed granules with respect to the uncrushed ones, conversely to Si release. Also in this case, for all the tested conditions, the concentrations of Na were not influenced by the crushing process.

Finally, the results obtained on Ca and Si leaching from crushed and uncrushed granules were compared, in order to gain further insights on the evolution of the carbonation through the particles formed as a result of the granulation-carbonation treatments.

Making reference to the granules based on water, it can be observed that Ca and Si concentrations achieved for the crushed and un-crushed granules obtained after carbonation (GC30'_W) were comparable. This result is somehow different from the one obtained in similar experiments discussed in chapter 2, where the formation of an external carbonated layer lead to a higher Si release and lower Ca release in the case of uncrushed coarser granules, and may be related to the coarser size of the granules. In this case, the different result may be hence related to a high degree of carbonation attained by the aggregates, characterized by a mean diameter lower than 4 mm, for which the formation of two distinct layers differently carbonated probably did not occur. On the other hand, the formation of a thin-carbonated layer covering the un-carbonated core may explain the great difference observed for Ca-eluate concentrations between the crushed and un-crushed coarser granules obtained from the test G30'_W. Comparing this result with the low CO₂ uptake achieved from these granules, it may be concluded that most of the particles forming the core of the aggregates, having a mean size of 10 mm, was actually not carbonated. As for the granules based on the alkali activator, it can be observed that, upon carbonation, the aggregates obtained after the test GC30'_AA_W/S=0.14 were characterized by a higher difference between both Ca and Si concentrations measured in the eluate of the crushed and un-crushed granules, than that observed for the test GC60'_AA_W/S=0.14. This finding may be once again related to a non-uniform diffusion of CO₂ into the larger granules (obtained in test

GC30'_AA_W/S=0.14), that were hence clearly constituted by an external layer characterized by a larger extent of carbonation with respect to the inner one.

4.3.4. Effect of the treatment on the mechanical properties of the material

The results in terms of the ACV of the produced granules are shown in Figure 4.8 and compared to the average values reported in the BS 812 part 110:1990 for mixed gravel (21%) and blast furnace slag (35%).

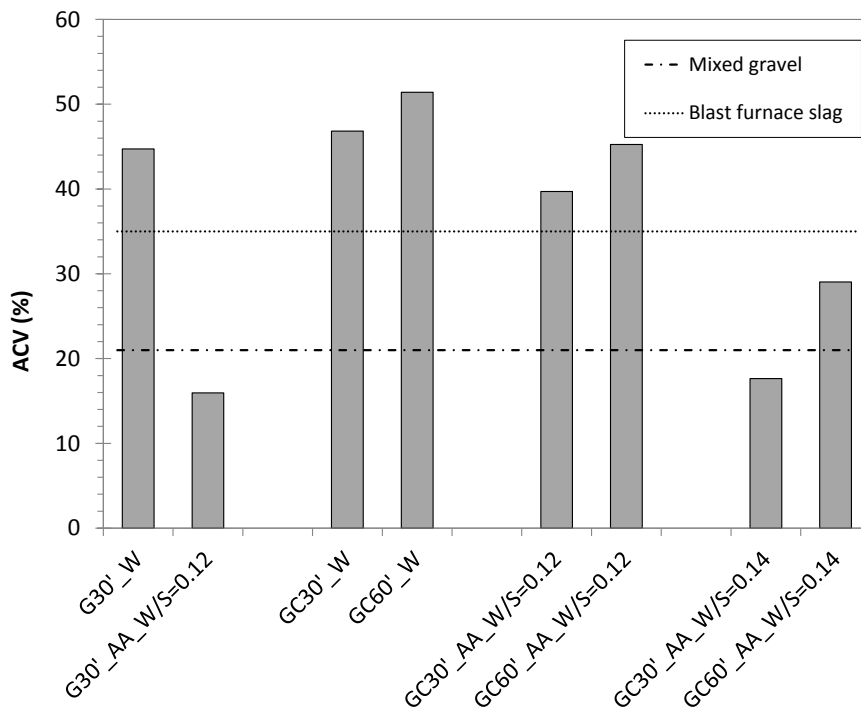


Figure 4.8 Aggregate Crushing Value (ACV) of the obtained granules at the different tested conditions. The dotted lines represent the values for the mixed gravel (21%) and blast furnace slag (35%), as reported in the BS 812 part 110:1990.

The mechanical resistance of the granules showed to be affected by the type of binder used and the type of treatment applied.

Namely, as shown in Figure 4.8, the granulation treatment employing the alkaline activator allowed to enhance the strength of the obtained granules, leading to an ACV value of 15%, notably lower than the one typical of mixed gravel, but also clearly lower than the ACV obtained after granulation using water as binder (around 45%). Combining the carbonation with granulation at a w/s equal to 0.12 l/kg led to higher ACV than those obtained after the granulation treatment. In this case, a slight improvement of the mechanical strength was achieved using the activator rather than water, whereas increasing the reaction time showed to reduce the granules strength with both binders. Finally, increasing the amount of the alkaline binder (see Figure 4.8) showed to improve the resistance of the granules; in fact, the granules obtained after 30 minutes of combined carbonation-granulation treatment, employing a w/s ratio of 0.14 l/kg, led to an ACV equal to 18%, that is about 50% less than the ACV achieved using a w/s ratio equal to 0.12 l/kg.

Thus summarizing, Figure 4.9 reports the ACV obtained from the different tests referred to that achieved from the one named G30'_AA_W/S=0.12, indicated as "reference". It can be observed that the ACV of the granules based on water, regardless the treatment applied, resulted three times higher than the reference one. A similar finding was also achieved for the granules containing the alkali solution, at a w/S ratio of 0.12 l/kg, obtained from the granulation-carbonation treatment at different reaction times. Conversely, it was possible to achieve strong granules from the granulation and carbonation treatment only increasing the amount of alkali binder and treating the material for 30 minutes. As an indication, Turk and Dearman (1989), quoting Shergold (1948), suggested that the ACV of an unbound aggregate used for the construction of a heavy traffic road should be not greater than 13%, while aggregate for concrete used in the body of the road with medium traffic conditions might have an ACV up to 40%. These differences underline that it does not exist a unique value to assess the mechanical strength of aggregates, but rather the upper limit depends on the specific civil engineering applications for which the aggregates are assigned.

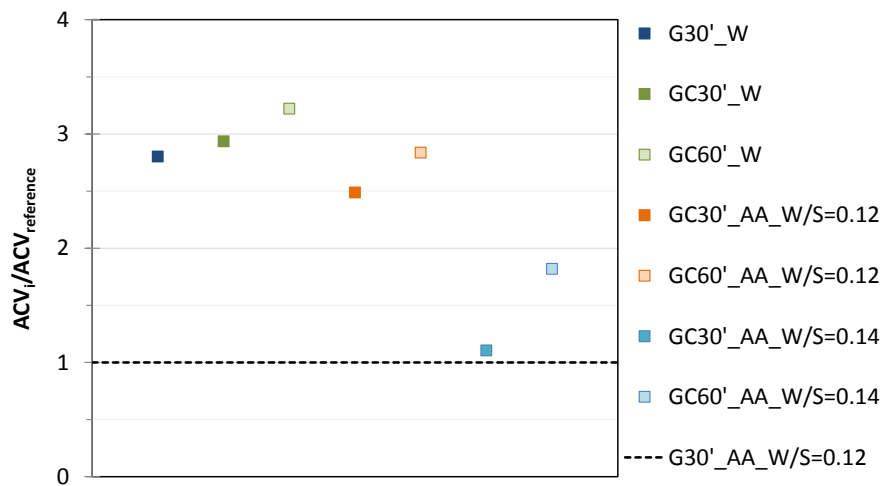


Figure 4.9 Ratio between the ACV of the granules obtained from the generic “i” test and the ACV of the granules obtained from the “reference” one, i.e. G30’_AA_W/S=0.12.

Nevertheless, based on these values and compared those set by British Standard for mixed gravel or blast furnace slag, it may be concluded that the granules produced using only the alkaline activator, or the alkaline solution at a w/s ratio of 0.14 l/kg and CO₂ as binder, presented adequate mechanical properties to be reused in civil engineering applications.

4.4. Main findings

In this chapter the results obtained from the granulation-carbonation treatment carried out with a sample of BOF slag mixed with a solution of sodium silicate and sodium hydroxide were reported and compared with those obtained with the granulation process performed employing the same binder type.

The main outcome of this chapter is that alkali activation surely allowed to improve the mechanical properties of the obtained granules, with respect to those achieved after the carbonation-granulation process using water as binder, discussed in Chapter 2.

Differently from the latter ones, the new set of experiments clearly lead to ACV values close to those typical of natural aggregates. Notably, the best performances were achieved for the granulation treatment (15%), whereas a slight increase of the w/s ratio to 0.14 l/kg was needed in order to get similar results for the combined carbonation-granulation processes (ACV=18%). The latter condition allowed also to achieve a fair storage of carbon dioxide, with a maximum average CO₂ uptake of 40 gCO₂/kg steel slag, achieved after 60 minutes of the combined treatment with the alkali activated slag at a w/s ratio of 0.12 l/kg.

The main difficulty was instead in the achievement of an environmental behavior suitable for reuse of these materials. Following the Italian legislation, it is clear that both Cr and V would exceed the limits set for waste reuse, in the case of the granules produced after the combined granulation-carbonation process with alkali-activation. All regulated elements would instead respect this limit in the case of the granules obtained from granulation only, despite in this case the pH limit (12) would be also exceeded.

Finally, with regard to the effects of the tested treatments on granule particle size, it was observed that also the combined process with alkali activation showed to achieve a remarkable increase of d₅₀ with respect to the starting material.

SECTION II

TREATMENTS AIMED AT THE VALORIZATION OF COAL GASIFICATION ASH

This section is based on a submitted paper:

Morone M., Costa G., Stendardo S., Baciocchi R. “*Characterization and density separation of coal gasification residues generated from the ZECOMIX experimental platform*”. Fuel Processing Technology.

Chapter 5

Background

5.1. Description of the Zecomix platform

Security of energy supply and CO₂ emissions are two growing concerns for an increasing number of countries. Coal, an abundant worldwide resource, will still play an important role in the domestic energy portfolio mix of the near future. Because of the high emissions associated to its utilization, however, countries are under strong pressure to exploit clean technologies for coal use and limit CO₂ emissions. Carbon capture and storage (CCS) appears as a promising technology option in the framework of decarbonised energy production. The research of new technologies based on more efficient materials and more efficient design for integration of CO₂ capture technologies in power cycles is a promising way to ensure, in the medium term, costs and energy performances comparable to those of current power plants without CCS. Zecomix (Zero Emission Coal mixed technology) represents an Italian initiative lead by ENEA, the National Italian Agency for New Technologies, Energy and Sustainable Economic Development, aimed at combining clean coal technologies and CCS in order to substantially reduce the environmental impacts related to coal use (Calabrò et al. 2008). Zecomix is an integrated pilot-scale platform where coal is gasified and the yielded synthetic gas is decarbonised in order to be used as a H₂ rich fuel in a gas turbine. The experimental activities of the Zecomix platform with regard to coal gasification started

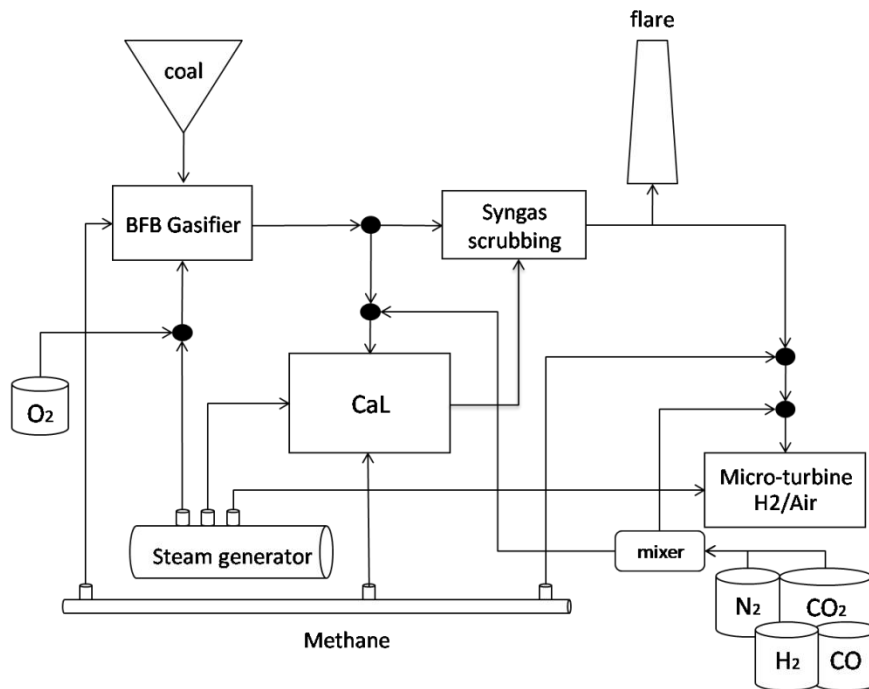


Figure 5.1 Schematic layout of the Zecomix platform

within the framework of a program funded by the Italian Ministry of Economic Development (Calabrò et al. 2009). The main aim of the project is to demonstrate, through a series of modelling and experimental activities, the feasibility of an innovative process for producing electricity and hydrogen. In the Zecomix project, a mix of different processes, such as coal gasification, syngas treatment, capture and storage of CO₂ and combustion of hydrogen in a gas turbine were coupled. The key factor for the high energetic and environmental performance of the overall process relies in the optimization of the integration of the different technologies described above. The Zecomix experimental pilot plant was designed and constructed to test each of these technologies independently. It is an advanced and flexible facility particularly oriented to the experimental investigation and modelling of both the process as a whole and of its components. The plant was presented in international research frameworks (e.g. CSLF, ZEP and EERA) as one of the advanced technological initiatives of the European and worldwide scientific community. Moreover, the Zecomix plant was evaluated and

inserted in the first Italian Roadmap towards large research facilities conceived by the Ministry of Research.

The main units of the platform, as shown in Figure 5.1, are: (i) the coal bubbling fluidized bed (BFB) gasifier, (ii) the calcium looping (CaL) decarbonising reactor and (iii) a 100 kWe micro-turbine modified to accommodate a mixture of H₂ and air.

The coal gasifier is a 300 kW_{th} steam/oxygen blown bubbling fluidised bed reactor. The coal feed system was designed for a nominal load of 1.2 t/d of coal. The system includes a 2 m³ unit for coal storage, which allows the stationary operation of the gasifier for up to 36 hours, and two screws driven by an engine connected to an inverter. The particulate solid bed of the coal gasifier is composed of olivine ([Fe, Mg]₂ SiO₄) which acts as a catalyst agent for tar cracking. The coal is gasified by means of a steam and oxygen flux which is fed at different points of the reactor in order to control the hydrodynamics of the solids and the reaction rate in all the reactor. The fuel obtained as a product of the gasification process, defined as synthetic gas or syngas, is composed of H₂, CO, CO₂ and steam at temperature of 850 °C, and is sent to a regenerative heat exchanger which reduces its temperature to around 600 °C. After this device, the syngas should be sent to the decarbonising reactor and then treated, or directly cleaned by scrubbing.

Although it is beyond the scope of this study, in this paragraph a short description of the decarbonising unit installed downstream the gasifier is provided. Among the various technologies for separating (or capturing) CO₂ from gas streams, the Calcium Looping (CaL) option with CaO-based solid sorbents was implemented in the Zecomix platform. One of the key advantages of this option, which makes it a valuable route for gas decarbonisation, is the low cost and wide availability of the feed material (a naturally occurring sorbent such as limestone or dolomite) and its high reactivity with CO₂. Moreover, CaO-based solid sorbents are more environmentally benign compared to other state-of-the-art reagents (e.g. amine-based liquid solvents). In the CaL process, CaO is converted into CaCO₃ by reacting with gaseous CO₂, then the spent solid sorbent is regenerated in a calcination step at a temperature range from 850 to 900 °C leading to the release of the captured CO₂ in a pure stream that can be sent to final storage. In addition, in the decarbonising unit, which is a fluidized bed reactor, CO-shift and steam

reforming are also carried out in order that the syngas is fully decarbonized and is mainly made up at the outlet of this unit by a mixture of steam and hydrogen.

Syngas cleaning consists in two-stage water scrubbing, then the H₂-rich gas is dried and compressed to make it suitable as a fuel for a 100 kWe micro-turbine. Moreover, a water steam generator is envisaged for feeding the gasifier, the carbonator and the micro-turbine (see Figure 5.1). Finally, there is an oxygen pre-heater for preventing condensation of water in the oxygen/steam mixture and a flare for the combustion of the syngas generated by the coal gasifier when the micro-turbine is not employed.

5.2. Overview of the main characteristics and reuse options of coal gasification ash

Besides syngas, during coal gasification also solid residues are generated, namely bottom or bed ash, the material left in the reactor after the thermal process, and fly ash, obtained from the cyclone placed downstream the gasifier for particulate removal from the produced syngas. The gasification bed ash is a typically amorphous and inert solid, mainly made up by the mineral matter of the feed coal, unburnt carbon due to incomplete coal gasification and other solid material employed in the process. Hence, the characteristics and composition of these by-products are strongly affected by the properties of the feed material and the operating conditions of the specific gasification technology adopted, such as feedstock dimensions and the operating temperature and pressure of the gasification chamber (Collot, 2006; Minchener, 2005). Gasification bed ash is generally characterized by a high content of glassy compounds (SiO₂ and Al₂O₃) related to the mineral constituents of the coal and, from an environmental point of view, by an overall limited release of potentially toxic metals compared to other types of thermal treatment residues, due to its vitreous character (Aineto et al., 2006; Pinto et al., 2008). However, depending on the coal conversion grade of the gasification technology employed, the slag sample may present various percentages of a carbon-rich fraction, called char. There are three main types of gasifier configurations depending on syngas

and coal flow characteristics: entrained flow, fixed (or moving bed) and fluidized bed (Minchener, 2005). The slag removed from an entrained bed gasifier is usually made up by a coarse, vitreous and inert fraction characterized by a low carbon content (around 30%), and a fine more porous ash presenting a higher unburnt carbon content (around 60%) compared to the coarse slag (Wu et al., 2007; Xu et al., 2009). Heterogeneous and irregularly shaped clinker samples, with a diameter greater than 1 cm, consisting of grey stone in which a black glassy matrix is included, as well as coarse particles of unburnt carbon-rich particles, are the main output stream of the Sasol Lurgi fixed bed gasifier (Matjie et al., 2006; Matjie et al. 2008a; Wagner et al., 2008). The residues resulting from a fluidised bed gasifier, such as the one installed in the Zecomix plant, are usually made up by both the mineral material that makes up the fluidised bed and acts as a catalyst (e.g. silica sand or olivine), and residual unconverted coal presenting a significant carbon content (more than 75% and depending on the coal used as feedstock) (Galhetas et al., 2012). The incomplete carbon conversion of the fluidized bed gasification technology is the consequence of the lower operating temperatures employed (typically in the range 800-1050 °C) that are kept well below ash fusion temperatures of the fuels in order to avoid ash melting and hence clinker formation (Minchener 2005). As for coal gasification fly ash, these residues are characterized by a particle size varying from 4 to 153 µm (Galhetas et al. 2012) and present a predominant Al-Si glass matrix and an amorphous character, along with different crystalline reduced phases, such as sulphides (Aineto et al., 2006).

It is estimated that a gasifier operating in a 425 net MW Integrated Gasification Combined-Cycle (IGCC) plant burning a coal characterized by a 10% ash content generates about 450 to 500 t/d of solid residues (Douglas and Chugh, 2006). So, considering that the coal gasification technology should be increasingly applied over the next years (NETL gasification worldwide database, 2010), it is important to identify potential industrial applications for gasification residues and limit so far landfill disposal. Moreover, since gasification bed ash is strongly heterogeneous because it is made up of a mixture of vitreous and carbonaceous fractions, it is necessary to identify methods for separating these two fractions in order to identify suitable reuse options for each one of them so to achieve the total utilization of the bulk sample. Indeed, the

presence of unburnt carbon in the ‘as-generated’ gasification slag may represent a detrimental factor to its utilization as sand or aggregate. The methods used to remove the carbonaceous fraction (char) from the vitreous or silicate rich one (i.e. slag) are sieving and density separation procedures (Praxis Eng.1998; Matjie et al., 2008a; Galhetas et al., 2012). Praxis Eng (1998) working on the bed ash generated from an entrained-flow gasifier, developed at a pilot scale a multi-step process for slag/char separation, through hydrocyclone or jigs, with the aim of obtaining a “char-free slag” to reuse as lightweight aggregate in the civil engineering field. Furthermore, in the work of Matjie et al. (2008), after initial characterization by CHNS analysis, a gasification slag sample obtained from a fixed bed gasifier was separated by sieving and density separation in order to obtain a specific carbon-rich size fraction to use as energy source for the cement industry, fine slag to use in the cement/concrete industry and coarse slag to employ as aggregate in road construction or brick manufacturing. In the study of Galhetas et al. (2012), the chars generated from a fluidized bed gasifier were separated from the sand bed by mechanical sieving to a size above 0.5 mm and analyzed in terms of composition and environmental behaviour as a function of the properties of the feed coal and in view of their valorization for energy production prior to landfilling. Generally, the main reuse option identified for the recovered char fractions is recycling as a fuel in the gasifier; however, depending on the type of coal used this may lead to an undesired increase of the ash content of the bed, in particular for fluidized bed units (Minchener 2005). Hence, hybrid systems consisting of a coal fluidized bed gasification process followed by char combustion in a dedicated unit may be employed to increase the carbon conversion (Minchener 2005). Alternatively, the potential of reusing high carbonaceous fractions as precursors for activated carbon production was also investigated (Maroto Valer et al., 2004; Gonzalez et al. 2009; Balsamo et al., 2013). As for the non-carbonaceous fraction of gasification bed and fly ash, based on its physical and chemical characteristics, specific reuse options have been investigated also for this material, including the production of a porous glass-ceramic product (Aineto et al., 2006), fired bricks (Acosta et al., 2002; Chen et al., 2009), and lightweight aggregates (Praxis Eng., 1998; Aineto et al., 2005).

Chapter 6

Characterization and density separation procedure of coal gasification residues generated from the Zecomix platform

6.1. Introduction

The previous section deals with the valorization of a BOF steelmaking slag, through the application of different treatments, i.e. the combination of the granulation and carbonation or the alkali activation process, with the aim of yielding a product with suitable characteristics for the reusing of this residue as aggregate in the civil application. The current work is related to another industrial residue coming from the gasification of coal, that was characterized and treated in order to assess its most suitable valorization-route. The ashes analyzed in this study come from the gasification unit of the Zecomix platform, an integrated pilot-scale system where the coal is gasified and the yielded synthetic gas is decarbonised in order to be used as a H₂ rich fuel in a

gas turbine. The overall description of the plant has been carried out in the previous chapter, hence subsequently a detailed description of the gasifier is reported.

The coal gasification unit of the Zecomix platform is mainly made up by a steam/oxygen-blown bubbling fluidised bed (BFB) gasifier and an over-bed feeding system. The gasifier has a variable cross sectional area surface whose smaller base area is a 0.38x0.36 m rectangle through which the fluidising/gasifying medium is injected. The height of the reactor is of 3.5 m. The operating temperature is 850 °C, whereas the pressure is 1.1 atm. In order to avoid clogging during coal feeding, an over-bed feeding system was selected. It consists of a funnel-shaped hopper connected with the feeding system via a vertical gravity chute. The coal metered by a screw is fed into the reaction chamber of the gasifier through a further screw which feeds the coal from above the bed. The revolution per minute of the screw-drive is remotely selected via a distributed control system. Since the operating pressure of the BFB gasifier is slightly greater than atmospheric pressure, a rotary valve is installed downstream the coal hopper with two slide valves which guard against any possible blow-back of the hot gas and fine particles from the fluidised bed to the coal hopper. The two slide valves work alternatively to accommodate a programmed quantity of coal into the charge hopper and then in a further lock hopper when needed. In order to prevent any formation of persistent clogging problems (e.g. rat-holing or bridging), a 55 l/min flow of nitrogen was added during the feeding of the olivine and coal. In addition a 22 mbar back pressure is maintained which prevents any blow-back of synthetic fuel gas from the gasification zone to the gravity chute. The steam and the oxygen during the gasification tests are fed through the smaller cross sectional area. The oxygen is stored into a cryogenic vessel and heated up via an electrical heat exchanger up to 150 °C whereas the steam is generated in a boiler by a heat exchanger fed by methane.

The experimental method adopted for the start-up of the BFB gasifier during the coal gasification tests is summarised briefly below:

- *Piping and gasifier heating up*: the temperature throughout the reaction chamber of the gasifier is increased up to 500 °C via an auxiliary methane combustor before supplying the feedstock. In the meantime, the steam generator is turned

- on in order to produce a 5 kg/h steam flow and to heat up the tubes for the injection of the steam during the coal gasification tests;
- *Feeding of the particulate olivine*: when a temperature of 500 °C is reached, the olivine is fed in order to build up the fluidised bed. The temperature in the reactor decreases and the feed rate of the olivine is adjusted to maintain a temperature in the range of 500-530 °C. The total amount of bed material used in each test is of approximately 200 kg;
 - *Fluidisation of the bed material*: the olivine is fluidised by using 120 kg/h air as fluidising medium. The pressure drop across the solid bed increases and reaches a stable value which does not further increase with an increase of the flow rate of the fluidising agent;
 - *Feeding of the particulate coal*: when the particulate olivine is well fluidised, the coal is fed via the previously described gravity feeding system. The coal flow rate is of 8 kg/h and the flow of the fluidising agent is maintained at 120 kg/h; the auxiliary methane combustor is turned off and the coal burns with the oxygen content of the fluidising agent. The temperature in the bed increases with time;
 - *Coal gasification*: when the temperature reaches 700 °C the air flow rate is slightly decreased whereas both the flow rate of oxygen and steam are increased to 25 kg/h (total mixture: 50 kg/h). The temperature during the gasification test, that has a duration of 20-30 min, is maintained at approximately 850 °C. The yielded synthetic fuel gas is depulverised in the cyclone, then scrubbed in two spray water columns and finally burnt in the flare torch.

During the gasification experiments performed in the Zecomix unit, the bed ash is typically left in the reactor for more than one cycle to increase carbon conversion, decrease the use of fresh olivine and also because the thermally treated olivine showed an enhanced performance in terms of tar catalytic cracking. However, after that the ash content of the bed increases above 5-10%, the reactor is emptied and the bed is re-composed with fresh olivine. Hence, specific management options for the discharged

bed ashes are required, as well as for the fly ashes produced from the cyclone downstream the gasification unit.

The aim of this study was to identify valorization strategies for the solid residues generated by the Zecomix gasification unit that may allow to both minimize or avoid landfill disposal while recovering energy and material that may be possibly reused within one of the processes making up the Zecomix platform. Hence, this chapter first presents the results of the characterization of the coarse and fine residues collected from the bed and the cyclone of the fluidized bed coal gasification unit of the Zecomix plant, respectively. Particle size distribution, elemental composition, total organic carbon (TOC) analysis, mineralogy and leaching behaviour were measured. Moreover, the TOC content of different particle size fractions of both types of residues was analysed to evaluate if by sieving the C-rich fraction could be removed. In addition, for the fractions presenting a prevalence of inorganic mineral material, a density separation procedure was developed and tested for each fraction with the aim of removing the residual char so to possibly use it (or specific particle size fractions of it) as a support material for producing CaO-based sorbents as indicated in the literature (Li et al., 2005; Martavaltzi and Lemonidou, 2008), to employ in the decarbonisation unit of the ZECOMIX plant.

6.2. Materials and methods

6.2.1. Materials and methods of characterization

The feed coal used for the gasification experiments was a South African coal that, along with the olivine used as bed material, was characterized in order to better understand the composition of the residues generated from the gasification process. The materials were analyzed in terms of particle size distribution, elemental and mineralogical composition and leaching behaviour.

The particle size distribution was assessed by following the ASTM D422 standard procedure. The ultimate analysis was carried out by employing a CHNS-O analyzer

(Fisher Scientific) and by following the ASTM D3173 and ASTM D3174 standard procedures for measuring the moisture and ash content of the coal, respectively. The major element and trace metal and metalloid content of the olivine, bed ash and fly ash was determined by alkali fusion which entails digesting the samples with $\text{Li}_2\text{B}_4\text{O}_7$ in platinum crucibles at 1050 °C, followed by the dissolution of the molten material with a 4% HNO_3 solution which is then analyzed by an Agilent 710-ES inductively coupled plasma optical emission spectrometer (ICP–OES). The total organic carbon (TOC) content of the residues was evaluated using a Shimadzu TOC VCPH analyser equipped with a SSM-5000A solid sampler. Moreover, the environmental behavior of the bed and fly ash was determined by performing the UNI EN 12457-2 batch standard compliance test that involves grinding the material below a grain size of 4 mm and contacting it with deionized water applying a liquid to solid (L/S) ratio of 10 l/kg for 24 h. The obtained leachates were then analyzed by ICP-OES to determine their major element and trace metal and metalloid content. All the chemical analysis, as well as the leaching tests were performed in triplicate. The mineralogical composition was determined by powder XRD analysis with Cu $K\alpha$ radiation using a Philips Expert Pro diffractometer equipped with a copper tube operated at 40 kV and 40 mA, applying an angular step of 0.02° for 2 s with 2θ spanning from 5° to 85° .

6.2.2. Particle size and density separation procedures of the gasification residues

Since the bed ash (BA) and fly ash (FA) samples analyzed in this work were heterogeneous in their particle size distribution, both samples were subdivided by sieving in different size fractions. In particular, the following classes were chosen for the BA bulk sample: Class A ($d < 0.425$ mm); Class B ($0.425 < d < 0.5$ mm); Class C ($0.5 < d < 0.6$ mm); Class D ($0.6 < d < 0.84$ mm); Class E ($0.84 < d < 9.53$ mm) while the FA bulk sample was divided in the following size fractions: Class F ($d < 0.25$ mm); Class G ($0.25 < d < 0.84$ mm) and Class H ($0.84 < d < 9.53$ mm). The TOC content was then evaluated for each fraction applying the methods reported in the previous section.

Mechanical sieving along with the TOC analysis, allowed to identify the particle size fractions with a high carbonaceous content, i.e. class E for the BA sample and classes F and H for the FA sample. However, since for the remaining fractions the sieving procedure did not allow to separate the char from the mineral material making up the gasifier bed, a density separation procedure was developed on a laboratory scale, with the aim of obtaining a carbon-rich low density fraction (float), i.e. char, and an inorganic high density fraction (sink), mainly made up of olivine. Following the experimental procedure reported in (Matjie et al., 2008), the separation medium used in this study was a mixture of bromoform and toluene, whose densities are 2890 g/l and 870 g/l, respectively. In this way, varying the amount of each compound in the final solution, it is possible to work within a range of densities close to that of coal or char, i.e. 1900 g/l. Actually, this specific density value was tested on the bulk sample of the residues but the char fraction showed not to float, indicating that to ensure that a suitable separation of the fractions could take place a higher density should be adopted. Based on this finding, the separation of classes A, B, C and D was tested with solutions presenting the following relative densities: 2000 g/l, 2200 g/l, 2400 g/l, 2600 g/l and 2890 g/l, while for class G of the fly ash, the separation process was tested employing a solution with a density of 2000 g/l. For each test, around 20 g of solid sample was mixed with the solution, whose volume was kept constant and equal to 75 ml. After the separation treatment, several washing cycles with acetone were performed on both the float and the sink fractions to remove the traces of the solution from the pores of the sample so to avoid interferences on the carbon content result. Each float and sink fraction was dried at 105 °C for 24 h, then weighted and analyzed to determine its TOC content.

6.3. Results and discussion

6.3.1. Results of the characterization

6.3.1.1. Physical properties

The coal used as feedstock material in the gasification experiments presented a particle size ranging from 1 to 6 mm with a d_{50} value of 3 mm (see Figure 6.1a), while the olivine was characterized by a mean diameter of 0.5 mm, with a particle size ranging from 0.2 to 0.84 mm (see Figure 6.1b).

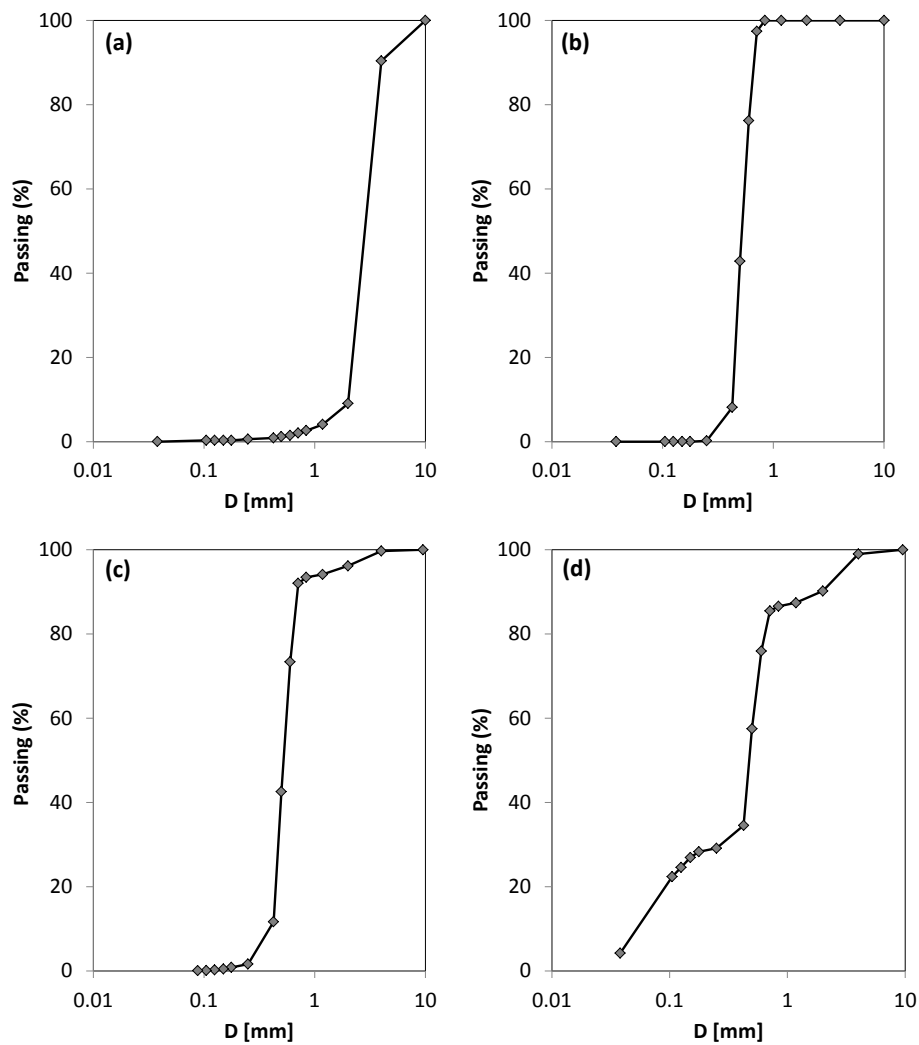


Figure 6.1 Particle size distribution of (a) the feed coal, (b) the feed olivine, (c) the bed ash and (d) fly ash.

The particle size distribution of the bed ash analyzed in this study resulted between 0.105 mm and 4 mm, with a d_{50} value of 0.5 mm (Figure 6.1c), similar to the fly ash sample, although the latter showed to be characterized by a higher amount of fine particles (see Figure 6.1d). Hence, it can be observed that the particle size distribution of the bed ash showed to be fairly comparable to that of the feed olivine, indicating that a low agglomeration occurred between the inorganic and organic fractions during gasification. This finding may be related to the relatively low operating temperature employed (850 °C), in agreement with the findings of Marinov et al. (1992) that found that agglomeration in a fluidized-bed gasifier took place usually for temperatures above 900 °C, which corresponded to the melting temperature of the iron phases present in the coal ash. The particle size of the bed and fly ash was slightly coarser than the ones reported in the study of Galhetas et al. (2012) for residues obtained from a similar type of gasification process, in which the maximum diameter observed was 1 mm for the bed ash and 0.5 mm for the fly ash.

6.3.1.2. Chemical properties

The results retrieved from the ultimate analysis of the feed coal (see Table 6.1) showed a total carbon content of 77% that, following the ASTM D388 “Standard Classification of coals by rank”, allowed to classify it as a medium volatile bituminous coal. The moisture and ash content of the coal resulted equal to 3% and 14%, respectively, consistent with the values reported for other South African coals (Pettinau et al., 2011). The hydrogen and sulfur values showed to be comparable, both equal to 1.2%, while the nitrogen content was of 0.7%.

Table 6.1 Ultimate analysis, expressed as % by weight for the coal and on bulk samples of the bed and fly ash.

	Coal	Bulk bed ash	Bulk fly ash
Total carbon	76.73	5.05	23.89
Hydrogen	1.21	0.06	0.23
Nitrogen	0.65	0	0.17
Sulfur	1.2	0.02	0.4

Regarding the residues, the findings shown in Table 6.1 indicate that the carbon content of the bulk bed ash sample was of 5%, quite similar to values reported in previous studies on slag generated by fluidized bed gasification of lignite (Li et al. 2011). The carbon content of the bulk fly ash showed to be quite significant (24%), indicating a higher amount of char present in this sample compared to the bed ash. However, both residues presented a much lower hydrogen and nitrogen content than that detected for the feed coal, due to a high degree of particle carbonization, especially for the bed ash, at the elevated operating temperatures of the gasification process, in agreement to what reported in Wagner et al. (2008). Moreover, both types of ash, the BA in particular, exhibited a low sulphur content, indicating a low retention of this element in the solid phase which, as suggested by Pinto et al. (2008), may be ascribed to the low iron content of olivine employed to make up the bed of the gasifier.

The major element and trace metal and metalloid content of olivine and the bulk bed and fly ash residues is reported in Table 6.2. The major constituents of the olivine sample were Mg (29%), Si (17.8%) and Fe (5.4%). Similar results were attained also for the residues, nevertheless, with respect to the amount retrieved in the feed olivine, the concentrations of these elements showed to be slightly lower in both ashes, and in particular in the fly ash sample, probably owing to its lower olivine content and higher char amount. Among the trace elements, the concentrations of K, Al, Ba, V and Zn were slightly higher in the fly ash sample with respect to the bed ash, while the opposite behaviour was found for Cr, Cu, Mn and Ni.

Table 6.2 Major element and trace metal and metalloid content, expressed as g/kg, of olivine and of the bulk samples of bed and fly ash.

Element (g/kg)	Olivine	Bulk bed ash	Bulk fly ash
Al	2.94	5.08	9.79
Ba	0.02	0.05	0.10
Ca	6.41	7.73	9.96
Cd	0.20	<0.002	0.38
Co	0.07	0.09	0.04
Cr	2.42	2.07	1.34
Cu	0.35	1.3	0.30
Fe	53.87	52.97	47.86
K	2.30	2.44	5.84
Mg	290.62	241.24	177.89
Mn	0.75	0.77	0.55
Mo	<0.04	<0.04	<0.04
Na	1.05	1.36	1.14
Ni	2.07	1.95	1.14
Si	178.4	161.35	125.84
V	0.02	0.02	0.04
Zn	0.29	0.07	0.40

6.3.1.3. Mineralogical properties

The XRD patterns of the residues and of the feed materials are reported in Figure 6.2. It can be seen that the main minerals detected in the coal sample were quartz, carbon and muscovite, with different peaks of Fe-containing phases, such as. Fe-sulphide and pyrite, while, as expected, olivine was the main mineral phase making up the mineral pattern of the material constituting the bed of the gasifier, along with different peaks of quartz, muscovite, enstatite and Fe-Al oxide. The mineralogy of both residues resulted very similar, pointing out the abundance of the inert material (olivine). Indeed, the most abundant mineral phase present in both residues showed to be olivine, consistent with the high content of the bed material retrieved in both bulk samples. Moreover, it is

interesting to notice that the slight hump in the diffractogram at 2θ values ranging from 15 to 30° , related to amorphous phases such as amorphous silica, was very evident for the coal but could also be detected in the fly ash sample, along with an intense peak associated to quartz or carbon. The latter peak showed to be less intense in the bed ash sample and, along with the slight presence of quartz, proved that most of the char particles characterized by a mineralogical pattern similar to that of coal were present in the fly ash. Furthermore, the sulfur containing species in the coal, i.e. pyrite and Fe sulfide, were not identified in either residue, in accordance to the lower sulfur content retrieved by chemical composition analysis for the two types of ash, indicating that during gasification sulfur was mainly converted in a volatile form and not retained in the solids (Matjie et al., 2008b; Skhonde et al., 2008).

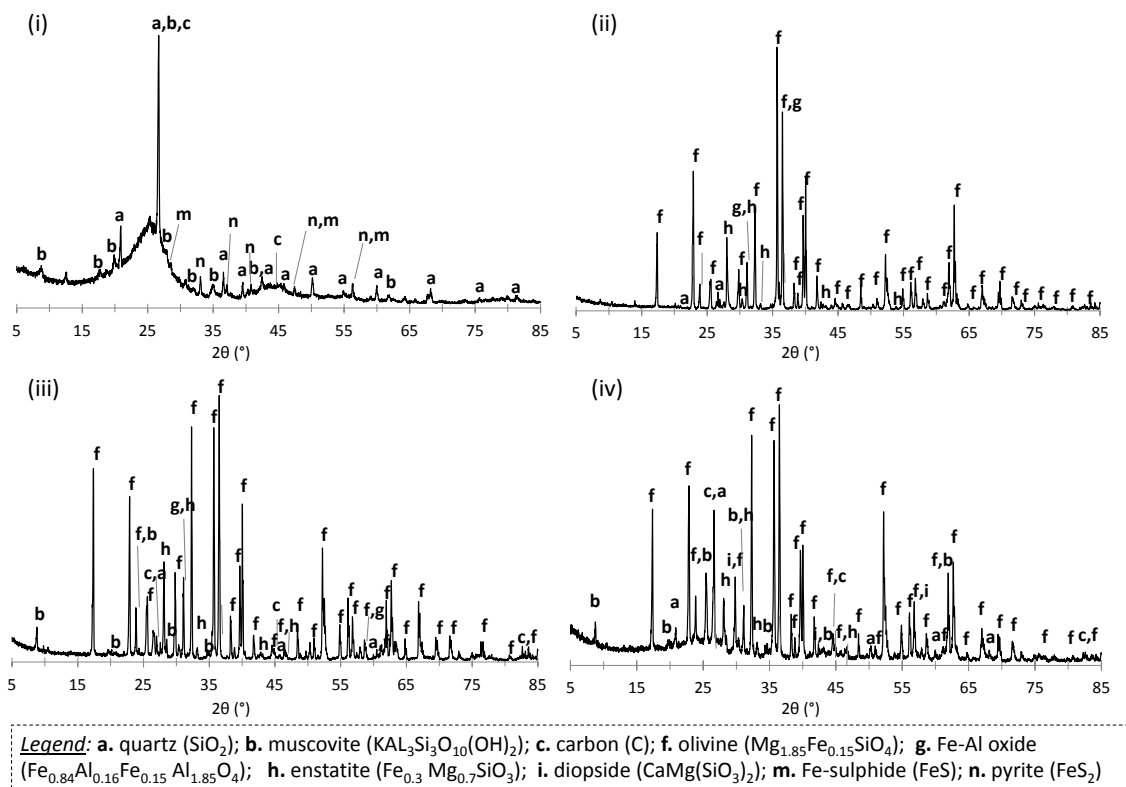


Figure 6.2 XRD pattern of the (i) coal, (ii) olivine and bulk samples of (iii) bed ash and (iv) fly ash.

6.3.1.4. Leaching behavior

The main results of the compliance leaching test carried out on the different types of residues are reported in Figure 6.3 and compared to the Italian regulatory limits for reuse. The pH of the eluates resulting for the two types of residues was comparable, showing alkaline values, lower than the reported limit (pH<12) and similar to the values reported by Galhetas et al. (2012) and Kim (2009).

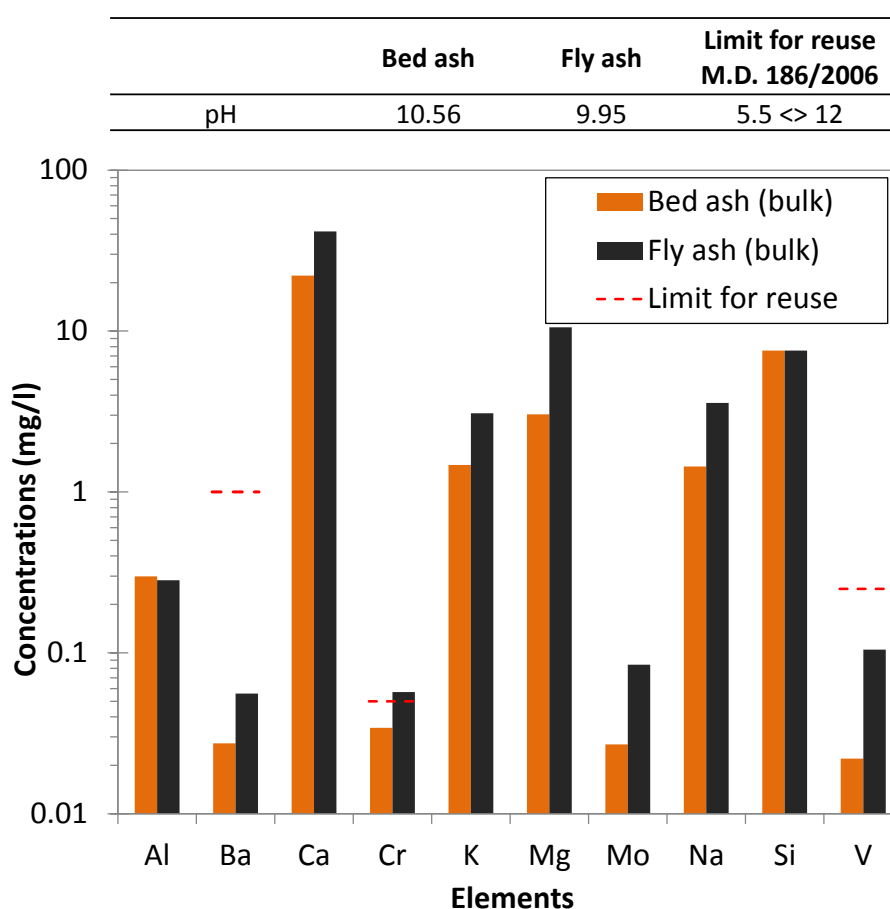


Figure 6.3 EN 12457-2 leaching test results, in terms of pH values and metal concentrations expressed in mg/l, for the bulk samples of bed and fly ash, compared to the Italian limit values for reuse (M.D. 186/2006).

The leaching of major and trace elements showed to differ depending on the type of residue analyzed since, for instance, the fly ash sample exhibited an overall higher metal

release with respect to that obtained for the bed ash. The Ca concentration was two times higher (42 mg/l) in the eluate of the FA sample compared to the BA one (22 mg/l). The Si concentration showed to be similar, for both residues around 8 mg/l, while Mg and Na release resulted to be almost three times higher in the eluate of the fly ash sample, for which concentrations of 11 and 4 mg/l were retrieved, respectively. Apart from Cr release, that in the fly ash sample showed to be slightly higher than the requirement for reuse (0.05 mg/l), the overall leachability of the regulated elements resulted low for both residues, in agreement with the findings of other studies (Pinto et al., 2008; Kim et al., 2009).

6.3.2. Results of the tested treatments on the gasification residues

6.3.2.1. Particle size procedure results

The content by weight of the different particle size classes obtained by sieving of the bed and fly ash samples is reported in Figure 5. For the bed ash (Figure 6.4i), it can be seen that classes B and C were the most abundant, representing more than the 60% by weight of the sample, followed by class D, with a 20% by weight, and classes A and E, with about 12% and 7% by weight, respectively. Moreover, based on a visual inspection of the bed ash sample (see Figure 6.5), it was observed that differently from the other particle size classes that appeared to be a mixture of mineral material with char particles, the coarser fraction (class E) consisted almost exclusively of char (see Figure 6.5c). This finding confirms that agglomeration of mineral fractions did not occur, since the olivine used in the tests presented a particle size below 0.84 mm.

Three main size fractions were identified by applying the particle size separation procedure on the fly ash sample, as reported in Figure 6.4ii. In particular, more than 50% of the total weight of the sample was collected in class G, characterized by a mixture of unburnt coal and olivine. The coarse and fine fractions, i.e. class H and F, representing respectively 13% and almost 30% by weight of the sample, were mainly characterized by unburnt coal or char.

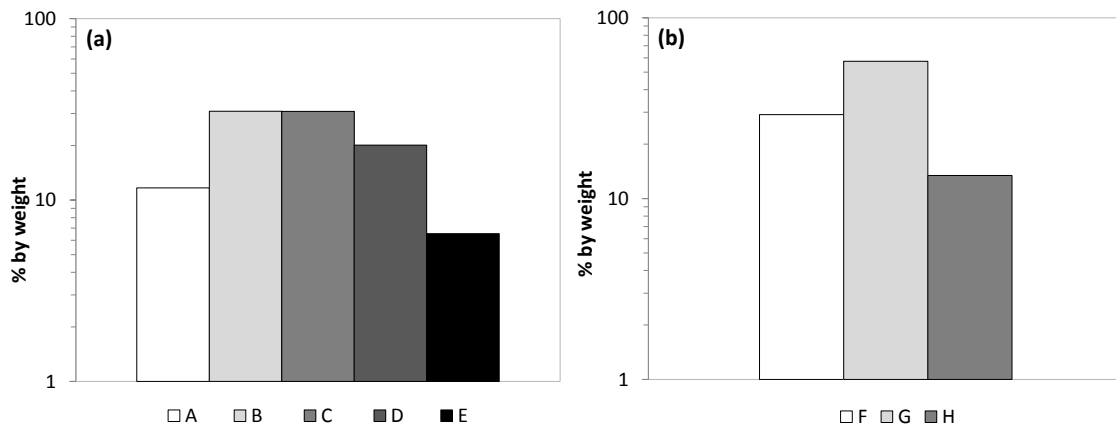


Figure 6.4 Content by weight of different particle size classes for (a) bed ash and (b) fly ash generated from the Zecomix gasification plant. Class A ($d < 0.425$ mm); Class B ($0.425 < d < 0.5$ mm); Class C ($0.5 < d < 0.6$ mm); Class D ($0.6 < d < 0.84$ mm); Class E ($0.84 < d < 9.53$ mm); Class F ($d < 0.25$ mm); Class G ($0.25 < d < 0.84$ mm); Class H ($0.84 < d < 9.53$ mm).

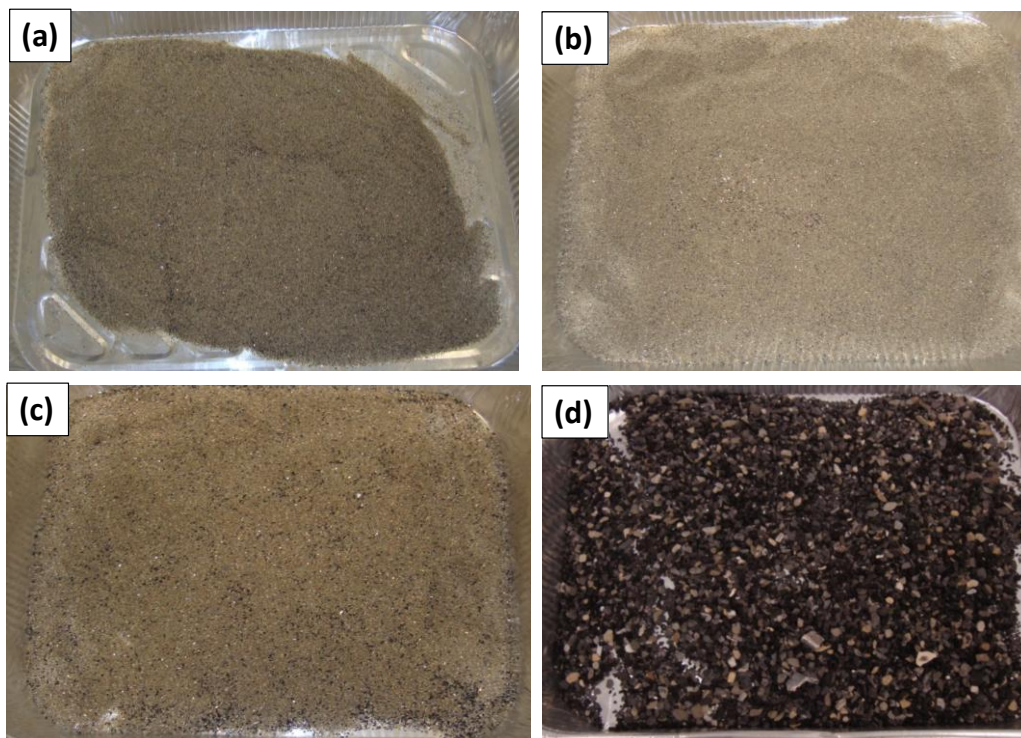


Figure 6.5 Pictures of (a) class A, (b) class B, (c) class D and (d) class E of the analyzed bed ash sample

The total organic carbon content was assessed for each size fraction of both types of residues, in order to evaluate its distribution as a function of particle size. The TOC of the bulk samples resulted equal to 5% for the bed ash sample and to 28% for the fly ash, which showed to be highly comparable with the results obtained by CHNS analysis (see Table 6.1). Regarding the TOC (%) distribution in the classes of the bed ash, it can be observed in Table 6.3 that the lowest amount of total organic carbon, less than 0.5%, was detected in the intermediate and most abundant fractions, i.e. classes B and C. For class D and class A, it showed to be almost 1.3 and 2.2%, respectively, while the coarser and less abundant class E presented a TOC content above 50%. On the other hand, considering the fly ash sample, it can be noticed that the intermediate class G presented the lowest TOC content, equal to 1%, while more than 50% was retrieved in both the fine (class F) and the coarse (class H) fractions.

Table 6.3 Total Organic Carbon (TOC) content results, along with the weight distribution of each particle class of the bed and fly ash samples

Size fractions	d (mm)	% by weight	TOC (%)
Bed ash			
Bulk			5
A	d<0.425	11.68	2.17
B	0.425<d<0.5	30.9	0.25
C	0.5<d<0.6	30.81	0.32
D	0.6<d<0.84	20.08	1.29
E	0.84<d<9.53	6.54	54.26
Fly ash			
Bulk			27.64
F	d<0.25	29.14	55.64
G	0.25<d<0.84	57.43	0.97
H	0.84<d<9.53	13.43	57.95

Hence, the TOC results indicated that, through the sieving procedure, it may be possible to achieve a good separation of the high carbonaceous fractions in the bulk sample of both the residues, which are characterized by a wide particle size range mixture of

olivine and unburnt coal. Indeed, class E of the bed ash and class H of the fly ash sample, that stand for 84% and 32% of the TOC content by weight for the respective total bulk samples (see Figure 6.6), are made up only by the coarser particles of char. Actually, the lower amount of unburnt coal detected in class H with respect to class E was ascribed to the different size distribution of the unburnt coal in the fly ash sample, since part of it was also present as a high carbonaceous fine fraction, namely class F, which represented 66% by weight of the total TOC content of the bulk fly ash sample. The higher content of char particles in the fly ash may be ascribed to the low retention time of this residue in the reactor leading to its partial or negligible gasification.

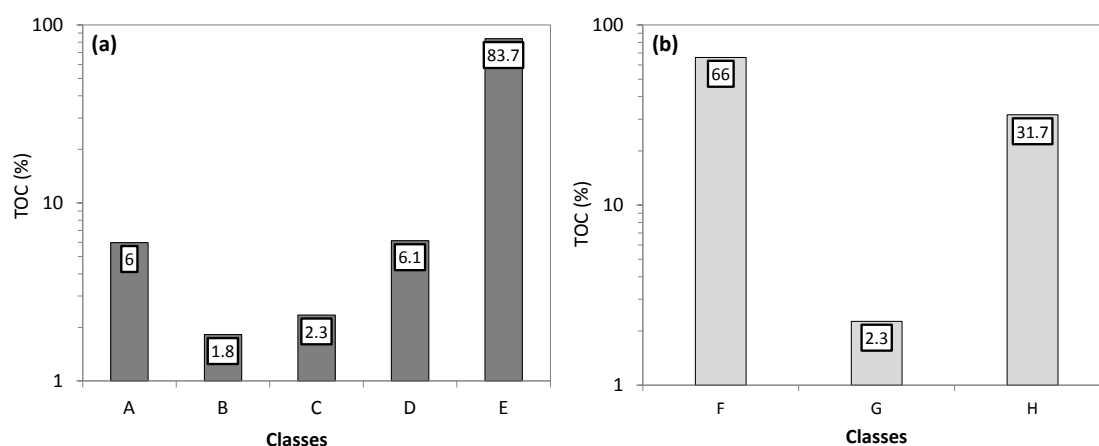


Figure 6.6 Distribution of the Total Organic Carbon (TOC) in the different particle size classes of (a) bed ash and (b) fly ash. The values were obtained considering the TOC and weight amount of each size fraction.

Thus summarizing, the particle size distribution of the tested residues proved to be one of the main factors controlling their char content, as also reported in Matjie et al. (2008) for a fixed-bed coal gasification ash. However, it should be noted that this finding cannot be generalized since it depends on the type of gasifier considered; in fact conversely to this work, Wu et al. (2007) found that the char distribution of slag generated from an entrained-bed gasifier presented a poor correlation with slag particle size.

The results of the particle size separation treatment hence indicated that, for the bed ash, sieving at 0.84 mm may allow to remove most of the TOC content of the ash present in the retained material; while for the fly ash, in order to remove the majority of the char fraction, the material should be sieved between 0.25 and 0.84 mm.

6.3.2.2. Density separation procedure results

The density separation procedure was performed on the classes that were characterized by a predominance of inorganic material and the presence of unburnt coal. Hence, based on the results obtained from the TOC analysis carried out on each size fraction, it was decided to perform the density separation procedure, aimed at removing the organic fraction from the inorganic one, on classes A, B, C and D of the bed ash sample and on class G of the fly ash.

The results achieved by applying the density separation procedure on classes A, B, C and D of the bed ash sample are reported in Figure 6.7. The amount of float or sink recovered after the treatment is reported in the figure as percentage of the initial weight of the untreated particle size fraction. As it can be observed in Figure 6.7a and b, the weight of the float and sink fractions showed to vary depending on the particle size class and density of the separation solution; however, for all the conditions tested, the sink fraction was always predominant, varying from a minimum of around 92% for class A with a 2890 g/l solution to 99.7% for class C with a 2000 g/l solution (see Figure 8b). The weight of the recovered float fraction (see Figure 6.7a) showed to vary both depending on the particle size class and density of the separation solution, appearing to increase with the solution density for all the classes, reaching the highest value, equal to 8.1% for class A at $\rho=2890$ g/l. Specifically, considering classes A and B, the weight of each recovered float fraction was quite comparable for densities below 2600 g/l, ranging from 1.7% to 2.2% for class A and from 0.25% to 0.75% for class B. The weight of the float fraction of Class C showed to increase of one order of magnitude from a density of 2000 to 2600 g/l, passing from 0.1% to 1.3%, while for class D the same values, around 2%, were achieved for both the lower (2000 g/l) and the

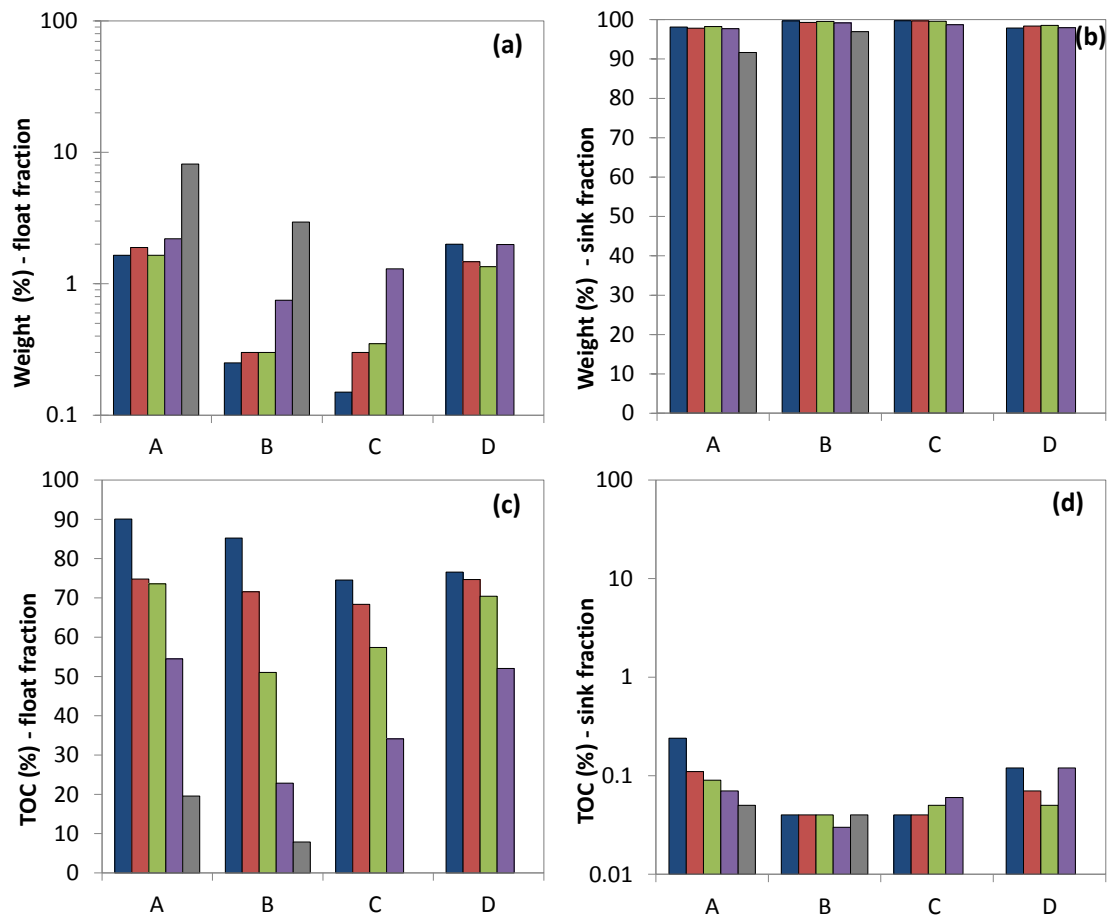


Figure 6.7 Density separation procedure results for particle size classes A, B, C and D of the bed ash as a function of the density of the solution employed (expressed in g/l), in terms of weight (%) with respect to the initial mass of the sample before the treatment of the (a) float and (b) sink fractions and of the TOC (%) of the (c) float and (d) sink fractions.

higher (2600 g/l) densities tested for this class. The highest weight recovery of float was achieved for the tests carried out with the 2890 g/l solution (8.14 and 2.95 % for classes A and B, respectively).

The distribution of the percentage of TOC in the float fraction for the different classes as a function of the density of the separation solution is reported in Figure 8c. It can be observed that increasing the density of the solution from 2000 to 2890 g/l, the TOC content decreased from 90% to 19.6% for class A and from 85% to 7.8% for class B. This result could be ascribed to the presence of light inorganic particles besides char in

the float fraction for the higher densities tested. Although to a lower extent, classes C and D showed a similar trend, since the TOC values ranged from 75% to 34% for class C and 77% to 52% for class D for increasing densities. Regarding the findings obtained for the coarser class (i.e. D), it can be observed that although the same percentages of float were obtained for the tests with 2000g/l and 2600 g/l solutions, the TOC concentrations differed considerably depending on the density adopted. Also in this case, for the lowest density a higher amount of char particles was achieved compared to the highest one for which inorganic particles may have also been included in the float fraction leading to a lower TOC concentration. The TOC content of the sink fraction, reported in Figure 6.7d, resulted well below 0.1% and close to the instrumental quantification limit (0.03-0.04 %) for all the classes and densities tested, except for class A, for which the sink contained 0.24% and 0.09% of TOC for solution densities of 2000 and 2400 g/l, respectively, and for class D, for which the same TOC content (0.12%) was found for densities of 2000 and 2600 g/l.

Hence, the results of these tests showed that, for all of the particle size fractions of the bed ash and solution densities tested, the TOC-rich fraction could be effectively separated from the far more abundant inorganic one. Actually, the classes presenting the lowest TOC content, i.e. class B and C, displayed for all the tested densities an almost completely organic carbon-free sink fraction; while for the classes presenting higher TOC contents (i.e. A=2.2% and D=1.3%) the concentrations obtained in the sink fraction showed to be of at least one order of magnitude lower.

The purity in terms of TOC content and amounts of the float fraction, however showed to vary significantly depending on the density of the solution, as well as on the particle size fraction tested. Hence, in order to assess which density value allowed to achieve the best separation efficiency for each class and also overall, the separation efficiency was calculated on the basis of the ratio between the amount of TOC in the float fraction and the total amount of organic carbon in both of the fractions achieved from the separation procedure, as shown in Eq. 6.1.

$$\xi(\%) = \frac{TOC(g)_{float}}{TOC(g)_{float} + TOC(g)_{sink}} \times 100 \quad (6.1)$$

where the amount of TOC of the obtained float ($TOC(g)_{float}$) and sink ($TOC(g)_{sink}$) fractions, expressed in g, was evaluated based on their respective weight and TOC contents (% by wt.) as reported in Equation 6.2.

$$TOC(g) = TOC(\%bywt.) \times Weight(g) \quad (6.2)$$

The results obtained in terms of the TOC content (expressed in g) of the float and sink fractions are shown respectively in Figure 6.8a and b. As for the float fraction, the TOC contents showed to vary less as a function of the solution density and more on the basis of the particle size fraction considered and, particularly, of its initial TOC content. Indeed, it can be observed that, for all the tested densities, classes B and C, both characterized by the lowest initial TOC content (see Figure 6.8), presented the lowest amount of TOC, generally below 1 g. Conversely, classes A and D showed a higher content of TOC, which also appeared to slightly differ depending on the tested densities. Moreover, if one considers all the four classes together and takes into account the TOC content recovered for each tested density, a total amount of TOC ranging from 0.5 g for a density of 2400 g/l to 0.7 g for 2000 g/l was recovered in the float fraction. As far as the sink fraction is concerned, it can be seen that, apart from class A at 2000 g/l, a negligible TOC content, generally lower than 0.05 g, was obtained after the density separation treatment.

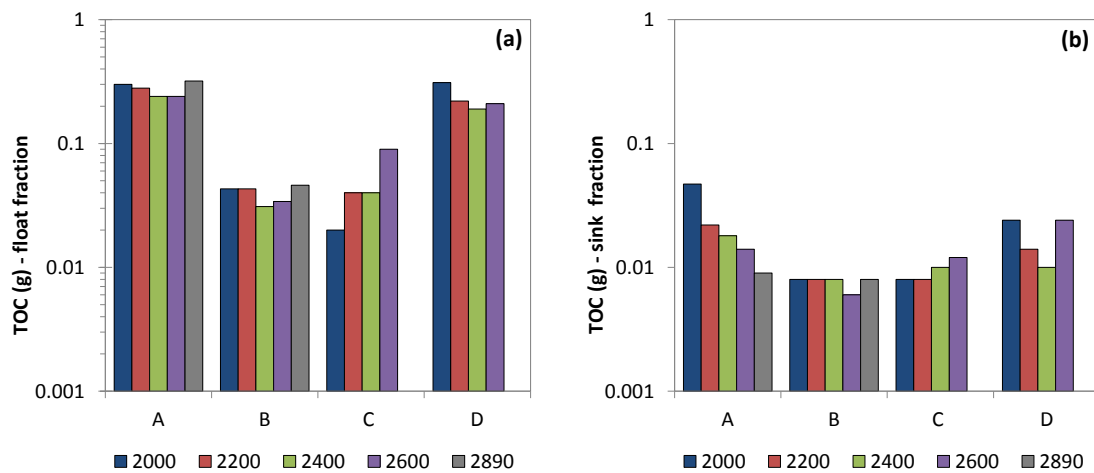


Figure 6.8 Density separation procedure results for particle size classes A, B, C and D of the bed ash as a function of the density of the solution employed (expressed in g/l) in terms of TOC (g) of the (a) float and (b) sink fractions.

The TOC separation efficiency, reported in Figure 6.9 as a function of the tested solution density, individually for each class and for the total sample with a size lower than 0.84 mm, resulted generally higher than 80% for all of the tested densities, except for the value of 74% achieved for class C at a density of 2000 g/l. For classes B and C, that presented the lowest initial content of TOC the separation efficiency was generally <85%, however for all the classes the TOC removal appeared to increase for higher solution densities. For the total sample, TOC separation proved above 90% for $\rho > 2000$ g/l, with the highest value (92%) retrieved employing a 2200 g/l solution.

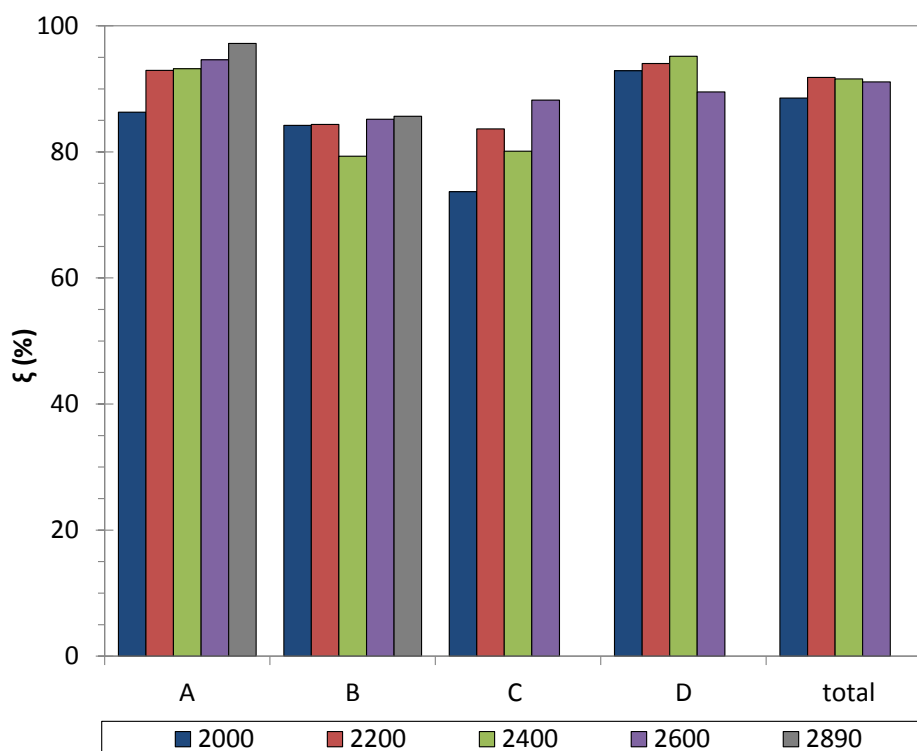


Figure 6.9 Density separation procedure results for particle size classes A, B, C and D of the bed ash, and the total, as a function of the density of the solution employed (expressed in g/l), in terms of the TOC efficiency of separation ξ (%).

In order to better analyze the effectiveness of the density separation procedure, the mineralogy of the float and sink fractions obtained by applying the procedure on class D with a solution presenting a density of 2200 g/l was analyzed and compared to the coal and olivine patterns (see Figure 6.10). The mineralogy of class D (not reported here) resulted similar to the bed ash bulk sample, since olivine and quartz were the main phases detected. Lower intensity peaks of carbon and muscovite, typical of the feed coal, were also identified, due to the presence of coarse particles of unburnt coal. The float fraction (Figure 6.10i) presented an amorphous pattern similar to the feed coal and a predominance of peaks of muscovite and carbon, whereas peaks of quartz were not detected, similarly to what observed in a previous study (Matjie et al., 2008).

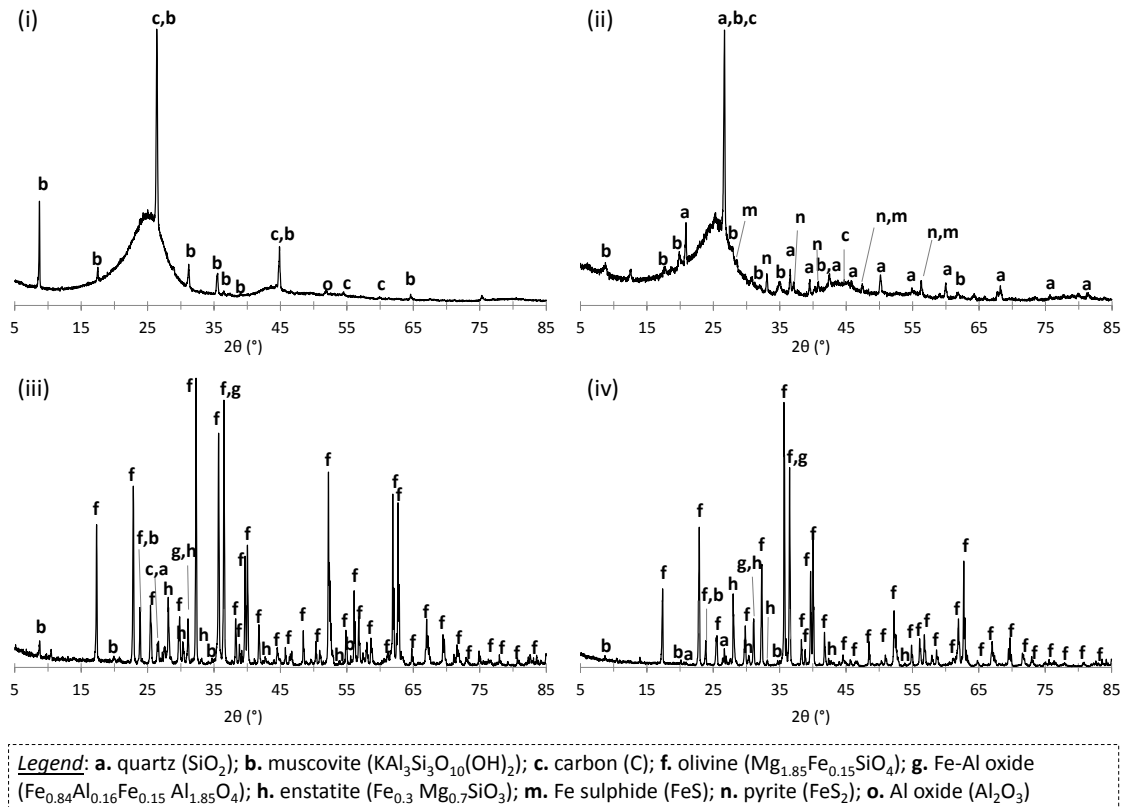


Figure 6.10 Comparison of the XRD pattern of (i) the float fraction of class D obtained after the density separation procedure at a density of 2200 g/l and (ii) the feed coal; (iii) the sink fraction of class D obtained after the density separation procedure at a density of 2200 g/l and (iv) the feed olivine.

Comparing the XRD patterns of the sink fraction (Figure 6.10iii) with that obtained for the feed olivine (Figure 6.10iv), it is evident that the main mineralogical phase in both samples was olivine. This result is in good agreement with the results of the TOC analysis, indicating that high purity float and sink fractions, with a mineralogy similar to that of the feed coal and olivine, respectively, was attained applying the developed procedure. Based on the results achieved for the bed ash, the density separation procedure was also applied on class G of the fly ash and in this case it was decided to test the lowest density, i.e. 2000 g/l, to avoid that light inorganic particles could be removed in the float fraction. Figure 6.11 reports the results in terms of weight (%) and TOC (%) of the float and sink fractions obtained. It can be seen that the float fraction, although representing only 2% of the sample, contained almost 90% of organic carbon.

Conversely, the sink fraction represented more than 98% of class G and was characterized by a negligible amount of organic carbon, equal to 0.13%. In this case, the TOC separation efficiency was equal to 92%, hence very similar to the optimum values achieved for the bed ash. Also mineralogy analysis (results not shown) lead to the same results previously reported for the bed ash (i.e. float fraction similar to the feed coal and sink fraction similar to the feed olivine).

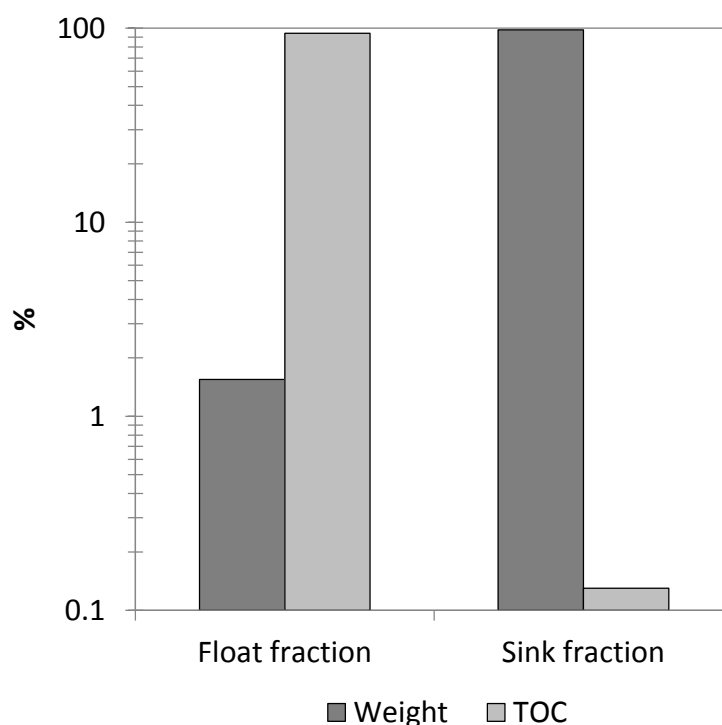


Figure 6.11 Density separation procedure results for the particle size class G of the fly ash at a density of 2000 g/l, in terms of weight (%), with respect to the initial mass of the sample before the treatment, and TOC (%) of the float and sink fractions.

6.4. Main findings

This chapter deals with the characterization, followed by treatment through a sieving and density separation procedure, of the solid residues produced from the coal gasification unit of the Zecomix plant, in view of defining an experimental protocol to

recover different fractions of these by-products and valorize them within the Zecomix testing rig. The chemical and mineralogical analysis performed on the residues derived from the bottom of the gasifier and from the cyclone positioned immediately downstream of the gasification chamber, namely bed and fly ash, showed that both were constituted by a mixture of unburnt feed coal and mineral material i.e. olivine added in the reactor as bed material. As for the environmental behavior, both ashes showed an alkaline pH and a low release of the main regulated elements, except for Cr leaching for the fly ash sample that showed to slightly exceed the limit for reuse. The carbon content analysis, which allowed to evaluate the amount of char particles in the residues, yielded a TOC of 5% for the bed ash sample, almost six times lower than that retrieved for the fly ash. In order to separate the carbon rich fraction from the inorganic one, both the residues were subdivided by sieving in different particle size classes and their TOC content was analyzed. Indeed, more than 80% of the bulk carbon content of the bed ash was concentrated in the particles presenting a diameter greater than 0.84 mm, while it was mainly distributed in the fine ($d < 0.25$ mm) and coarse ($d > 0.84$ mm) fractions of the fly ash sample. Thus, based on this preliminary separation procedure, it was possible to discriminate by sieving the fractions containing the major content of unburnt coal to feed back to the gasifier to increase the energy yield. For the other size classes mainly containing inorganic material, a density separation procedure was applied using solutions of bromoform and toluene with different densities, ranging from 2000 g/l to 2890 g/l, so to achieve a carbonaceous float fraction and an inorganic sink one, with the aim of recovering both of them. The results of these tests showed that it was possible to achieve a sink fraction with an overall negligible carbon content, lower than 0.1%, for all of the particle size classes and most solution densities investigated. The float fraction was characterized by a TOC content that was variable as a function of the solution density, decreasing generally for higher densities. In particular, considering the application of this procedure to the bulk bed ash with a particle size below 0.84 mm, the highest TOC separation yield (92%) was achieved for a density of 2200 g/l. An analogous separation efficiency was achieved also for the intermediate particle size fraction of the fly ash with a density of 2000 g/l.

Conclusions and final remarks

This thesis was addressed to investigate suitable treatments aimed at the valorization of two specific types of residues, i.e. BOF steel slags and the ashes derived from a coal gasifier, that currently are not properly exploited or reused.

The main research topic was the development of an innovative treatment of BOF slags, based on the combination of a granulation process for aggregates production, with carbonation and alkali activation, aimed at reducing GHG emissions of steelmaking plants and at improving the end product properties.

The application of either granulation or granulation-carbonation treatments to BOF slags allowed to produce granules with a particle size tenfold larger than the untreated slag and to obtain promising CO₂ uptakes. The leaching behavior of the yielded aggregates showed to comply with the Italian limit for reuse, except for pH values, while the mechanical performance of the achieved aggregates (measured in terms of ACV) was poor with respect to natural gravel. The mechanical properties of the aggregates obtained by either granulation or granulation-carbonation were notably improved by partially replacing the BOF slags with up to 20% cement, leading to ACV values comparable with those of natural gravel, although a slightly detrimental effect on the CO₂ uptake was observed with respect to tests performed without cement.

Alkali-activation was then successfully investigated as an alternative option to the use of cement as binder for aggregates production. Namely, a preliminary study allowed to select a specific solution of sodium hydroxide and sodium silicate as the most suitable one to activate BOF slags. The application of this solution to the granulation and granulation-carbonation treatments also allowed to obtain aggregates with mechanical properties comparable to those of natural gravel, with CO₂ uptakes close to those achieved without adding an alkali activator. The leaching behavior of the aggregates obtained from the granulation process were again in compliance with the Italian limit for reuse, except for the pH, whereas also Cr and V were found to exceed the Italian limits set for waste reuse for the aggregates obtained from the granulation-carbonation process.

A secondary topic was the characterization of coal gasification ashes (bed- and fly-) and the application of a separation process, aimed at obtaining a char-rich fraction and an inorganic fraction both suitable for reuse. Based on the finding that more than 80% of the organic carbon content is in bed-ash particles with size above 0.84 mm, while it is mainly distributed in the fine ($d < 0.25$ mm) and coarse ($d > 0.84$ mm) fractions of the fly-ash, a sieving process was applied to the bulk material, allowing to obtain fractions with an organic carbon content comparable to that of coal. A density-separation process was then applied to the remaining size fractions, allowing to obtain a sink fraction with an overall negligible carbon content and a float fraction once again with an organic carbon content comparable to that of coal.

Perspectives

The techniques developed and investigated in this work may represent feasible options for valorizing both investigated residues, although different aspects of the research still need to be addressed.

Indeed, as far as the work on BOF valorization is concerned, it should be underlined that alkali activation has a two-fold effect: to activate the hydration reactions of BOF slag and to provide increased alkaline conditions to promote CO₂ uptake and thereby carbonation reactions. Low CO₂ uptake trend observed in the work cannot be related to low CO₂ uptake but to the limited solubility of the Ca and Mg containing minerals present in the analyzed steel slag. In that case, how to master the carbonation of this material remains a challenging task to further investigate.

The environmental benefits of the treatment applied to BOF steel slag could be also further explored by Life Cycle Assessment (LCA), assessing the impacts related to the use of recycled aggregates produced through the innovative treatment proposed in this thesis in comparison to the use of natural aggregates. Moreover, raw alkali solutions used in this work as a source of silica, whose production may lead to CO₂ emissions and to other environmental impacts as well, could be replaced by suitable waste streams (e.g. glass waste, gasification bottom ash or blast furnace slag), possibly allowing to make the whole process more sustainable. Besides, based on the findings achieved in

this study on a lab-scale base, future research may also regard the scale-up of the treatment to pilot-scale, so to identify the optimum conditions for the production of marketable aggregates.

As far as the process for the valorization of gasification residues is concerned, future research could investigate treatments for exploiting the inorganic fraction obtained from the applied separation process, as a support for catalysts (i.e. for steam reforming) or sorbents (i.e. dispersed CaO sorbent for CO₂ capture). Hence, further work is needed to verify the suitability of the obtained inorganic fraction for these applications.

References

- Acosta, A., Iglesias, I., Aineto, M., Romero, M., Rincón, J. M. (2002). Utilisation of IGCC slag and clay steriles in soft mud bricks (by pressing) for use in building bricks manufacturing. *Waste management*, 22(8), 887-891.
- Adetayo, A. A., Litster, J. D., Desai, M. (1993). The effect of process parameters on drum granulation of fertilizers with broad size distributors. *Chemical engineering science*, 48 (23), 3951-3961.
- Aineto, M., Acosta, A., Rincón, J.M., Romero, M. Production of lightweight aggregates from coal gasification fly ash and slag, *World of Coal Ash (WOCA) Conference*, April 11-15 2005, Lexington, Ky, USA
- Aineto, M., Acosta, A., Iglesias, I. (2006). The role of a coal gasification fly ash as clay additive in building ceramic. *Journal of the European Ceramic Society*, 26(16), 3783-3787.
- Allahverdi, A., Kani, E. N., Esmailpoor, S. (2008). Effects of Silica Modulus and Alkali Concentration on Activation of Blast-Furnace Slag. *Iranian Journal of Materials Science and Engineering*, 5 (2), 32-35.
- Altan, E., Erdoğan, S. T. (2012). Alkali activation of a slag at ambient and elevated temperatures. *Cement and Concrete Composites*, 34(2), 131-139.
- Altun, I. A., Yılmaz, I. (2002). Study on steel furnace slags with high MgO as additive in Portland cement. *Cement and Concrete Research*, 32 (8), 1247-1249.
- Arickx, S., Van Gerven, T., Vandecasteele, C. (2006). Accelerated carbonation for treatment of MSWI bottom ash. *Journal of hazardous materials*, 137 (1), 235-243.
- Atiş, C. D., Bilim, C., Çelik, Ö., Karahan, O. (2009). Influence of activator on the strength and drying shrinkage of alkali-activated slag mortar. *Construction and building materials*, 23 (1), 548-555.
- Babu, K. G., Kumar, V. S. R. (2000). Efficiency of GGBS in concrete. *Cement and Concrete Research*, 30(7), 1031-1036.

- Baclocchi, R., Costa, G., Polettini, A., Pomi, R. (2009). Influence of particle size on the carbonation of stainless steel slag for CO₂ storage. *Energy Procedia*, 1(1), 4859-4866.
- Baclocchi, R., Costa, G., Di Bartolomeo, E., Polettini, A., Pomi, R. (2010a). Carbonation of stainless steel slag as a process for CO₂ storage and slag valorization. *Waste and biomass valorization*, 1 (4), 467-477.
- Baclocchi, R., Costa, G., Lategano, E., Marini, C., Polettini, A., Pomi, R., Postorino, P., Rocca, S. (2010b). Accelerated carbonation of different size fractions of bottom ash from RDF incineration. *Waste management*, 30(7), 1310-1317.
- Baclocchi, R., Costa, G., Di Gianfilippo, M., Polettini, A., Pomi, R., Stramazzo, A.. Evaluation of the CO₂ storage capacity of different types of steel slag subjected to accelerated carbonation. In: *Proceedings of the 3rd International Conference on Industrial and Hazardous Waste Management*. Crete, Greece, 12-14 September 2012.
- Baclocchi, R., Costa, G., Di Gianfilippo, M., Polettini, A., Pomi, R., Stramazzo, A., Zingaretti, D. Influence of CO₂ partial pressure on direct accelerated carbonation of steel slag. In: *Proceedings of the 4th International Conference on Accelerated carbonation for environmental and material Engineering (ACEME)*. Leuven, Belgium, 9-12 April 2013.
- Baclocchi, R., Costa, G., Di Gianfilippo, M., Polettini, A., Pomi, R., Stramazzo, A. (2015a). Thin-film versus slurry-phase carbonation of steel slag: CO₂ uptake and effects on mineralogy. *Journal of hazardous materials*, 283, 302-313.
- Baclocchi, R., Costa, G., Polettini, A., Pomi, R. (2015b). Effects of thin-film accelerated carbonation on steel slag leaching. *Journal of hazardous materials*, 286, 369-378.
- Bakharev, T., J. G. Sanjayan, Y-B. Cheng. (1999a). Effect of elevated temperature curing on properties of alkali-activated slag concrete. *Cement and concrete research*, 29(1), 1619-1625.
- Bakharev, T., Sanjayan, J. G., Cheng, Y. B. (1999b). Alkali activation of Australian slag cements. *Cement and Concrete Research*, 29(1), 113-120.
- Balsamo, M., Di Natale, F., Erto, A., Lancia, A., Montagnaro, F., Santoro, L. (2013). Gasification of coal combustion ash for its reuse as adsorbent. *Fuel*, 106, 147-151..

- Baykal, G., Döven, A. G. (2000). Utilization of fly ash by pelletization process; theory, application areas and research results. *Resources, Conservation and Recycling*, 30 (1), 59-77.
- Belhadj, E., Diliberto, C., Lecomte, A. (2012). Characterization and activation of Basic Oxygen Furnace slag. *Cement and Concrete Composites*, 34 (1), 34-40.
- Bernal, S.A., Provis, J. L., Brice, D. G., Kilcullen, A., Duxson, P., van Deventer, J. S. (2012). Accelerated carbonation testing of alkali-activated binders significantly underestimates service life: the role of pore solution chemistry. *Cement and Concrete Research*, 42(10), 1317-1326.
- Bernal, S. A., Provis, J. L., Walkley, B., San Nicolas, R., Gehman, J. D., Brice, D. G., Kilcullen, A.R., Duxson, P., van Deventer, J. S. (2013). Gel nanostructure in alkali-activated binders based on slag and fly ash, and effects of accelerated carbonation. *Cement and Concrete Research*, 53, 127-144.
- Bohmer, S., Moser, G., Neubauer, C., Peltoniemi, M., Schachermayer, E., Tesar, M., Walter, B., Winter, B. (2008). Aggregate case study, final report.
- Bonenfant, D., Kharoune, L., Sauve, S., Hausler, R., Niquette, P., Mimeault, M., Kharoune, M. (2008). CO₂ sequestration potential of steel slags at ambient pressure and temperature. *Industrial Engineering Chemistry Research*, 47(20), 7610-7616.
- Brough, A. R., Atkinson, A. (2002). Sodium silicate-based, alkali-activated slag mortars: Part I. Strength, hydration and microstructure. *Cement and Concrete Research*, 32(6), 865-879.
- Bullard, J. W., Jennings, H. M., Livingston, R. A., Nonat, A., Scherer, G. W., Schweitzer, J. S., Scrivener, K. L., Thomas, J. J. (2011). Mechanisms of cement hydration. *Cement and Concrete Research*, 41(12), 1208-1223.
- Burciaga-Díaz, O., Díaz-Guillén, M. R., Fuentes, A. F., Escalante-Garcia, J. I. (2013). Mortars of alkali-activated blast furnace slag with high aggregate: binder ratios. *Construction and Building Materials*, 44, 607-614.
- Butensky, M., Hyman, D. (1971). Rotary drum granulation. An experimental study of the factors affecting granule size. *Industrial Engineering Chemistry Fundamentals*, 10(2), 212-219.
- Calabrò, P. Deiana, G. Girardi, P. Fiorini, S. Stendardo, Possible optimal configurations for the ZECOMIX high efficiency zero emission hydrogen and power plant. *Energy* 33 (6) (2008) 952-962.

- Calabrò, A., Samela F., Bassano C., Deiana P., Analisi di un impianto sperimentale per la coproduzione di energia elettrica e di idrogeno da carbone con “quasi” zero emissioni di anidride carbonica, ENEA Report RSE/2009/25, in italian
- Capobianco O., Innovative technology trains for treating excavated material in the framework of Brownfield regeneration, PhD thesis, 2014.
- Chaurand, P., Rose, J., Domas, J., Bottero, J. Y. (2006). Speciation of Cr and V within BOF steel slag reused in road constructions. *Journal of Geochemical Exploration*, 88(1), 10-14.
- Chaurand, P., Rose, J., Briois, V., Olivi, L., Hazemann, J. L., Proux, O., Domas, J., Bottero, J. Y. (2007). Environmental impacts of steel slag reused in road construction: A crystallographic and molecular (XANES) approach. *Journal of Hazardous Materials*, 139(3), 537-542.
- Cheeseman, C. R., Makinde, A., Bethanis, S. (2005). Properties of lightweight aggregate produced by rapid sintering of incinerator bottom ash. *Resources, Conservation and Recycling*, 43(2), 147-162.
- Chen, Q., Johnson, D.C., Zhu, L., Yuan, M., Hills, C.D., Accelerated carbonation and leaching behavior of the slag from iron and steel making industry. *Journal of University of Science and Technology Beijing*, 2007, 14 (4), 297.
- Chen, L. M., Chou, I.M., Chou, S-F J., Stucki, J.W. Producing fired bricks using coal slag from a gasification plant in Indiana, World of Coal Ash (WOCA) Conference, May 4-7, 2009, Lexington, KY, USA.
- Cioffi, R., Colangelo, F., Montagnaro, F., Santoro, L. (2011). Manufacture of artificial aggregate using MSWI bottom ash. *Waste Management*, 31 (2), 281-288.
- Cizer, Ö., Van Balen, K., Elsen, J., Van Gemert, D. (2012). Real-time investigation of reaction rate and mineral phase modifications of lime carbonation. *Construction and Building Materials*, 35, 741-751.
- Collot, A. G. (2006). Matching gasification technologies to coal properties. *International Journal of Coal Geology*, 65(3), 191-212.
- Criado, M., Fernández-Jiménez, A., Palomo, A. (2010). Alkali activation of fly ash. Part III: Effect of curing conditions on reaction and its graphical description. *Fuel*, 89(11), 3185-3192.

- Das, B., Prakash, S., Reddy, P. S. R., Misra, V. N. (2007). An overview of utilization of slag and sludge from steel industries. *Resources, conservation and recycling*, 50(1), 40-57.
- Davidovits, J., Cordi, S. A. (1979). Synthesis of new high-temperature geo-polymers for reinforced plastics/composites. *SPE PACTEC*, 79, 151-4.
- De Vargas, A. S., Dal Molin, D. C., Vilela, A. C., Da Silva, F. J., Pavão, B., Veit, H. (2011). The effects of Na₂O/SiO₂ molar ratio, curing temperature and age on compressive strength, morphology and microstructure of alkali-activated fly ash-based geopolymers. *Cement and concrete composites*, 33(6), 653-660.
- De Windt, L., Chaurand, P., Rose, J. (2011). Kinetics of steel slag leaching: batch tests and modelling. *Waste Management*, 31 (2), 225-235.
- Deneele, D., De Larrard, F., Rayssac, E., Reynard, J. (2005). Control of basic oxygen steel slag swelling by mixing with inert material. In *Proceedings of the 4th European Slag Conference, Oulu* (pp. 187-98).
- Douglas, E., Brandstetr, J. (1990). A preliminary study on the alkali activation of ground granulated blast-furnace slag. *Cement and concrete research*, 20(5), 746-756.
- Douglas, F., Chugh, Y.P. (2006), Feasibility of utilizing integrated gasification combined cycle (IGCC) by-products for novel materials development, Final Report.
- Duxson, P., Provis, J. L., Lukey, G. C., Van Deventer, J. S. (2007). The role of inorganic polymer technology in the development of 'green concrete'. *Cement and Concrete Research*, 37(12), 1590-1597.
- Escalante, J. I., Gomez, L. Y., Johal, K. K., Mendoza, G., Mancha, H., Mendez, J. (2001). Reactivity of blast-furnace slag in Portland cement blends hydrated under different conditions. *Cement and Concrete Research*, 31(10), 1403-1409.
- Etxeberria, M., Pacheco, C., Meneses, J. M., Berridi, I. (2010). Properties of concrete using metallurgical industrial by-products as aggregates. *Construction and Building Materials*, 24(9), 1594-1600.
- Euroslag Statistics, 2012. <http://www.euroslag.com/products/statistics/2012/> (accessed on April 2015).
- Fernández-Bertos, M., Simons, S. J. R., Hills, C. D., Carey, P. J. (2004). A review of accelerated carbonation technology in the treatment of cement-based materials and sequestration of CO₂. *Journal of Hazardous Materials*, 112(3), 193-205.

- Fernández-Jiménez, A., Puertas, F., Arteaga, A. (1998). Determination of kinetic equations of alkaline activation of blast furnace slag by means of calorimetric data. *Journal of thermal analysis and calorimetry*, 52(3), 945-955.
- Fernández-Jiménez, A., Palomo, J. G., Puertas, F. (1999). Alkali-activated slag mortars: mechanical strength behaviour. *Cement and Concrete Research*, 29(8), 1313-1321.
- Fernández-Jiménez, A., Palomo, A. (2003). Characterisation of fly ashes. Potential reactivity as alkaline cements. *Fuel*, 82(18), 2259-2265.
- Fernández-Jiménez, A., Palomo, A. (2005). Composition and microstructure of alkali activated fly ash binder: effect of the activator. *Cement and concrete research*, 35(10), 1984-1992.
- Galhetas, M., Lopes, H., Freire, M., Abelha, P., Pinto, F., Gulyurtlu, I. (2012). Characterization, leachability and valorization through combustion of residual chars from gasification of coals with pine. *Waste management*, 32(4), 769-779.
- Garcia-Lodeiro, I., Fernandez-Jimenez, A., Palomo, A. (2013). Hydration kinetics in hybrid binders: early reaction stages. *Cement and Concrete Composites*, 39, 82-92.
- Geiseler, J. (1996). Use of steelworks slag in Europe. *Waste management*, 16(1), 59-63.
- Glukhovsky, V. D. (1981). Slag-alkali concretes produced from fine-grained aggregate. Kiev: Vishcha Shkolay.
- Glukhovsky, V. D., Rostovskaja, G. S., Rumyna, G. V. (1980). High strength slag-alkaline cements. In *Proceedings of the 7th international congress on the chemistry of cement*, Paris, June.
- González, J. F., Román, S., Encinar, J. M., Martínez, G. (2009). Pyrolysis of various biomass residues and char utilization for the production of activated carbons. *Journal of Analytical and Applied Pyrolysis*, 85(1), 134-141.
- Greenberg, S. A., Chang, T. N. (1965). The hydration of tricalcium silicate. *The Journal of Physical Chemistry*, 69(2), 553-561.
- Gunning, P., Hills, C.D., Carey, P.J., Commercial Application of Accelerated Carbonation: Looking Back at the First Year, In: *Proceedings of the Fourth International Conference on Accelerated Carbonation for Environmental and Materials Engineering*, April 9-12, (Leuven, Belgium), 2013, 185-192.

-
- Gunning, P.J., Hills, C.D., Carey, P.J. (2009). Production of lightweight aggregate from industrial waste and carbon dioxide. *Waste Management*, 29 (10), 2722-2728.
- Habert, G., De Lacaillerie, J. D. E., Roussel, N. (2011). An environmental evaluation of geopolymer based concrete production: reviewing current research trends. *Journal of Cleaner Production*, 19(11), 1229-1238.
- Haha, M. B., Lothenbach, B., Le Saout, G., Winnefeld, F. (2011). Influence of slag chemistry on the hydration of alkali-activated blast-furnace slag—Part I: Effect of MgO. *Cement and Concrete Research*, 41(9), 955-963.
- Haha, M. B., Lothenbach, B., Le Saout, G., Winnefeld, F. (2012). Influence of slag chemistry on the hydration of alkali-activated blast-furnace slag—Part II: Effect of Al₂O₃. *Cement and Concrete Research*, 42(1), 74-83.
- Hänchen, M., Prigiobbe, V., Storti, G., Seward, T. M., Mazzotti, M. (2006). Dissolution kinetics of fosteritic olivine at 90–150 C including effects of the presence of CO₂. *Geochimica et cosmochimica acta*, 70(17), 4403-4416.
- Hapgood, K. P., Tan, M. X., Chow, D. W. (2009). A method to predict nuclei size distributions for use in models of wet granulation. *Advanced Powder Technology*, 20(4), 293-297.
- Herrmann, I., Andreas, L., Diener, S., Lind, L. (2010). Steel slag used in landfill cover liners: laboratory and field tests. *Waste Management Research*, 28 (12), 1114-1121.
- Huijgen, W. J. J., Comans, R. N. J. (2005). Mineral CO₂ sequestration by carbonation of industrial residues. The Netherlands: Energy Research Centre of the Netherlands (ECN).
- Huijgen, W. J., Witkamp, G. J., Comans, R. N. (2005). Mineral CO₂ sequestration by steel slag carbonation. *Environmental science technology*, 39(24), 9676-9682.
- Huijgen, W. J., Comans, R. N. (2006). Carbonation of steel slag for CO₂ sequestration: leaching of products and reaction mechanisms. *Environmental science technology*, 40(8), 2790-2796.
- Huntzinger, D. N., Gierke, J. S., Kawatra, S. K., Eisele, T. C., Sutter, L. L. (2009). Carbon dioxide sequestration in cement kiln dust through mineral carbonation. *Environmental science technology*, 43(6), 1986-1992.
- IEA, GHG (2002). *Transmission of CO₂ and Energy*, RD Programme, Cheltenham, UK.
-

- Iveson, S. M., Litster, J. D., Ennis, B. J. (1996). Fundamental studies of granule consolidation part 1: effects of binder content and binder viscosity. *Powder Technology* 88, 15-20.
- Iveson, S. M., Litster, J. D. (1998a). Fundamental studies of granule consolidation part 2: quantifying the effects of particle and binder properties. *Powder technology*, 99(3), 243-250.
- Iveson, S. M., Litster, J. D. (1998b). Growth regime map for liquid-bound granules. *AIChE journal*, 44(7), 1510-1518.
- Iveson, S.M., Litster, J.D., Hapgood, K., Ennis, B.J. (2001a), Nucleation, growth and breakage phenomena in agitated wet granulation processes: a review. *Powder Technology*, 117 (1-2), 3-39.
- Iveson, S. M., Wauters, P. A., Forrest, S., Litster, J. D., Meesters, G. M., Scarlett, B. (2001b). Growth regime map for liquid-bound granules: further development and experimental validation. *Powder Technology*, 117(1), 83-97.
- Minchener J., (2005), Coal gasification for advanced power generation, *Fuel* 84, 2222-2235.
- Johnson, D. R., Robb, W. A. (1973). Gaylussite: thermal properties by simultaneous thermal analysis. *Am. Mineral*, 58, 778-784.
- Johnson, D. C., MacLeod, C. L., Carey, P. J., Hills, C. D. (2003). Solidification of stainless steel slag by accelerated carbonation. *Environmental technology*, 24(6), 671-678.
- Keningley, S. T., Knight, P. C., Marson, A. D. (1997). An investigation into the effects of binder viscosity on agglomeration behaviour. *Powder Technology*, 91(2), 95-103.
- Kim A. G.(2009). Soluble metals in coal gasification residues, *Fuel* 88, 1444-1452.
- Kriskova, L., Pontikes, Y., Zhang, F., Cizer, Ö., Jones, P. T., Van Balen, K., Blanpain, B. (2014). Influence of mechanical and chemical activation on the hydraulic properties of gamma dicalcium silicate. *Cement and Concrete Research*, 55, 59-68.
- Krizan, D., Zivanovic, B. (2002). Effects of dosage and modulus of water glass on early hydration of alkali-slag cements. *Cement and Concrete Research*, 32(8), 1181-1188.

-
- Kuramochi, T., Ramírez, A., Turkenburg, W., Faaij, A. (2012). Comparative assessment of CO₂ capture technologies for carbon-intensive industrial processes. *Progress in energy and combustion science*, 38(1), 87-112.
- Lackner, K. S., Wendt, C. H., Butt, D. P., Joyce, E. L., Sharp, D. H. (1995). Carbon dioxide disposal in carbonate minerals. *Energy*, 20(11), 1153-1170.
- Lange, L. C., Hills, C. D., Poole, A. B. (1996). The influence of mix parameters and binder choice on the carbonation of cement solidified wastes. *Waste Management*, 16(8), 749-756.
- Li, Z. S., Cai, N. S., Huang, Y. Y., Han, H. J. (2005). Synthesis, experimental studies, and analysis of a new calcium-based carbon dioxide absorbent. *Energy Fuels*, 19(4), 1447-1452.
- Li, X., Bertos, M. F., Hills, C. D., Carey, P. J., Simon, S. (2007). Accelerated carbonation of municipal solid waste incineration fly ashes. *Waste management*, 27(9), 1200-1206.
- Li, C., Sun, H., Li, L. (2010a). A review: The comparison between alkali-activated slag (Si+ Ca) and metakaolin (Si+ Al) cements. *Cement and Concrete Research*, 40(9), 1341-1349.
- Li, F., Huang, J., Fang, Y., Wang, Y. (2010b). Formation mechanism of slag during fluid-bed gasification of lignite. *Energy Fuels*, 25(1), 273-280.
- Litster, J. D., Sarwono, R. (1996). Fluidized drum granulation: studies of agglomerate formation. *Powder technology*, 88(2), 165-172.
- Litster, J. D. (2003). Scale up of wet granulation processes: science not art. *Powder Technology*, 130(1), 35-40.
- Liu, L. X., Litster, J. D., Iveson, S. M., Ennis, B. J. (2000). Coalescence of deformable granules in wet granulation processes. *AIChE Journal*, 46(3), 529-539.
- Liu, L., Ha, J., Hashida, T., Teramura, S. (2001). Development of a CO₂ solidification method for recycling autoclaved lightweight concrete waste. *Journal of materials science letters*, 20(19), 1791-1794.
- Macphee, D. E., Luke, K., Glasser, F. P., Lachowski, E. E. (1989). Solubility and aging of calcium silicate hydrates in alkaline solutions at 25 C. *Journal of the American Ceramic Society*, 72(4), 646-654.
-

- Mahieux, P. Y., Aubert, J. E., Escadeillas, G. (2009). Utilization of weathered basic oxygen furnace slag in the production of hydraulic road binders. *Construction and Building Materials*, 23(2), 742-747.
- Manso, J. M., Polanco, J. A., Losañez, M., González, J. J. (2006). Durability of concrete made with EAF slag as aggregate. *Cement and Concrete Composites*, 28(6), 528-534
- Maries, A. (1985). The activation of Portland cement by carbon dioxide. In *Proceedings of Conference in Cement and Concrete Science*, Oxford, UK.
- Marinov, V., Marinov, S. P., Lazarov, L., Stefanova, M. (1992). Ash agglomeration during fluidized bed gasification of high sulphur content lignites. *Fuel processing technology*, 31(3), 181-191.
- Maroto-Valer, M. M., Zhang, Y., Miller, B. (2004). Development of activated carbons from coal and biomass combustion and gasification chars. *Prepr. Pap.-Am. Chem. Soc., Div. Fuel Chem*, 49(2), 690.
- Marruzzo, G., Medici, F., Panei, L., Piga, L., Rinaldi, G. (2001). Characteristics and properties of a mixture containing fly ash, hydrated lime and an organic additive. *Environmental Engineering Science*, 18 (3), 159-165.
- Marsh, B. K., Day, R. L. (1988). Pozzolanic and cementitious reactions of fly ash in blended cement pastes. *Cement and Concrete Research*, 18(2), 301-310.
- Martavaltzi, C. S., Lemonidou, A. A. (2008). Parametric study of the $\text{CaO}-\text{Ca}_{12}\text{Al}_{14}\text{O}_{33}$ synthesis with respect to high CO_2 sorption capacity and stability on multicycle operation. *Industrial Engineering Chemistry Research*, 47(23), 9537-9543.
- Matjie, R. H., Van Alphen, C., Pistorius, P. C. (2006). Mineralogical characterisation of Secunda gasifier feedstock and coarse ash. *Minerals engineering*, 19(3), 256-261.
- Matjie, R. H., Van Alphen, C. (2008a). Mineralogical features of size and density fractions in Sasol coal gasification ash, South Africa and potential by-products. *Fuel*, 87(8), 1439-1445
- Matjie, R. H., Li, Z., Ward, C. R., French, D. (2008b). Chemical composition of glass and crystalline phases in coarse coal gasification ash. *Fuel*, 87(6), 857-869.

- McLellan, B. C., Williams, R. P., Lay, J., Van Riessen, A., Corder, G. D. (2011). Costs and carbon emissions for geopolymer pastes in comparison to ordinary portland cement. *Journal of Cleaner Production*, 19(9), 1080-1090.
- Medici, F., Piga, L., Rinaldi, G. (2000). Behaviour of polyaminophenolic additives in the granulation of lime and fly-ash. *Waste Management*, 20 (7), 491-498.
- Mehta, P. K. (1991). Durability of concrete--fifty years of progress?. *ACI Special Publication*, 126.
- Melton, J.S., Tarabadkar, K., Gardner, K. H., 2008. Accelerated carbonation of contaminated sediment to immobilize heavy metals. *Proceedings of the 2nd International Conference on Accelerated Carbonation for Environmental and Materials Engineering*. (Rome, Italy), 1-3 October 2008.
- Ministerial Decree 04/05/2006, n.186. Regolamento recante modifiche al decreto ministeriale 5 Febbraio 1998 "Individuazione dei rifiuti non pericolosi sottoposti alle procedure semplificate di recupero, ai sensi degli articoli 31 e 33 del Decreto Legislativo 5 Febbraio 1997 n.22", Published on *Gazzetta Ufficiale* n.115 dated 05/19/2006, (in italian).
- Mishra, B. K., Thornton, C., Bhimji, D. (2002). A preliminary numerical investigation of agglomeration in a rotary drum. *Minerals Engineering*, 15(1), 27-33.
- Motz, H., Geiseler, J. (2001). Products of steel slags an opportunity to save natural resources. *Waste Management*, 21(3), 285-293.
- Mounanga, P., Khokhar, M. I. A., El Hachem, R., Loukili, A. (2011). Improvement of the early-age reactivity of fly ash and blast furnace slag cementitious systems using limestone filler. *Materials and structures*, 44(2), 437-453.
- National Energy Technology Laboratory, *Gasification Worldwide Database*, 2010.
- Navarro, C., Diaz, M., Villa Garcia, M.A. (2010). Physico-chemical characterization of Steel Slag. Study of its behaviour under simulated environmental conditions. *Environmental Science Technology*, 44, 5383-5368.
- Ngala, V. T., Page, C. L. (1997). Effects of carbonation on pore structure and diffusional properties of hydrated cement pastes. *Cement and Concrete Research*, 27(7), 995-1007.

-
- Nicolae, M., Vilciu, I., Zăman, F. (2007). X-ray diffraction analysis of steel slag and blast furnace slag viewing their use for road construction. *UPB Sci. Bull*, 69(2), 99-108.
- Oner, A., Akyuz, S. (2007). An experimental study on optimum usage of GGBS for the compressive strength of concrete. *Cement and Concrete Composites*, 29(6), 505-514.
- Pacheco-Torgal, F., Castro-Gomes, J., Jalali, S. (2008a). Alkali-activated binders: A review: Part 1. Historical background, terminology, reaction mechanisms and hydration products. *Construction and Building Materials*, 22(7), 1305-1314.
- Pacheco-Torgal, F., Castro-Gomes, J., Jalali, S. (2008b). Alkali-activated binders: a review. Part 2. About materials and binders manufacture. *Construction and Building Materials*, 22(7), 1315-1322.
- Pal, S. C., Mukherjee, A., Pathak, S. R. (2003). Investigation of hydraulic activity of ground granulated blast furnace slag in concrete. *Cement and Concrete Research*, 33(9), 1481-1486.
- Palomo, A., Grutzeck, M. W., Blanco, M. T. (1999). Alkali-activated fly ashes: a cement for the future. *Cement and concrete research*, 29(8), 1323-1329.
- Papadakis, V. G., Vayenas, C. G., Fardis, M. N. (1989). A reaction engineering approach to the problem of concrete carbonation. *AIChE Journal*, 35(10), 1639-1650.
- Park, A. H. A., Jadhav, R., Fan, L. S. (2003). CO₂ mineral sequestration: chemically enhanced aqueous carbonation of serpentine. *The Canadian Journal of Chemical Engineering*, 81(3-4), 885-890.
- Pettinau, A., Frau, C., Ferrara, F. (2011). Performance assessment of a fixed-bed gasification pilot plant for combined power generation and hydrogen production. *Fuel Processing Technology*, 92(10), 1946-1953.
- Pinto, F., Lopes, H., André, R. N., Gulyurtlu, I., Cabrita, I. (2008). Effect of catalysts in the quality of syngas and by-products obtained by co-gasification of coal and wastes. 2: Heavy metals, sulphur and halogen compounds abatement. *Fuel*, 87(7), 1050-1062.
- Poh, H. Y., Ghataora, G. S., Ghazireh, N. (2006). Soil stabilization using basic oxygen steel slag fines. *Journal of materials in Civil Engineering*, 18(2), 229-240.
- Praxis Engineers Inc., (1998), Utilization of lightweight materials made from coal gasification slags, Quarterly Report No. 17.
-

- Prigiobbe, V., Hänchen, M., Werner, M., Baciocchi, R., Mazzotti, M. (2009). Mineral carbonation process for CO₂ sequestration. *Energy Procedia*, 1(1), 4885-4890.
- Proctor, D. M., Fehling, K. A., Shay, E. C., Wittenborn, J. L., Green, J. J., Avent, C., Bigham, R.D, Connolly, M., Lee, B., Shepker, T.O., Zak, M. A. (2000). Physical and chemical characteristics of blast furnace, basic oxygen furnace, and electric arc furnace steel industry slags. *Environmental Science Technology*, 34(8), 1576-1582.
- Puertas, F., Martínez-Ramírez, S., Alonso, S., Vazquez, T. (2000). Alkali-activated fly ash/slag cements: strength behavior and hydration products. *Cement and Concrete Research*, 30(10), 1625-1632.
- Puertas, F., Fernández-Jiménez, A., Blanco-Varela, M. T. (2004). Pore solution in alkali-activated slag cement pastes. Relation to the composition and structure of calcium silicate hydrate. *Cement and Concrete Research*, 34(1), 139-148.
- Puertas, F., Torres-Carrasco, M. (2014). Use of glass waste as an activator in the preparation of alkali-activated slag. Mechanical strength and paste characterization. *Cement and Concrete Research*, 57, 95-104.
- Purdon, A. O. (1940). The action of alkalis on blast-furnace slag. *Journal of the Society of Chemical Industry*, 59(9), 191-202.
- Rashad, Alaa M. A comprehensive overview about the influence of different additives on the properties of alkali-activated slag—A guide for Civil Engineer. *Construction and Building Materials*, 2013, 47: 29-55.
- Reddy, A. S., Pradhan, R. K., Chandra, S. (2006). Utilization of basic oxygen furnace (BOF) slag in the production of a hydraulic cement binder. *International journal of mineral processing*, 79(2), 98-105.
- Richardson, I. G. (1999). The nature of C-S-H in hardened cements. *Cement and concrete research*, 29(8), 1131-1147.
- Salman, M., Cizer, Ö., Pontikes, Y., Vandewalle, L., Blanpain, B., Van Balen, K. (2014a). Effect of curing temperatures on the alkali activation of crystalline continuous casting stainless steel slag. *Construction and Building Materials*, 71, 308-316.
- Salman, M. (2014b), Sustainable materialization of residues from thermal processes into construction materials, PhD thesis.

- Salman, M., Cizer, Ö., Pontikes, Y., Snellings, R., Vandewalle, L., Blanpain, B., Van Balen, K. (2015). Cementitious binders from activated stainless steel refining slag and the effect of alkali solutions. *Journal of hazardous materials*, 286, 211-219.
- Santos, R. M., Ling, D., Sarvaramini, A., Guo, M., Elsen, J., Larachi, F., Beaudoin, G., Blanpain, B., Van Gerven, T. (2012). Stabilization of basic oxygen furnace slag by hot-stage carbonation treatment. *Chemical Engineering Journal*, 203, 239-250.
- Scanferla, P., Ferrari, G., Pelay, R., Volpi Ghirardini, A., Zanetto, G., Libralato, G. (2009). An innovative stabilization/solidification treatment for contaminated soil remediation: demonstration project results. *Journal of Soils Sediments*, 9 (3), 229-236.
- Shariq, M., Prasad, J., Ahuja, A. K. (2008). Strength development of cement mortar and concrete incorporating GGBFS. *Asian Journal of Civil Engineering (Building and Housing)*, 9(1), 61-74.
- Shen, H., Forssberg, E. (2003). An overview of recovery of metals from slags. *Waste Management* 23 (10), 933-949.
- Shen, D.-H., Wu, C.-M., Du, J.-C. (2009). Laboratory investigation of basic oxygen furnace slag for substitution of aggregate in porous asphalt mixture. *Construction and Building Materials* 23 (1), 453-461.
- Shergold, F. A. (1948). A review of available information on the significance of roadstone tests. HM Stationery Office.
- Sherritt, R. G., Chaouki, J., Mehrotra, A. K., Behie, L. A. (2003). Axial dispersion in the three-dimensional mixing of particles in a rotating drum reactor. *Chemical Engineering Science*, 58(2), 401-415.
- Shi, C., Day, R. L. (1995). A calorimetric study of early hydration of alkali-slag cements. *Cement and Concrete Research*, 25(6), 1333-1346.
- Shi, C., Day, R.L. (1996). Some factors affecting early hydration of alkali-slag cements. *Cement and Concrete Research* 26 (3): 439-447.
- Shi, C. (2002). Characteristics and cementitious properties of ladle slag fines from steel production. *Cement and Concrete Research*, 32(3), 459-462.
- Shi, C., Jiménez, A. F., Palomo, A. (2011). New cements for the 21st century: the pursuit of an alternative to Portland cement. *Cement and Concrete Research*, 41(7), 750-763.

- Shi, C., He, F., Wu, Y. (2012). Effect of pre-conditioning on CO₂ curing of lightweight concrete blocks mixtures. *Construction and Building Materials*, 26(1), 257-267.
- Skhonde, M. P., Matjie, R. H., Bunt, J. R., Strydom, A. C., Schobert, H. (2008). Sulfur Behavior in the Sasol– Lurgi Fixed-Bed Dry-Bottom Gasification Process. *Energy Fuels*, 23(1), 229-235.
- Song, S., Sohn, D., Jennings, H. M., Mason, T. O. (2000). Hydration of alkali-activated ground granulated blast furnace slag. *Journal of materials science*, 35(1), 249-257.
- Stade, H. (1989). On the reaction of C-S-H (di, poly) with alkali hydroxides. *Cement and Concrete Research*, 19(5), 802-810.
- Suzuki, K., Nishikawa, T., Ito, S. (1985). Formation and Carbonation of C-S-H in Water. *Cement and Concrete Research*, 15(2), 213-224.
- Tardos, G. I., Khan, M. I., Mort, P. R. (1997). Critical parameters and limiting conditions in binder granulation of fine powders. *Powder Technology*, 94(3), 245-258.
- Taylor, H. F. (1997). *Cement chemistry*. Thomas Telford.
- Taylor, R., Richardson, I. G., Brydson, R. M. D. (2010). Composition and microstructure of 20-year-old ordinary Portland cement–ground granulated blast-furnace slag blends containing 0 to 100% slag. *Cement and Concrete Research*, 40(7), 971-983.
- Tossavainen, M., Engstrom, F., Yang, Q., Menad, N., Lidstrom Larsson, M., Bjorkman, B. (2007). Characteristics of steel slag under different cooling conditions. *Waste Management* 27 (10), 1335-1344.
- Turk, N., Dearman, W. R. (1989). An investigation of the relation between ten per cent fines load and crushing value tests of aggregates (UK). *Bulletin of the International Association of Engineering Geology-Bulletin de l'Association Internationale de Géologie de l'Ingénieur*, 39(1), 145-154.
- UNI EN 1097-6, Tests for mechanical and physical properties of aggregates – determination of particle density and water absorption, February 2002
- UNI EN 12457-2, Leaching: compliance test for leaching of granular waste materials and sludges-Part 2: one stage batch test at a liquid to solid ratio of 10 l/kg for materials with particle size below 4 mm, October 2004.

- Valls, S., Vazquez, E. (2001). Accelerated carbonatation of sewage sludge–cement–sand mortars and its environmental impact. *Cement and Concrete Research*, 31(9), 1271-1276.
- Van Gerven, T., Van Baelen, D., Dutré, V., Vandecasteele, C. (2004). Influence of carbonation and carbonation methods on leaching of metals from mortars. *Cement and Concrete Research*, 34(1), 149-156.
- Van Jaarsveld, J. G. S., Van Deventer, J. S. J., Lorenzen, L. (1998). Factors affecting the immobilization of metals in geopolymerized flyash. *Metallurgical and materials transactions B*, 29(1), 283-291.
- van Zomeren, A., Van der Laan, S. R., Kobesen, H., Huijgen, W. J., Comans, R. N. (2011). Changes in mineralogical and leaching properties of converter steel slag resulting from accelerated carbonation at low CO₂ pressure. *Waste management*, 31(11), 2236-2244.
- Wagner, N. J., Matjie, R. H., Slaghuis, J. H., Van Heerden, J. H. P. (2008). Characterization of unburned carbon present in coarse gasification ash. *Fuel*, 87(6), 683-691.
- Wang, S. D., Scrivener, K. L., Pratt, P. L. (1994). Factors affecting the strength of alkali-activated slag. *Cement and Concrete Research*, 24(6), 1033-1043.
- Wang, G., Wang, Y., Gao, Z. (2010). Use of steel slag as a granular material: volume expansion prediction and usability criteria. *Journal of Hazardous Materials*, 2010, 184 (1-3), 555-560.
- Wang, Q., Yan, P. (2010). Hydration properties of basic oxygen furnace steel slag. *Construction and Building Materials*, 24(7), 1134-1140.
- Wang, Q., Yan, P., Han, S. (2011). The influence of steel slag on the hydration of cement during the hydration process of complex binder. *Science China Technological Sciences*, 54(2), 388-394.
- Wauters, P.A.L., van de Water, R., Litster, J.D., Meesters, G.M.H., Scarlett, B. (2002). Growth and compaction behaviour of copper concentrate granules in a rotating drum. *Powder Technology* 124 (3), 230-237.
- Wieczorek-Ciurowa, K., Paulik, J., Paulik, F. (1980). Influence of foreign materials upon the thermal decomposition of dolomite, calcite and magnesite part I. Influence of sodium chloride. *Thermochimica Acta*, 38(2), 157-164.

World Steel association, world steel in figures, 2014

Wu, T., Gong, M., Lester, E., Wang, F., Zhou, Z., Yu, Z. (2007). Characterisation of residual carbon from entrained-bed coal water slurry gasifiers. *Fuel*, 86(7), 972-982.

Xu, H., Van Deventer, J. S. J. (2000). The geopolymerisation of alumino-silicate minerals. *International Journal of Mineral Processing*, 59(3), 247-266.

Xu, S., Zhou, Z., Gao, X., Yu, G., Gong, X. (2009). The gasification reactivity of unburned carbon present in gasification slag from entrained-flow gasifier. *Fuel Processing Technology*, 90(9), 1062-1070.

Xue, Y., Wu, S., Hou, H., Zha, J. (2006). Experimental investigation of basic oxygen furnace slag used as aggregate in asphalt mixture. *Journal of Hazardous Materials*, 138 (2), 261-268.

Yildirim, I. Z., Prezzi, M. (2009). Use of steel slag in subgrade applications (No. FHWA/IN/JTRP-2009/32).

Yildirim, I. Z., Prezzi, M. (2011). Chemical, mineralogical, and morphological properties of steel slag. *Advances in Civil Engineering*, 2011

Yip, C. K., Lukey, G. C., Van Deventer, J. S. J. (2005). The coexistence of geopolymeric gel and calcium silicate hydrate at the early stage of alkaline activation. *Cement and Concrete Research*, 35(9), 1688-1697.

Young, J. F., Berger, R. L., Breese, J. (1974). Accelerated curing of compacted calcium silicate mortars on exposure to CO₂. *Journal of the American Ceramic Society*, 57(9), 394-397.

Zevenhoven, R., Teir, S., Eloneva, S. (2008). Heat optimisation of a staged gas–solid mineral carbonation process for long-term CO₂ storage. *Energy*, 33(2), 362-370.

Zhan, B., Poon, C., Shi, C. (2013). CO₂ curing for improving the properties of concrete blocks containing recycled aggregates. *Cement and Concrete Composites*, 42, 1-8.

Živica, V. (2007). Effects of type and dosage of alkaline activator and temperature on the properties of alkali-activated slag mixtures. *Construction and Building Materials*, 21(7), 1463-1469.

Publications

Scientific journal

Morone M., Costa G., Stendardo S., Baciocchi R. “Characterization and density separation of coal gasification residues generated from the ZECOMIX experimental platform”. *Fuel Processing Technology* (submitted).

Morone M., Costa G., Poletini A., Pomi R., Baciocchi R. (2014), “Valorization of steel slag by a combined carbonation and granulation treatment”. *Minerals Engineering* 59, 82-90.

Baciocchi R., Capobianco O., Costa G., Morone M., Zingaretti D. (2014), “Carbonation of industrial residues for CO₂ storage and utilization as a treatment to achieve multiple environmental benefits”. *Energy Procedia*, 63, 5879-5886.

Conference proceedings

Baciocchi R., Capobianco O., Costa G., Morone M., Gavasci R., “Production of aggregates from recycled industrial soil and residues”. XII Simpòsio Italo-Brasileiro de Engenharia Sanitária e Ambiental 2014 (19-21th May 2014, Natal, Brasil).

Baciocchi R., Capobianco O., Costa G., Morone M., Zingaretti D., “Carbonation of industrial residues for CO₂ storage and utilization as a treatment to achieve multiple environmental benefits”. International conference on Greenhouse Gas Technologies (GHGT), 5-9th October 2014, Austin, Texas.

Baciocchi R., Costa G., Morone M., Poletini A., Pomi R., “Valorization of steel slag by a combined carbonation and granulation treatment”. 4th International Conference on Accelerated Carbonation for Environmental and Materials Engineering (ACEME), 9-12th April 2013.